

**THE POTENTIAL OF MICRO-HYDROPOWER  
GENERATION IN THE INKOMATI RIVER CATCHMENT  
IN MOZAMBIQUE**

**Daniel Macaringue**

Submitted in fulfilment of the requirements for the degree of  
MASTER OF SCIENCE

School of Engineering  
University of KwaZulu-Natal  
Pietermaritzburg  
May 2014

## PREFACE

I ..... declare that

- (i) The research reported in this thesis, except where otherwise indicated, and is my original work.
- (ii) This thesis has not been submitted for any degree or examination at any other university.
- (iii) This thesis does not contain other persons' data, pictures, graphs or other information, unless specifically acknowledged as being sourced from other persons.
- (iv) This thesis does not contain other persons' writing, unless specifically acknowledged as being sourced from other researchers. Where other written sources have been quoted, then:
  - (a) their words have been re-written but the general information attributed to them has been referenced;
  - (b) where their exact words have been used, their writing has been placed inside quotation marks, and referenced.
- (v) Where I have reproduced a publication of which I am an author, co-author or editor, I have indicated in detail which part of the publication was actually written by myself alone and have fully referenced such publications.
- (vi) This thesis does not contain text, graphics or tables copied and pasted from the Internet, unless specifically acknowledged, and the source being detailed in the thesis and in the References sections.

Signed.....

Supervisor.....

Co- supervisor.....

## ACKNOWLEDGEMENTS

The accomplishment of this thesis would not have been possible without the kind collaboration and encouragement of many people.

**Hence, I would like therefore to thank the following:**

- First and foremost, I thank to Almighty God for giving me this opportunity, strength and guidance that make the conclusion of this study possible, although it seemed very difficult.
- My sincere gratitude goes to my supervisor, **Professor Jeff Smithers** (former Head of School of Bioresources Engineering and Environmental Hydrology at UKZN). It has been an honor to be his MSc student. His excellent leadership and supervision were so invaluable that without his guidance and invaluable help, this thesis would not have been possible.
- Many thanks to my co-supervisor, **Mr. Mark Horan** for his invaluable advice, valuable contributions of information and input data throughout the study.
- My heartfelt thanks and appreciation go to **Eng. Benon Zaake, Dr. V. Chaplot, Professor T. Seyoum** and **Dr. Habteab Ghebrehiwot** for their assistance and advice from the alpha to the omega of this research work, and my special thanks go also to **Dr. Gaetan Kabera for statistical analysis support.**
- Thank you very much to my coordinators **Dr. Boaventura Cuamba and Dr. Geraldo Nhumai** (Eduardo Mondlane University (UEM), Mozambique), for believing in me and for their generosity in giving me the opportunity to fulfil my dream of pursuing a Masters degree. Your support and encouragement will never be forgotten.
- I owe special thanks to **SIDA-SAREC** for funding this project” Energy Science and Technology Research Program” during my stay in South Africa. Special thanks also to my Directors of Instituto Nacional de Meteorologia (INAM), **Eng. Vicente Benessene and Dr. Atanásio Manhique** for providing me a study leave to enable to pursue this MSc study. I am very grateful

- I am very grateful to **Mrs. Vilanculos, Zucule and Clemente** for their support, and effort in making available the necessary data for this study. I am also grateful to all **DNA/ARA-SUL's staff** for providing the valuable data for this study.
- I would like to express my warm thanks to all Mozambican friends, classmates and all BEEH participants and staff for helping me in many ways during my studies in South Africa. Special thanks go to **Pshesheya, Brian, Chauque, Paula, Fato, Macucule, Gazelane, Luis, Dito, Mpume, Rogerio, Lameck, Sequeira, Couto, Daute, Mugabe and others.**
- Finally, my gratitude and thanks to my wife (**Odete**) and children (**Quim, Aka and Kelvin**) for their endurance and sacrifice, and to my parents, brothers and sisters in Mozambique for their moral support and encouragement.

## ABSTRACT

Hydropower is the leading source of renewable energy. It provides more than 97% of all electricity generated by renewable sources internationally. Small hydropower plants (SHPs) can be an alternative and a complement to large power generating plants, especially in the less developed world where the demand for electricity is growing rapidly. The socio-economic development in the Inkomati River Catchment has experienced slow growth in recent years. One of the major reasons identified is the lack of availability of electrical energy, which hinders agricultural production, job creation and economic growth, particularly in small rural communities. The installation of small hydropower plants in the Inkomati River Catchment which experiences variable flows has the potential to produce clean and cheap energy for boosting and sustaining economic growth in the region.

Numerous hydrological studies conducted in the Inkomati River Catchment have focused on the mitigation of floods and droughts, while little attention has been given to the hydropower potential of the catchment. The objectives of this study were to: (i) derive and verify a simple methodology to estimate daily streamflow quantiles at gauged sites using flow duration curves (FDCs), (ii) to regionalise the FDCs in order to estimate daily streamflow quantiles at ungauged sites, and (iii) to demonstrate the use of the regionalised FDCs to estimate potential hydropower production at selected sites in the Inkomati River Catchment. To address these objectives, FDCs were computed using only reliable daily streamflow data gathered from twelve gauged stations across the Inkomati River Catchment. Since most of the gauged stations in the catchment are sparse, regionalisation was performed using morphoclimatic characteristics (drainage area, hypsometric fall, Mean Annual Precipitation (MAP) and river length) parameterized using a Geographic Information System (GIS). The methodology developed enables daily streamflow quantiles to be estimated at both gauged and ungauged sites. The verification of the accuracy of the regionalisation was done by calculating the root mean square error at two selected gauging stations, which were not used in the calibration procedure. The power equation was applied to determine the power potential at the Mac-Mac River and Ressano Garcia gauging stations, assuming a 50% and 70% overall plant efficiency ( $\epsilon$ ) of the turbine. The method estimates the flow and, given adequate head, the potential hydropower can be estimated, especially from small catchments (<100 km<sup>2</sup> drainage area).

# TABLE OF CONTENTS

	Page
1. INTRODUCTION .....	1
2. SMALL HYDRO-ELECTRIC POWER PLANTS .....	3
2.1 Definition of Small Hydropower Plants .....	3
2.2 Classification of Hydropower Plants .....	5
2.3 Factors that need to be considered for the Installation of SHPs .....	5
2.4 Method for Estimating Power Potential .....	8
2.4.1 Flow duration curve method .....	8
2.4.2 Flow duration curves in hydropower applications .....	9
2.4.3 Regionalization of flow duration curves .....	12
3. METHODOLOGY .....	15
3.1 Description of the Study Area .....	15
3.1.1 Description of hydrometric and meteorological stations .....	18
3.1.2 Reliability of Mozambican observed flow and rainfall data .....	21
3.1.2.1 Moamba gauging station .....	23
3.1.2.2 Ressano Garcia gauging station .....	24
3.1.2.3 Chinhanganine gauging station .....	26
3.1.2.4 Magude gauging station .....	29
3.1.2.5 Chobela gauging station .....	30
3.1.2.6 Incoluane gauging station .....	32
3.1.3 Assessment and reliability of South African observed flow data .....	36
3.1.3.1 Sassenheim gauging station .....	37
3.1.3.2 Bellevue gauging station .....	38
3.1.3.3 Glenthorpe gauging station .....	38
3.1.3.4 Kindergoed gauging station .....	40
3.1.3.5 Kruger National Park gauging station .....	40
3.1.3.6 Sabie gauging station .....	42
3.1.3.7 Ethna gauging station .....	42
3.1.3.8 Injaka gauging station .....	43
3.1.3.9 Dawsonsspruit gauging station .....	44
3.1.3.10 Mac-Mac River gauging station .....	45
3.2 Determination of Catchment Physical Parameters .....	47

3.2.1	Mean annual precipitation .....	48
3.2.2	Drainage area .....	50
3.2.3	Hypsometric fall .....	51
3.2.4	River length .....	51
3.3	Derivation of Flow Duration Curve for the Gauged Sites.....	51
3.4	Development of Regional Flow Duration Frequency Curves .....	52
3.4.1	Statistical analysis .....	52
3.4.2	Regional Model .....	53
3.4.3	Determination of hydro-potential for Small Hydropower Plants .....	55
4.	RESULTS .....	56
4.1	Determination of Catchment Physical Parameters .....	56
4.2	Derivation of Flow Duration Curve for the Gauged Sites.....	57
4.3	Regionalization using the Multiple Regressions Technique .....	60
4.3.1	Calibration of the flow duration curves.....	61
4.3.2	Regionalization of the flow duration curves .....	71
4.3.3	Estimation of the parameter $a$ .....	72
4.3.4	Estimation of the parameter $b$ .....	81
4.3.5	Summary of regionalization .....	83
4.4	Verification .....	82
4.5	Calculation of the power at Mac-Mac River and Ressano Garcia gauging .....stations (X3H003 and E-23).....	83
5.	DISCUSSION ,CONCLUSIONS AND RECOMMENDATIONS .....	85
6.	REFERENCES .....	91
7.	APPENDICES .....	97
7.1	Appendix 1 .....	97
7.2	Appendix 2.....	104

## LIST OF FIGURES

	Page
Figure 2. 1 Layout of small hydropower plant.....	4
Figure 2. 2 Planning for small hydropower plants.....	6
Figure 2. 3 Typical Flow Duration Curve.....	9
Figure 2. 4 Illustration of flow duration and power duration curves .....	12
Figure 3. 1 Map of the study area showing location of flow gauging and rainfall stations	17
Figure 3. 2 Length of observation periods at gauging stations in the Inkomati River .....	22
Figure 3. 3 Daily average discharge at the Moamba gauging station (E-22).....	24
Figure 3. 4 Rainfall and flow data of the represented station (E-22).....	24
Figure 3. 5 Daily average discharge at R.Garcia gauging station (E-23).....	26
Figure 3. 6 Rainfall and flow data of the represented station (E-23).....	26
Figure 3. 7 Daily average discharge at Chinhanganine gauging station (E-27).....	28
Figure 3. 8 Rainfall and flow data of the represented station (E-27).....	28
Figure 3. 9 Daily average discharge at Magude gauging station (E-43).....	30
Figure 3. 10 Rainfall and flow data of the represented station (E- 43).....	30
Figure 3. 11 Daily average discharge at Chobela gauging station (E-44) .....	32
Figure 3. 12 Rainfall and flow data of the represented station (E-44).....	32
Figure 3. 13 Daily average discharge at Incoluane gauging station (E-45).....	34
Figure 3. 14 Rainfall and flow data of the represented station (E-45).....	35
Figure 3. 15 Daily average discharge at Sassenhein gauging station (X2H008).....	37
Figure 3. 16 Daily average discharge at Bellevue gauging station (X2H010).....	38
Figure 3. 17 Daily average discharge at Glenthorpe gauging station (X2H024).....	39
Figure 3. 18 Daily average discharge at kindergoed gauging station (X2H047).....	41
Figure 3. 19 Daily average discharge at Kruger National Park gauging station (X2H072)	42
Figure 3. 20 Daily average discharge at Sabie gauging station (X3H001).....	42
Figure 3. 21 Daily average discharge at Ethna gauging station (X3H007) .....	43
Figure 3. 22 Daily average discharge at Injaka gauging station (X3H011).....	44
Figure 3. 23 Daily average discharge at Dawsonsspruit gauging station (X2H012) .....	45
Figure 3. 24 Daily average discharge at Geelhoutboom gauging station (X3H003).....	46
Figure 3. 25 Map of Inkomati River Catchment showing the Thiessen polygon method ...	49
Figure 4. 1 Superimposed daily Flow Duration Curves for all selected flow gauges.....	58
Figure 4. 2 Daily Flow Duration Curves of observed and estimated flow data for (E-22)..	62
Figure 4. 3 Daily Flow Duration Curves of observed and estimated flow data for (E-27)..	61

Figure 4. 4 Daily Flow Duration Curves of observed and estimated flow data for (E-43)..	62
Figure 4. 5 Daily Flow Duration Curves of observed and estimated flow data for (E-44)..	63
Figure 4. 6 Daily Flow D Curves of observed and estimated flow data for (X2H008)....	66
Figure 4. 7 Daily Flow Duration Curves of observed and estimated flow data for (X2H010)	65
Figure 4. 8 Daily Flow Duration Curves of observed and estimated flow data for (X2H024)	66
Figure 4. 9 Daily Flow Duration Curves of observed and estimated flow data for (X2H047)	67
Figure 4.10 Daily Flow Duration Curves of observed and estimated flow data for (X3H001)	70
Figure 4.11 Daily Flow Duration Curves of observed and estimated flow data for (X2H012)	71
Figure 4. 12 Scatter matrix for variables $a, P, A, H$ and $L$ for Model 3.7.....	71
Figure 4. 13 Plotted graph of residual versus fitted values for model 3.7 .....	73
Figure 4. 14 Scatter matrix for the variables $a, P, A, H$ and $L$ for Model 3.8.....	74
Figure 4. 15 Plotted graph of residual versus fitted values for model 3.8 .....	75
Figure 4. 16 Scatter matrix for the variables $a, P, A, H$ and $L$ for Model 3.9.....	76
Figure 4. 17 Plotted graph of residual versus fitted values for model 3.9 .....	77
Figure 4. 18 Scatter matrix for the variables $a, P, A, H$ and $L$ for Model 3.10.....	78
Figure 4. 19 Scatter matrix for the variables $b, P, A, H$ and $L$ for Models 3.7 to 3.10.	82
Figure 4. 20 Flow Duration Curves at the Geelhoutboom gauging station X3H003	84
Figure 4. 21 Flow Duration Curves at the Ressano Garcia gauging station E-23 .....	85
Figure 7. 1 Flow Duration Curve on logarithmic scale at Moamba station .....	97
Figure 7. 2 Flow Duration Curve on logarithmic scale at Ressano Garcia station .....	98
Figure 7. 3 Flow Duration Curve on logarithmic scale at Chinhanganine station .....	98
Figure 7. 4 Flow Duration Curve on logarithmic scale at Magude station .....	100
Figure 7. 5 Flow Duration Curve on logarithmic scale at Chobela station.....	100
Figure 7. 6 Flow Duration Curve on logarithmic scale at Sassenheim station .....	101
Figure 7. 7 Flow Duration Curve on logarithmic scale at Bellevue station .....	101
Figure 7. 8 Flow Duration Curve on logarithmic scale at Glenthorpe station .....	102
Figure 7. 9 Flow Duration Curve on logarithmic scale at Kindergoed station .....	102
Figure 7. 10 Flow Duration Curve on logarithmic scale at Sabie station .....	102
Figure 7. 11 Flow Duration Curve on logarithmic scale at Dawsonsspruit station .....	102

Figure 7. 12 Flow Duration Curve on logarithmic scale at Geelhoutboom station .....103

## LIST OF TABLES

	Page
Table 2. 1 Classification of hydropower plants (Balat, 2006) .....	5
Table 3. 1 Characteristics of the raingauges stations in Mozambique.....	19
Table 3. 2 Characteristics of the flow gauging stations in Mozambique.....	19
Table 3. 3 Characteristics of the flow gauging stations in South Africa .....	20
Table 3. 4 Summary of Mozambican gauging stations analysis and assessment of data...	36
Table 3. 5 Summary of South African gauging stations analysis and assessment of data...	47
Table 4.1 Morphoclimatic characteristics for the Mozambique and South Africa catchments .....	56
Table 4. 2 Flow estimates for various levels of probability of exceedance (D) (%) .....	57
Table 4. 3 Coefficient of determination ( $R^2$ ) of the five mathematical models.....	61
Table 4. 4 Parameters, morphoclimatic data used in the MRA .....	72
Table 4. 5 Correlation matrix for variables $a$ , $P$ , $A$ , $H$ and $L$ for Model 3.7.....	71
Table 4. 6 Correlation matrix for the variables $a$ , $P$ , $A$ , $H$ and $L$ for Model 3.8.....	74
Table 4. 7 Correlation matrix for variables $a$ , $P$ , $A$ , $H$ and $L$ for Model 3.9.....	76
Table 4. 8 Correlation matrix for variables $a$ , $P$ , $A$ , $H$ and $L$ for Model 3.10.....	78
Table 4. 9 Correlation matrix for variables $b$ , $P$ , $A$ , $H$ and $L$ for Models 3.7 to 3.10...	82
Table 4. 10 Performance of Regional model .....	81
Table 4. 11 Results of power from observed discharge at two selected stations.....	84
Table 7. 1 Results of analysis of the mathematical models at Moamba station .....	104
Table 7. 2 Results of analysis of the mathematical models at Chinhanganine station ...	105
Table 7. 3 Results of analysis of the mathematical models at Magude station.....	106
Table 7. 4 Results of analysis of the mathematical models at Chobela station .....	107
Table 7. 5 Results of analysis of the mathematical models at Sassenheim station.....	108
Table 7. 6 Results of analysis of the mathematical models at Bellevue station .....	109
Table 7. 7 Results of analysis of the mathematical models at Glenthorpe station.....	110
Table 7. 8 Results of analysis of the mathematical models at Kindergoed station.....	111
Table 7. 9 Results of analysis of the mathematical models at Sabie station.....	112
Table 7. 10 Results of analysis of the mathematical models at Dawsonsspruit station.....	113

## 1. INTRODUCTION

The ability to meet the demand for energy is currently a serious problem in many countries, particularly in developing countries, as a result of increasing population and slow economic growth (Bakis and Demirbas, 2004; Balat, 2006). Moreover, there is a growing need to construct hydro-electric schemes because of the serious environmental effects associated with the production of energy when using fossil fuels (Aslan *et al.*, 2008). The use of Small Hydropower Plants (SHPs) offers an alternative to generate renewable electricity at a relatively low cost for sustainable socio-economic growth (Blanco *et al.*, 2008).

(SHPs) are generally constructed as “run-of-river” with no dam (Aslan *et al.*, 2008) and are a development of hydropower on a small scale (Yuksel, 2008). They can also be developed at existing dams which have been constructed for the control of water levels of rivers and lakes and for irrigation schemes (Aslan *et al.*, 2008).

Hydropower plants play an important role in the generation of cleaner renewable energy and can be useful for water resources management (Kaygusuz, 2002; Yuksel, 2008). The development of SHPs can contribute to meeting the energy needs of local people in remote and mountainous areas and thus improve their standard of living and quality of life (Bakis and Demirbas, 2004; Balat, 2006; Dudhani *et al.*, 2006). One significant advantage for the installation of SHPs is that they have less of an environmental impact than other energy sources (Paish, 2002). The environmental impact of hydropower plants is minimal because they do not cause pollution through carbon dioxide emissions (Yuksel, 2008). SHPs can be installed in a large range of environmental conditions, but there are several factors that need to be addressed prior to their installation, including technical, environmental, ecological, human and legal considerations (Dudhani *et al.*, 2006; Kaldellis, 2007).

Globally, hydropower is starting to become a “success story”. It contributes to one-fifth of the world’s power generation and provides the majority of the electricity supply in 55 countries (Yuksel, 2008). In Africa, hydropower contributes to more than 50% of electricity generated in approximately 25 countries (Bartle, 2002). Mozambique has a natural potential for the efficient

and effective use of SHPs (Associates, 2003). The country has small-scale hydropower potential and adequate topographical conditions in which water resources could be utilized to generate electricity (Consultec and BKS, 2001). However, electricity production in the country is far from satisfying the needs of the population, especially in the rural areas (Associates, 2003). Consequently, there is a need to develop additional energy production systems by promoting the development of small-scale hydropower systems.

As the demand for water resources increases and becomes more complex and diversified, the need for hydrological information becomes more important (Vogel and Fennessey, 1995). Flow duration curves are a key concept in the estimation of hydropower production potential and are thus important for the operation of SHPs along the rivers (Karamouz *et al.*, 1991).

The objective of this dissertation was to (i) derive and verify a simple methodology to estimate daily streamflow quantiles at gauged sites using flow duration curves (FDCs), (ii) to regionalise the FDCs in order to estimate daily streamflow quantiles at ungauged sites, and (iii) to demonstrate the use of the regionalised FDCs to estimate potential hydropower production at selected sites in the Inkomati River Catchment. This document contains seven chapters. Chapter 1 contains a general introduction, while Chapter 2 provides theoretical concepts related to SHPs and highlights the methods of estimating the power potential from hydropower plants. This includes the concept of flow duration curves and their application in hydropower plant design. Chapter 3 contains details of the methodology employed in this study, which includes the description, assessment and reliability of observed rainfall and flow data of the selected stations, the determination of physical catchment parameters, the derivation of flow duration curves at gauged sites and the regionalization of flow duration characteristics, using multiple regression techniques and hydro-potential determination for SHPs. The results obtained from the application of the method in the Inkomati River Catchment are presented in Chapter 4. The discussion, conclusions drawn from the results and recommendations for future studies are detailed in Chapter 5. Finally, the references used and the appendices are presented in Chapters 6 and 7, respectively.

## 2. SMALL HYDRO-ELECTRIC POWER PLANTS

This chapter defines Small Hydropower Plants (SHPs), classifies hydropower plants, highlights the factors that need to be considered for the installation of small hydro plants and describes the concept of estimating power potential using the Flow Duration Curve approach.

### 2.1 Definition of Small Hydropower Plants

Small Hydropower Plants are defined as a development of hydroelectric power on a small scale to serve small communities or industries, mainly in the rural areas. This kind of project varies according to the generating capacity of up to 10 megawatts (MW), which is accepted as the upper limit. (Paish, 2002) and (Yüksel, 2007) defined an SHP as a ‘run-of-river’ or a small dam installation, which uses the flow of water within a natural river. Small hydropower plants depend on a suitable flow available in the river and an adequate head of water (Balat, 2006; Dudhani *et al.*, 2006; Aslan *et al.*, 2008). Head and flow are used to determine the magnitude of the power that can potentially be produced at the selected site. Head can be expressed in the form of gross head and net head. Gross head is the difference between headwater and tail-water elevation. The calculation of the elevation of head-water and tail-water can be obtained by surveying the area. The variation of the elevation must be observed throughout the year. Net head (rated head, effective head and design head) is considered as gross head minus losses in the water passage entrances, the penstocks and valves, down to the turbine. When the flow is known, the losses can be estimated. Hydropower plants are generally described as Low Head, when the head is between 2-30 m, Medium Head, when the range is between 30-100 m and High Head, when the head is greater than 100 m and not greater than 305 m. Mountainous catchments with significant hydraulic heads are usually considered for the development of small hydropower plants (Niadas, 2005).

Small hydropower plants are one of the most cost-effective and environmentally-benign energy technologies that can be considered for the electrification of rural communities in less-developed countries (Paish, 2002; Kaldellis, 2007). This kind of technology can be extremely

robust and can work for long periods, with minimal maintenance requirements (Paish, 2002; Bakis and Demirbas, 2004).

The use of the hydropower resources in small catchments in the region, combined with the minimization of the environmental impacts by SHPs, not only fulfills the energy demand of the small communities of the regions, but is also viable economically through job creation, revenue generation and by supporting sustainable development (Blanco *et al.*, 2008). Small hydropower plants are especially important in poor rural communities which lack the resources, because they are the most basic, self-sustaining and least-cost methods of power generation (Blanco *et al.*, 2008).

Figure 2.1 shows an example of the layout of a small hydropower plant. Water is diverted from the river by a weir, which is constructed across it. The water then passes through to the forebay tank, where it can be filtered, and then descends to the turbine, where the power is generated by the rotating turbines (Paish, 2002).

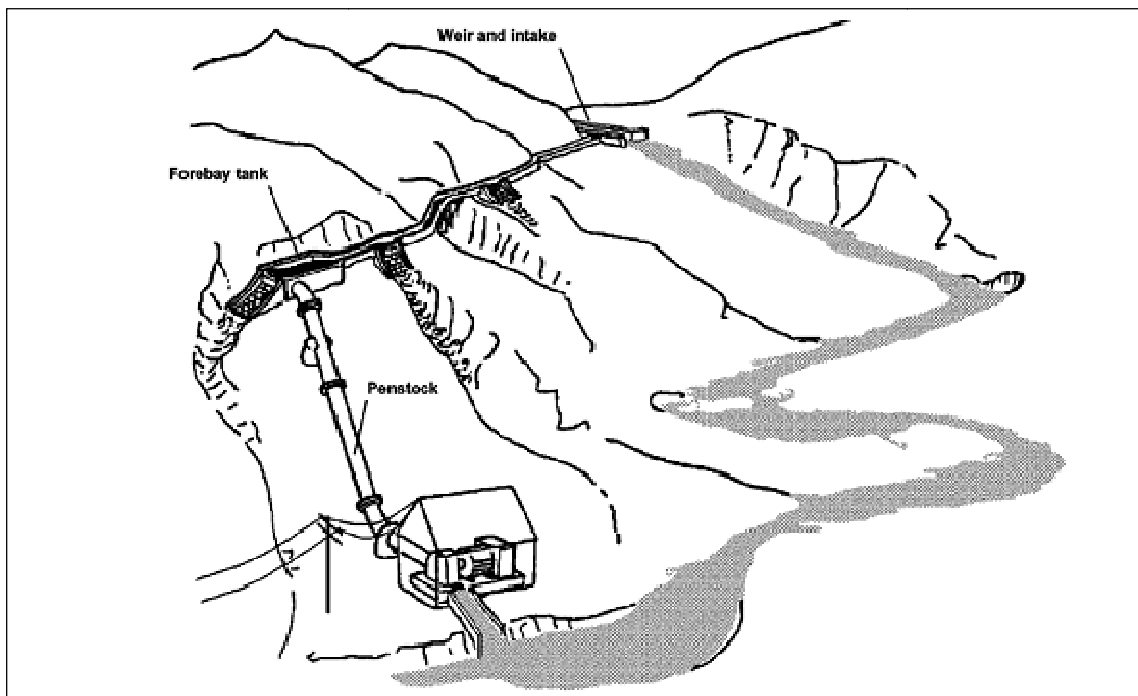


Figure 2. 1 Layout of small hydropower plant, (Paish, 2002)

## 2.2 Classification of Hydropower Plants

There is no standard or clear consensus regarding the classification ranges of hydropower plants (Ballance *et al.*, 2000; Paish, 2002). According to the European classification, hydropower plants can be categorized into large-scale, mini- or micro- and small hydropower plants. Hydropower plants can be classified into categories, as shown in Table 2.1 (Balat, 2006; Ramachandra and Shruthi, 2007). Small hydropower plants were chosen to be the focus of this study.

Table 2. 1 Classification of hydropower plants (Balat, 2006)

Size Class	Range
Micro	< 100 kW
Mini	100 – 500 kW
Small	500 kW – 50 MW
Large	> 50 MW

In addition to the scale of development, there are different philosophies behind large and small hydropower plants. Small hydropower plants are generally dependent on instantaneous streamflow, are susceptible to variations in flow and designed to be connected with smaller grids (Ballance *et al.*, 2000; Blanco *et al.*, 2008). The determination of flow is more difficult because it involves a hydrological study of the stream or source of water to be used in producing power and it is needed to estimate how the flow varies with time. Flow in hydropower studies can be characterized by Flow Duration Curves (FDCs) and the flow hydrographs.

## 2.3 Factors that need to be considered for the Installation of SHPs

A small hydropower plant can be developed by the simple design of turbines, generators and civil works, as shown in Figure 2.2 (Dudhani *et al.*, 2006).

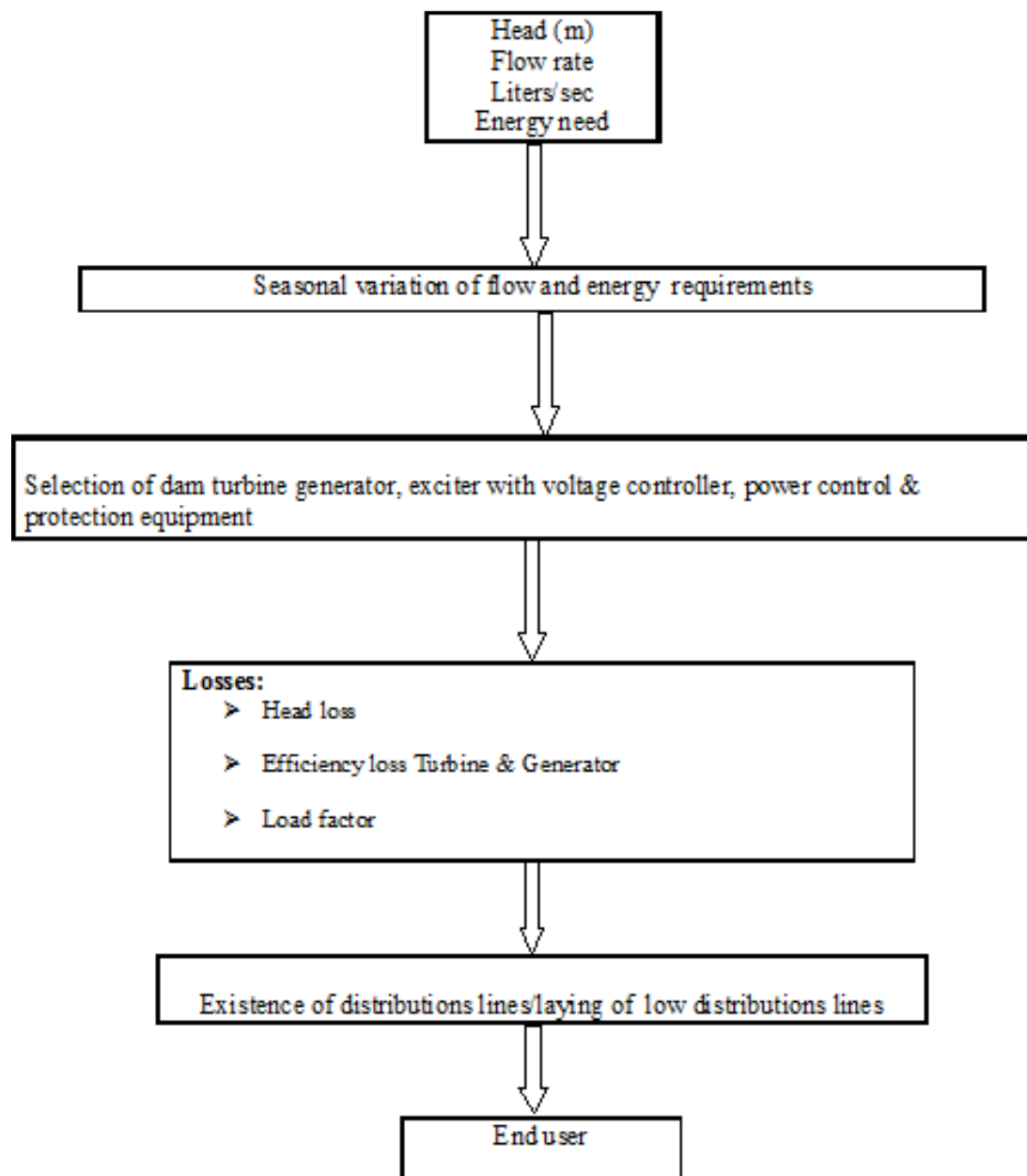


Figure 2.2 Planning for small hydropower plants (Dudhani *et al.*, 2006)

Yüksel (2007) suggests that the principal requirements that should be considered when developing small hydropower plants are:

- suitable rainfall and runoff in the catchment area,
- adequate hydraulic head of water across the turbine,

- a means of transporting water from the intake to the turbine, where the energy can be generated,
- a turbine housing structure containing the power generation equipment and valve gear, and
- a tailrace, to return the water to the natural water course.

In addition, legislative and administrative issues must be considered in order to mobilize and accelerate the development of SHPs (Tsoutsos *et al.*, 2007). The following requirements also need to be considered when developing small hydropower plants (Kaldellis, 2007) including:

- environmental issues, for example, ecological needs,
- the location of the proposed installation and the legal rights to the water resources,
- installation safety, and
- the integrity of documents required by legislation.

The installation of hydropower plants has advantages as well as disadvantages. Some of the advantages of SHPs (Tsoutsos *et al.*, 2007) are:

- They are a more concentrated energy resource, compared to wind and solar power,
- the energy available is readily predictable,
- power is usually continuously available on demand,
- no fuel is required,
- they are durable,
- do not lead to adverse environmental impacts,
- have low operating and maintenance costs, and
- most importantly, they improve living conditions.

The disadvantages include (Yüksek and Kaygusuz, 2006):

- modifications to the hydrological regimes that may have negative impacts on the environment,
- high investment requirements,
- dependency on runoff,

- local land use modification, and
- requirement for good management of competing water uses and water quality.

## **2.4 Method for Estimating Power Potential**

Of the several methods that can be used to estimate the potential power from hydropower plants, two primary methods have been widely used. The first method is the non-sequential or Flow Duration Curve (FDC) and the second method is Sequential Streamflow Routing (SSR) (Karamouz *et al.*, 1991). The FDC is generally selected for high-head, run-of-river projects, where the head is generally fixed and, in some cases, for low-head projects, where the head varies with discharge. The SSR method is selected for multipurpose projects and is more appropriate for examining the feasibility of power at constructed water conservation and flood control projects (Karamouz *et al.*, 1991; Bekoe *et al.*, 2012; Younis and Hasan, 2014). This review focuses on the FDC method.

### **2.4.1 Flow duration curve method**

A FDC is defined as the relationship between discharge ( $Q$ ) and the percentage of time during the period analyzed, in which the particular flow is equalled or exceeded ( $D$ ) (Mimikou and Kaemaki, 1985a; Vogel and Fennessey, 1994; Castellarin *et al.*, 2004; Niadas, 2005; Rojanamon *et al.*, 2007).

FDCs are used for many water resources development and management purposes, including the installation of small hydropower plants (Yu *et al.*, 2002; Castellarin *et al.*, 2007). A FDC is described as a simple cumulative function of daily, weekly and monthly streamflow (Fennessey and Vogel, 1990; Vogel and Fennessey, 1994; Vogel and Fennessey, 1995). FDCs show the relationship between the time excess probability and the discharge corresponding to the probability (Kim, 2004). Streamflow data is used to derive a FDC, which determines the design flow for hydroelectric power plants (Blanco, 2008). FDCs are useful graphical and analytical tools for illustrating and evaluating the relationships between the magnitude and frequency of

streamflow (Vogel and Fennessey, 1995). A typical flow duration curve is illustrated in Figure 2.3.

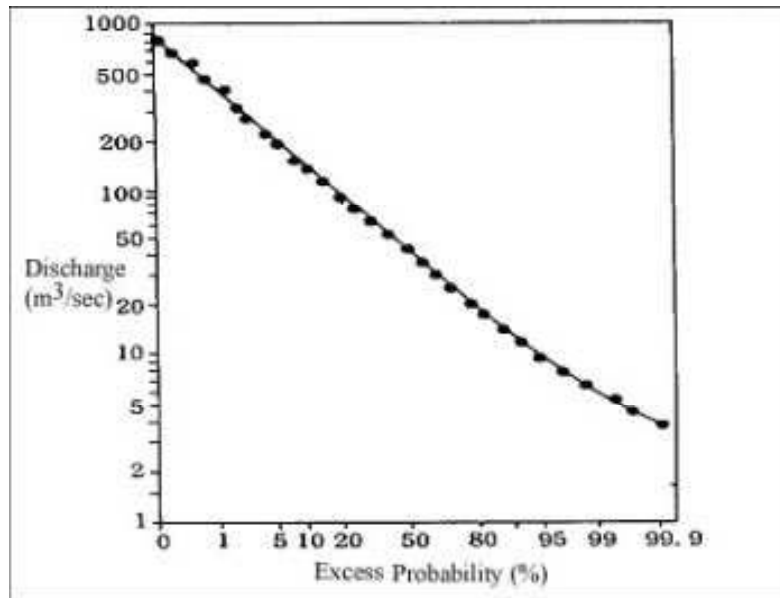


Figure 2.3 Typical Flow Duration Curve (Karamouz *et al.*, 1991)

#### 2.4.2 Flow duration curves in hydropower applications

FDCs can be applied to a wide variety of water resource problems, such as hydropower planning, water quality management and flood frequency analysis (Vogel and Fennessey, 1994). In the context of hydropower estimation, FDCs are applied in hydropower feasibility studies for run-of-the river operations (Vogel and Fennessey, 1995; Nobert *et al.*, 2011). The FDC method is a suitable method for preliminary or screening studies (Karamouz *et al.*, 1991). One of the requirements for developing a FDC is a sufficient period of record (Vogel and Fennessey, 1995; Nobert *et al.*, 2011). In this method, streamflow values are related to their corresponding exceedance percentage values, which show the percentage of time that different levels of stream flows are exceeded. FDCs are developed by ranking all daily flow data according to discharge, but not in the sequence in which they occurred. It means that streamflow data can be organized in a descending order of magnitude (Karamouz *et al.*, 1991).

In order to plot the FDC for a given river, it is necessary to analyze the streamflow data at gauged sites for a sufficient period of recorded data. The data is ranked according to the probability of exceedance. The probability of exceedance ( $Pe_i$ ) is estimated using Equation 2.1 (Karamouz *et al.*, 1991; Castellarin *et al.*, 2004):

$$Pe_i = \frac{i}{N+1} 100 \quad \text{Equation (2.1)}$$

where

- $Pe_i$  = probability that a given flow will be equalled or exceeded (% of time),
- $i$  = rank in descending order position on the listing (dimensionless), and
- $N$  = number of events for period of record (dimensionless).

In order to determine the power potential at a given site, under conditions where monthly data are available, the available head at the site, plant efficiency and turbine discharge must be known. According to Karamouz *et al.* (Karamouz *et al.*, 1991), the firm power is estimated using Equation 2.2:

$$P = e \cdot \gamma \cdot Q \cdot H \quad \text{Equation (2.2)}$$

where

- $P$  = potential power (W),
- $H$  = gross head (m),
- $Q$  = discharge through turbine ( $\text{m}^3 \cdot \text{s}^{-1}$ ),
- $e$  = overall plant efficiency (%), and
- $\gamma$  = specific weight of water, ( $9.8 \text{ N} \cdot \text{m}^{-3}$ ).

Flow duration curves can be converted to power duration curves, using the power equation. The equation for the conversion of a flow duration curve to a power duration curve is described in Equation 2.3 (Karamouz *et al.*, 1991; Ramachandra and Shruthi, 2007):

$$P_i = \frac{e_i \cdot \gamma \cdot Q_i \cdot H_i}{1000} \quad \text{Equation (2.3)}$$

where

- $P_i$  = power production at exceedance percentage  $i$  (kW),
- $Q_i$  = turbine discharge at percentage exceedance  $i$  (%),
- $H_i$  = net head available with river flow at exceedance percentage  $i$  (m),
- $e_i$  = overall plant efficiency with turbine discharge equal to  $Q_i$  (%), and
- $\gamma$  = specific weight of water (9.8 N.m<sup>-3</sup>)

The application of the Equation 2.3 can be from the plant intake, through the penstock, turbine intake, turbine, draft tube and tail water. Generally, the relationship between the turbine efficiency, discharge and water head are provided by the manufacturer (Vogel and Fennessey, 1995).

The power generation for each calendar month can be estimated, using Equation 2.3 and streamflow data, as illustrated in Figure 2.4. From the power duration curve, maximum power that can be generated and consequently the firm energy for a given level of reliability (e.g. 90%), can be determined.

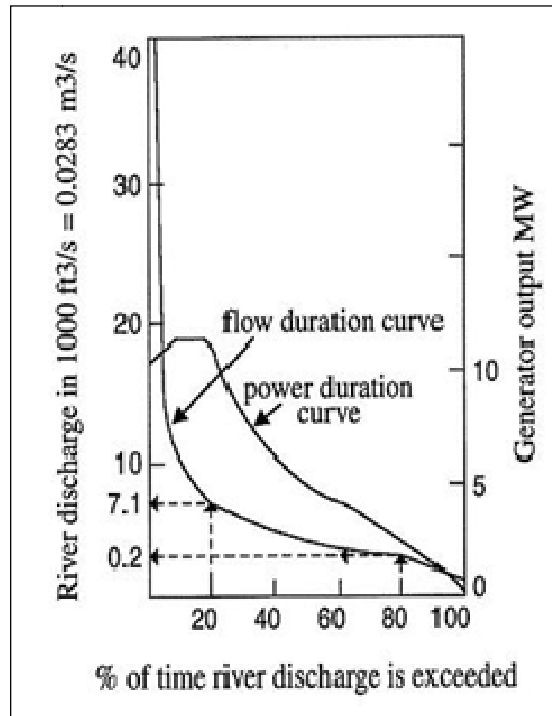


Figure 2. 4 Illustration of flow duration and power duration curves (Karamouz *et al.*, 1991)

### 2.4.3 Regionalization of flow duration curves

In most cases, potential sites for SHPs are ungauged, therefore regionalisation is necessary to estimate the required hydrological information at the ungauged site from a limited number of available streamflow gauging stations (Castellarin *et al.*, 2004). Regionalisation methods are still a challenge and several methods have been developed to predict at ungauged sites. In general, the regionalisation techniques can provide a mechanism to estimate the hydrological regime at ungauged sites. Regionalisation techniques are classified in the following categories: spatial proximity, flow duration curves, regression and physical similarity (Nobert *et al.*, 2011; Archfield *et al.*, 2013; Shoaib *et al.*, 2013).

The regionalisation of FDCs can be developed, using parametric and graphical approaches (Castellarin *et al.*, 2004; Kim, 2004; Castellarin *et al.*, 2007; Patel, 2007; Mohamoud, 2008).

The parametric methods use a parametric representation of FDCs and can be used in the estimation of FDCs at ungauged sites and the regional relationships can also obtain through different methods, such as multiple regression models, kriging, etc (Cheng *et al.*, 2012). The parametric approach can be further divided in two categories, *i.e.* statistical and analytical methods.

The statistical approach requires extensive catchment, climate and soils information. The statistical methods have a probabilistic approach to FDCs and are characterized by viewing of the FDC as the complement of the cumulative frequency distribution. The common steps for the application of this approach are the following:

- a suitable frequency distribution can be chosen for a particular region and the parameters of the distribution can be estimated from the gauged streamflow observations in the study area, and
- regional regression models can be identified to predict the parameters of the distribution at ungauged sites using the geo-morphological and climatic characteristics of the catchments (Fennessey and Vogel, 1990; Castellarin *et al.*, 2004; Kim, 2004; Castellarin *et al.*, 2007).

Analytical methods can be divided into two different groups, namely:

- the first procedure includes the representation of FDCs by analytical relationships for ungauged river catchments estimated through regional models, and
- the second procedure includes a regional procedure that uses standardized graphical representations of FDCs (Mimikou and Kaemaki, 1985a; Franchini and Suppo, 1996; Castellarin *et al.*, 2004; Kim, 2004).

The graphical approach is based on the following steps:

- Firstly, it is necessary to standardize the flow duration curves for all gauged river basins through the division by the mean or median discharge.
- Secondly, through an average of the standardized FDC in different sites, the graphical regional flow duration curve is estimated, and

- Finally, the FDC for a particular basin can be estimated using the mean or median discharge in the gauged stations with the dimensionless FDC (Smakhtin *et al.*, 1997; Ganora *et al.*, 2009)

Overall, the main objective of regionalization is to estimate FDCs at ungauged river catchments (Castellarin *et al.*, 2004; Castellarin *et al.*, 2007) . Gauged data are used to estimate the regional FDC, where there is a limited amount of hydrological information (Yu *et al.*, 2002). Regionalization techniques can also be applied to selected catchments, to compute daily flow time series for a selected period (Smakhtin and Toulouse, 1998; Kim, 2004). The sites can be assumed to be ungauged for the purpose of comparison between observed data and simulated time series (Kim, 2004).

This chapter addressed a detailed review of the concept of Small Hydropower Plants and their classification according to the class size and range. Some of the factors that need to be considered for the development of SHPs were highlighted. The review also defined and described the FDC method and its application in hydropower plants. The next chapter of this document describes the methodology used in this research and includes detailed information about the gauged and ungauged sites, statistical analyses and the regional model.

### **3. METHODOLOGY**

This chapter contains a description of the hydrometric and meteorological stations located in the Inkomati River Catchment, which is the focus area for this study. This is followed by the presentation of observed flow and rainfall data for all selected stations. The third part presents the estimation of physical catchment parameters, which are calculated by using available spatial data processed through a Geographic Information System (GIS). The FDCs are calibrated using the gauged data and then regionalized regressions are developed to estimate the parameters of the FDCs at ungauged sites using Multiple Regressions Techniques. Finally, the hydro-potential for Small Hydropower Plants is determined using the power equation.

#### **3.1 Description of the Study Area**

The Inkomati River Catchment is a trans-national catchment shared by Mozambique, Swaziland and South Africa. This catchment has an area of approximately 46,700 km<sup>2</sup> in total, with 28,600 km<sup>2</sup> in South Africa, 2,500 km<sup>2</sup> in Swaziland and 15,600 km<sup>2</sup> in Mozambique (Taucala, 2007). The layout of the Inkomati River Catchment is shown in Figure 3.1.

On the Mozambican side, this study was conducted, using data in the Inkomati River Catchment, ranging from Ressano Garcia in the western region bordering on South Africa to the Marracuene District in the east (Indian Ocean). The catchment is situated between the Limpopo River to the north and the Umbeluzi, Matola and Infulene Rivers to the south and is characterized by coastal dunes in the east. The river mouth is approximately 20 km from Maputo City (NDW, 1991; JIBS, 2001; Vaz and Van der Zaag, 2003). Data from flow gauging stations in both Mozambique and South African side have been utilized in this study.

The Inkomati River Catchment rises in the Drakensberg mountains and plateau with elevations above 2000 m in the west of the catchment and drops to the homogeneous flat plain to the east of the Libombo Mountains at an elevation of generally below 150 m. Five rivers originate in the plateau area, namely the Komati, Crocodile, Sabie, Massintonto and Uanetze Rivers. The Komati and Crocodile Rivers are the two main branches in the upper river catchment. The

confluence of the Komati and Crocodile Rivers is upstream of the Mozambican border, where the river is called the Inkomati (Consultec and BKS, 2001).

The Crocodile River is the larger tributary in the South African part of the catchment. It gathers additional flows from the Elands and Kaap Rivers. In addition, a significant tributary to the Inkomati River Catchment is the Mlumati River.

The Sabie, Massintonto and Uanetze Rivers are important tributaries to the Inkomati and all of them rise in South Africa and flow through the Kruger National Park, before crossing the border to their confluences with the Inkomati River in Mozambique. The Mazimechopes River has its sub-catchments in Mozambique, draining the northern extremes of the Inkomati River Catchment, mainly downstream of the Magude District (NDW, 1991; JIBS, 2001; Vaz and Van der Zaag, 2003).

The altitude of the Inkomati Catchment varies between 0 and 2700 m, and close to the border between South Africa and Mozambique the highest altitudes do not exceed 750 m (Consultec and BKS, 2001).



The climate in the catchment is characterized by two different seasons. The hot and rainy season (summer) is from October to March. High precipitation occurs mainly in December and March. The cool and dry season (winter) lasts (six) months (from April to September), with little to no precipitation recorded during that season (Consultec and BKS, 2001).

The mean annual precipitation in the Mozambican part of the Catchment varies from 1073 mm along the coast to 509 mm along/near the South African border in the west. The average annual precipitation is approximately 650 mm on the Mozambique side, while it reaches 740 mm in the South African side. The mean annual potential evaporation in the Catchment is 1900 mm (NDW, 1991; JIBS, 2001; Vaz and Van der Zaag, 2003).

The mean annual temperature ranges between 22°C and 24°C on the Mozambican side and between 14°C to 22°C on the South African side. Maximum temperatures are observed in December and January and the minimum temperatures usually occur from June to July.

### **3.1.1 Description of hydrometric and meteorological stations**

The observed daily rainfall and flow data from twelve rain gauges and eleven hydrometric stations from National Institute of Meteorology and Directorate of Water Resources in Mozambique were collected, with each data set having a different period of record. From the information on the website of the Department of Water Affairs in South Africa, it was possible to identify thirteen gauged stations which were considered in the study. Consistent procedures were adopted as a means of checking the quality of the data. Some characteristics of the stations in the catchment are summarised in Tables 3.1, 3.2 and 3.3.

Table 3. 1 Characteristics of the raingauges stations in Mozambique

Name of Station	Latitude	Longitude	Period	Record length (years)	Elevation (m)
R. Garcia	25°26' S	31°59' E	May1956 – Jul 1983	27	130
Moamba	25°36' S	32°14' E	Jan 1951 – Dec 1983	32	110
Sabie	25°19' S	32°14' E	Jan1951 – Dec 1983	32	80
Magude	25°02' S	32°39' E	Aug 1915 – Sep 1941	26	18
Chobela	25°00' S	32°44' E	Jan 1951 – Dec 2004	53	15
Macia	25°02' S	33°06' E	Jan 1951 – Mar 2009	58	56
Manhiça	25°22' S	32°48' E	Jan 1951 – Oct 2007	56	35
M.Maragra	25°27' S	32°48' E	Mar 1970 – May 1996	26	100
Bobole	25°37' S	32°40' E	Jan 1974 – Dec 1974	1	66
Marracuene	25°44' S	32°41' E	Jan 1951 – Jul 2007	56	26
Praia do Bilene	25°17' S	33°15' E	Sep 1958 – Jan 2005	47	20
Mapulanguene	24°29' S	32°05' E	Sep 1971 – May 1981	10	418

Table 3. 2 Characteristics of the flow gauging stations in Mozambique

Name of Station	Latitude	Longitude	Period	Catchment Area (km <sup>2</sup> )	Record length (years)
Moamba E-22	25°34'30"S	32°15'06"E	June 1954 – Jan 2009	21850	28
R.Garcia E-23	25°26'05"S	31°59'37"E	Jan 1949 – Feb 2009	21200	53
R.Garcia E-24	25°26'14"S	31°59'35"E	Oct 1987 – Jul 1999	-	-
Machatuine E-26	25°19'18"S	32°15'18"E	Oct 1997 – May 2008	-	-
Chinhanguanine E-27	25°17'00"S	30°30'29"E	Dec 1983 – Dec 2006	31037	19
Bobole E-29	25°36'46"S	32°40'20"E	Oct 2001 – Sep 2006	72	-
Magude E-43	25°01'47"S	32°39'01"E	Apr 1955 – May 2008	37500	47
Chobela E-44	25°01'05"S	32°45'03"E	Dec 1957 –May 2005	37600	46
Incoluane E-45	25°04'42"S	32°53'27"E	Feb 1957 – Sep 1974	42942	19
M.Major E-396	25°33'16"S	32°11'55"E	Oct 2008 – Dec 2008	-	-
Sabie E-413	25°18'58"S	32°17'29"E	Jan 1999 – Sep 2000	-	-

Table 3. 3 Characteristics of the flow gauging stations in South Africa

<b>Name of Station</b>	<b>Place</b>	<b>Latitude</b>	<b>Longitude</b>	<b>Catchment Area (km<sup>2</sup>)</b>	<b>Period</b>	<b>Record length (years)</b>
X2H008	Queens River	25°47'14"S	30°55'28"E	180	1948-2005	57
X2H010	Noordkaap River	25°36'55"S	30°52'30"E	126	1948-2005	57
X2H012	Dawsonsspruit	25°39'43"S	30°15'38"E	91	1952-2005	53
X2H024	Suidkaap River	25°42'60"S	30°50'06"E	80	1964-2005	41
X2H035	Kruisfonteinspruit	25°11'14"S	30°52'48"E	16	1982-2005	23
X2H047	Suarkoppiesspruit	25°37'05"S	30°24'06"E	110	1985-2005	20
X2H068	Sand River	25°37'05"S	30°53'59"E	64	1969-2005	57
X2H072	Nsikazi River	25°16'25"S	31°15'23"E	240	1989-2002	20
X3H001	Sabie River	25°05'28"S	30°46'41"E	174	1948-2005	57
X3H003	Mac-Mac River	24°59'50"S	30°48'51"E	52	1948-2005	57
X3H007	White Water River	25°09'15"S	31°00'09"E	46	1963-1991	28
X3H011	Marite River	24°53'21"S	31°05'29"E	212	1978-2005	27
X3H020	White Waters River	25°08'42"S	31°01'05"E	62	1973-2005	32

### **3.1.2 Reliability of Mozambican observed flow and rainfall data**

The periods of observed daily streamflow data for the 11 gauging stations in the Inkomati River Catchments in Mozambique are shown in Figure 3.2 and Table 3.2. Most of the stations have been operating since their inception, but many are not operational because of technical problems. Among these gauging stations, six stations have been selected and were considered for this study. The selected gauging stations are Moamba E-22, Ressano Garcia E-23, Chinhanganine E-27, Magude E-43, Chobela E-44 and Incoluane E-45. The gauging stations that have a short record of flow data and large amounts of missing flow were identified from Figure 3.2.

The streamflow data from the Moamba, Ressano Garcia, Chinhanganine, Magude, Chobela and Incoluane gauging stations revealed that most of the stations have high values of streamflow, mainly in 1976 and 2000. Therefore, these values indicate floods in the catchment. In order to obtain a general assessment of the reliability of the observed flow and rainfall data, percentages of missing flow and rainfall data were compared, as shown in Figures 3.4, 3.6, 3.8, 3.10, 3.12 and 3.14, using the selected rainfall stations for the sub-catchment where the gauging stations are located. Based on the period and reliability of the data, stations at Ressano Garcia E-24, Machatuine E-26, Bobole E-29, Moamba Major E-396 and Sabie E-413 were excluded from further analysis.

The plotted daily streamflow data revealed that, in some data sets, gaps or missing data periods make streamflow records shorter than the period of record. In order to minimize this limitation, all observations were used in the analysis despite periods of missing data within the record.

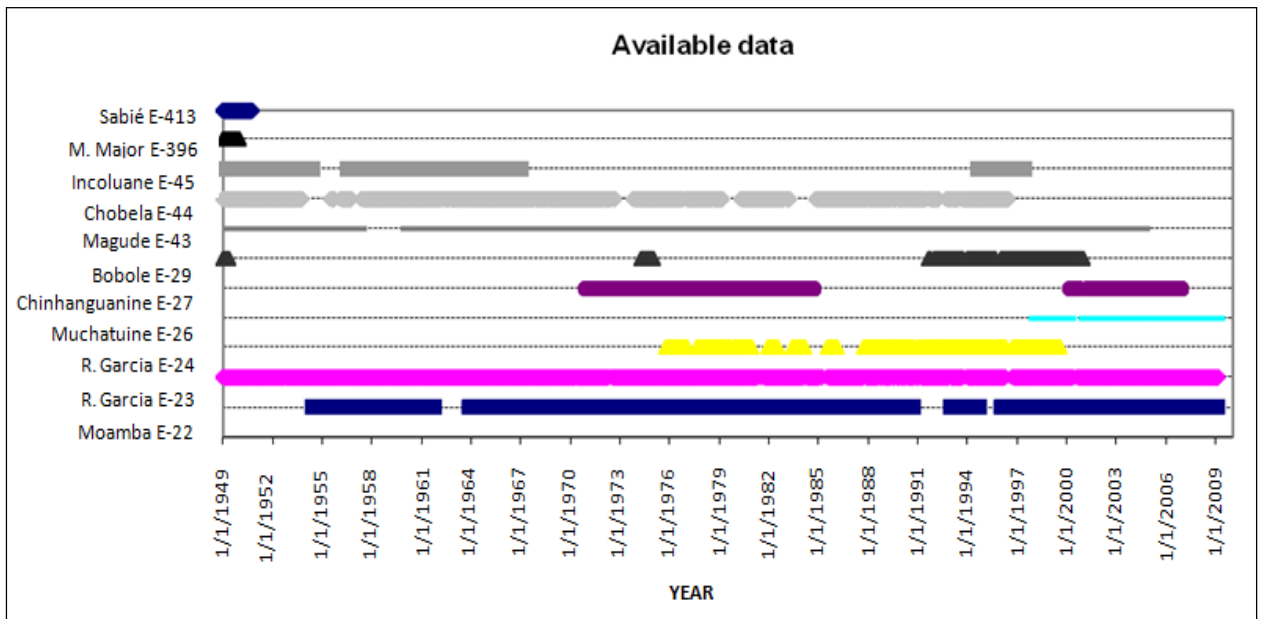


Figure 3. 2 Length of observation periods at gauging stations in the Inkomati River Catchments in Mozambique

### 3.1.2.1 Moamba gauging station

As shown in Figure 3.1, the Moamba (E-22) gauging station is located downstream of the Ressano Garcia E-23 station. Observed daily streamflow data are available from this station for the period June 1954 to December 1984. These periods of available records were linked into a single time series record, representative of the longest period record (June 1954 to September 1961, February 1964 to December 1984 (Copestake and Young, 2008)). The missing flow data amounts to approximately 21.4 % of the entire period and the drainage area is 21850 km<sup>2</sup>. The period of data (June 1954 to September 1961, February 1964 to September 1990, and December 1996 to January 2009) was selected from Figure 3.3 and it was used to generate the FDC. The FDC for the Moamba (E-22) gauging station is shown in Figure 7.1 in Appendix 1.

The Moamba District has a rainfall station, as shown in the Figure 3.1. This station was established in January 1951 and the observed rainfall was available up until December 1983. The rainfall data has some periods of missing rainfall or suspect data, when compared to the records of the surrounding rainfall stations, as shown in Figure 3.4. Missing data and annual rainfall and flows are shown in Figures 3.3 and 3.4. Figure 3.4 illustrates total rainfall from the Moamba, Ressano Garcia and Sabie raingauges, and total flow data from the Moamba gauging station and was used to obtain a general assessment of the reliability of the flow and, rainfall data, and to illustrate the percentages of missing flow and rainfall data. The Moamba gauging station is surrounded by Ressano Garcia and Sabie raingauges upstream and downstream, respectively. The Ressano Garcia and Moamba rainfall stations are located in the same catchment. The altitude of the Moamba rainfall station is approximately 110 meters. Data from the Moamba rainfall station was available from 1951 to 2009. The highest and lowest values of the observed rainfall are 865 mm in 1966 and 3.1 mm in 2005, respectively. Flow data from 1954 to 1984 was used in this study. Periods of missing flow data were from 1961 to 1963 and 1990 to 1996. The highest and lowest values of the observed flow data are 145.1 mm (1981) and 32.6 mm (1970), respectively as shown in Figure 3.4.

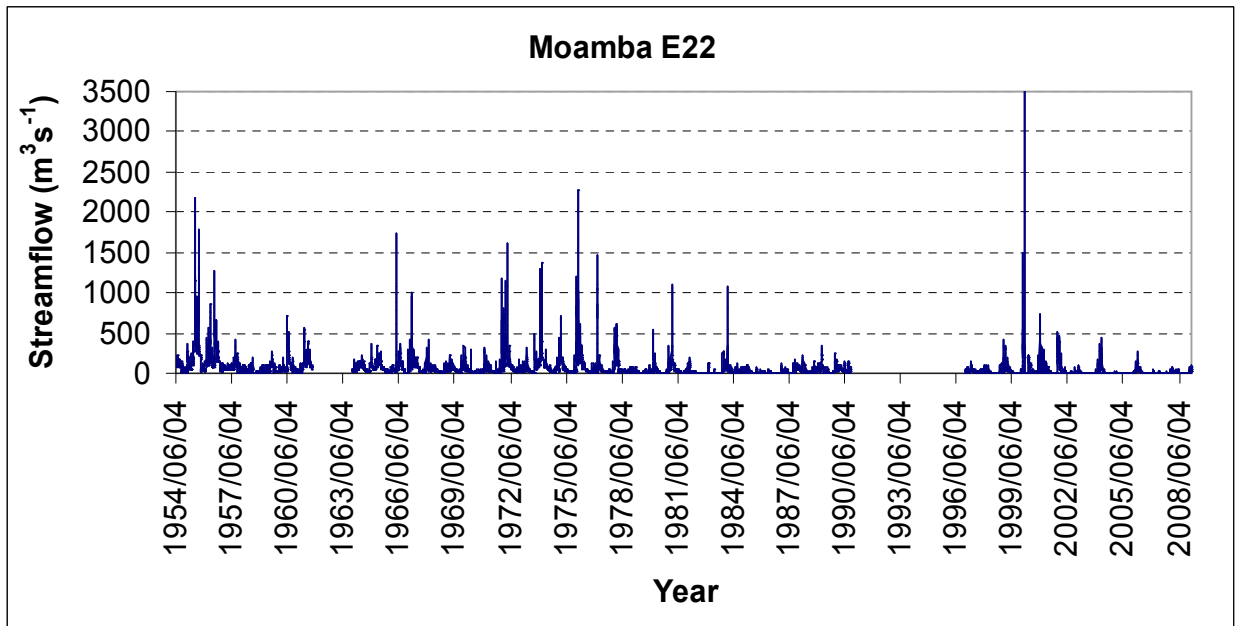


Figure 3.3 Daily average discharge at the Moamba gauging station (E-22)

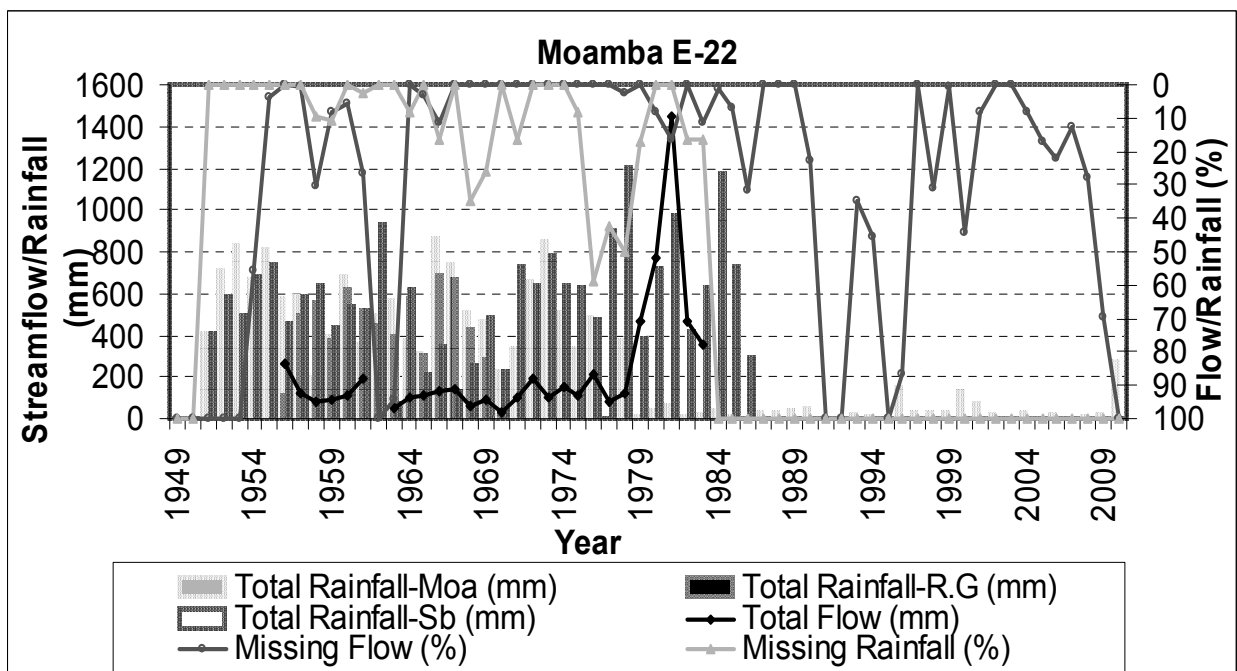


Figure 3.4 Rainfall and flow data of the represented station (E-22)

### 3.1.2.2 Ressano Garcia gauging station

The Ressano Garcia gauging station (E-23) is located downstream of the confluence of the Crocodile and Komati Rivers. Observed daily streamflow data is available from this station for the period January 1949 to February 2009. Suspect flow data (constant at  $1.0 \text{ m}^3 \cdot \text{s}^{-1}$ )

were detected because of repeated flow values, therefore the suspect data was excluded from the original data (January 1949 to September 1952). Approximately 11.3% of the flow data is missing. The time series of the daily flow data used in the analysis was from October 1952 to February 2009. The drainage area is 21200 km<sup>2</sup>. The period of data used in the analysis (October 1952 to February 2009) was selected from Figure 3.5, which was used to generate the FDC. The FDC for the Ressano Garcia (E-22) gauging station is shown in Figure 7.2 in Appendix 1.

The Ressano Garcia rain gauge station has measured daily rainfall data, from its establishment in May 1956 to December 1983. The total annual rainfall was calculated from monthly rainfall data. This station is situated downstream of the Komatipoort border in South Africa and upstream of the Moamba rainfall station on Mozambique side. The Ressano Garcia and Moamba rainfall stations are located in the same catchment. The Ressano Garcia gauging station is located upstream of the Moamba and Sabie raingauges and downstream of the Komatipoort border, respectively. The elevation of the Ressano Garcia rainfall station is approximately 130 meters. For this study data used from 1956 to 1970 was used. The highest and lowest values of rainfall are 687.9 mm (1966) and 28.1 mm (1970), respectively. A period of missing flow data was from 1994 to 2001. The highest and lowest values of flow data are 258.9 mm (1955) and 4.7 mm (2003), respectively (Figure 3.6).

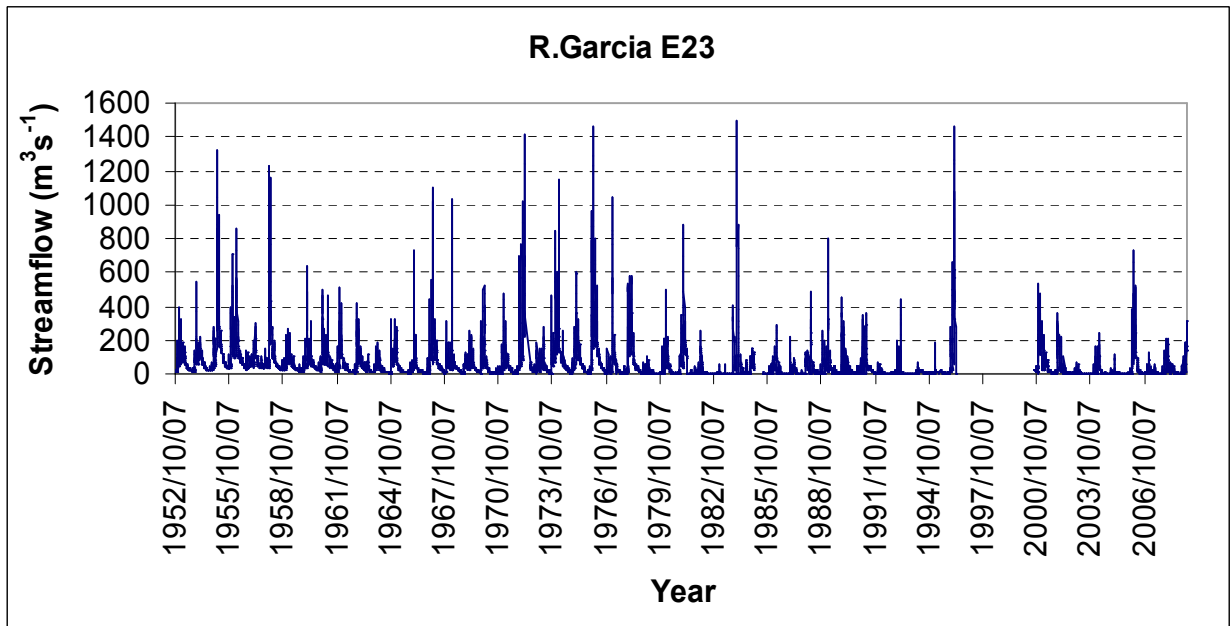


Figure 3. 5 Daily average discharge at R.Garcia gauging station (E-23)

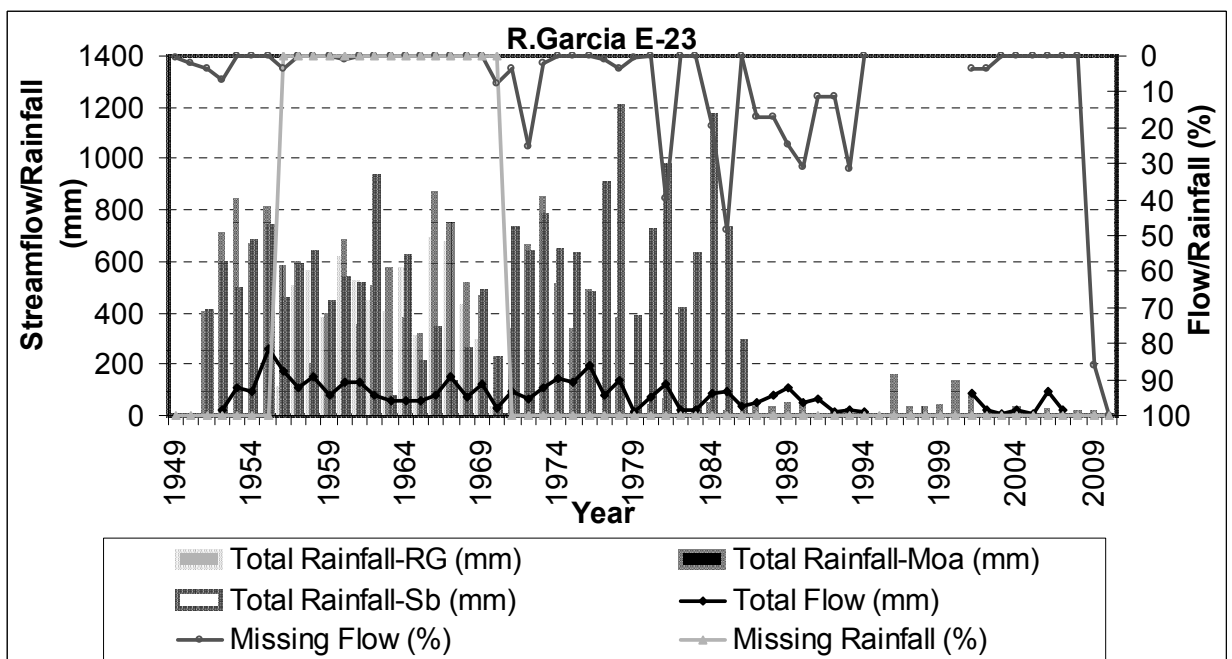


Figure 3. 6 Rainfall and flow data of the represented station (E-23)

### 3.1.2.3 Chinhanganine gauging station

Chinhanganine (E-27) is a gauging station situated downstream of the Moamba gauging station along the Inkomati River Catchment. The area of this catchment is 31073 km<sup>2</sup> and its

flow is gauged downstream of the Magude gauging station. This station has been operating from December 1970 to December 2006, with daily streamflow data available. For this station, flow data is missing from October 1984 up to February 2000. Therefore, the time series (December 1970 to September 1984) was used to estimate the FDC and (March 2000 to December 2006) was not used because the data was unreliable. The missing data amounts to approximately 63.15% of the entire period. The period of data used in the analysis was selected from Figure 3.7 and the data used was up to 1984, which was used to generate the FDC. FDC for the Chinhanguanine (E-27) gauging station is shown in Figure 7.3 in Appendix 1.

At the Chinhanguanine gauging station area, there is no rainfall station with a significant period of record. Hence, the closest rainfall stations used for comparison were the Sabie and Moamba stations (upstream) and the Chobela station (downstream). The elevation of the Sabie rainfall station is 80.0 m and the Moamba rainfall station is 110.0 m. The Moamba, Sabie and Chobela rainfall stations are not located in the same catchment. The Chinhanguanine gauging station is surrounded by Moamba and Sabie raingauges (upstream) and Chobela raingauge (downstream), respectively. The Sabie rainfall station selected for comparison between rainfall and flow data. Flow data from 1970 to 1984 was used in this study. The highest and lowest values of rainfall are 1202.7 mm (1978) and 728.3 mm (1963), respectively. The highest and lowest values of flow data of the Chinhanguanine gauging station are 270.8 mm (1976) and 4.4 mm (1983), respectively (Figure 3.8).

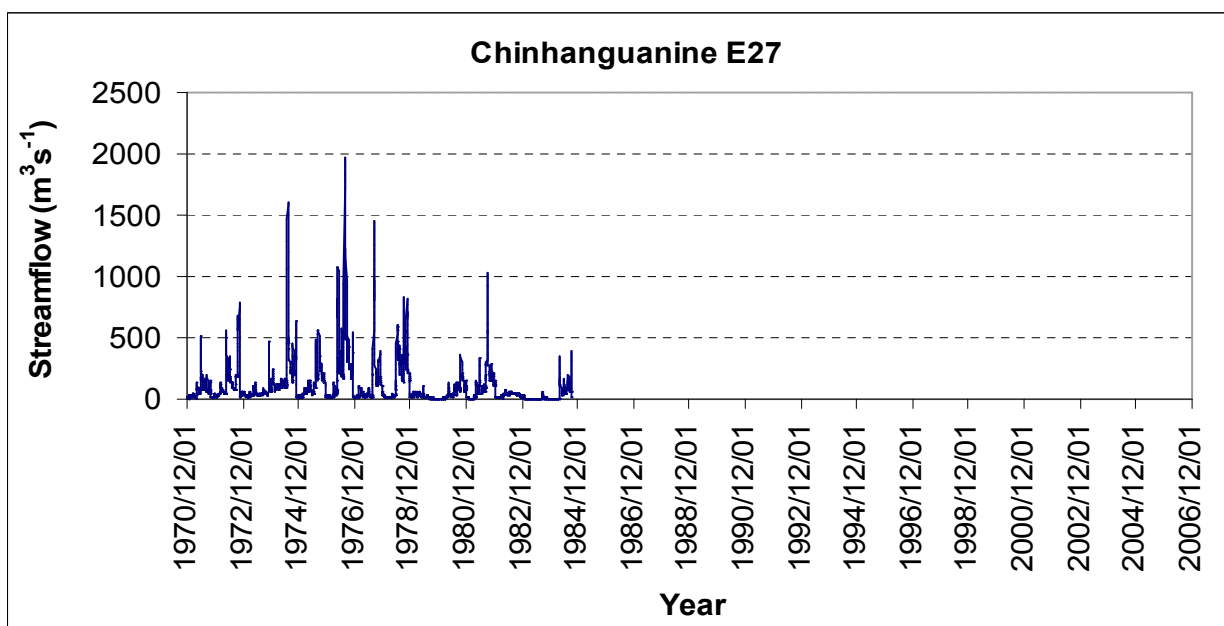


Figure 3.7 Daily average discharge at Chinhanguanine gauging station (E-27)

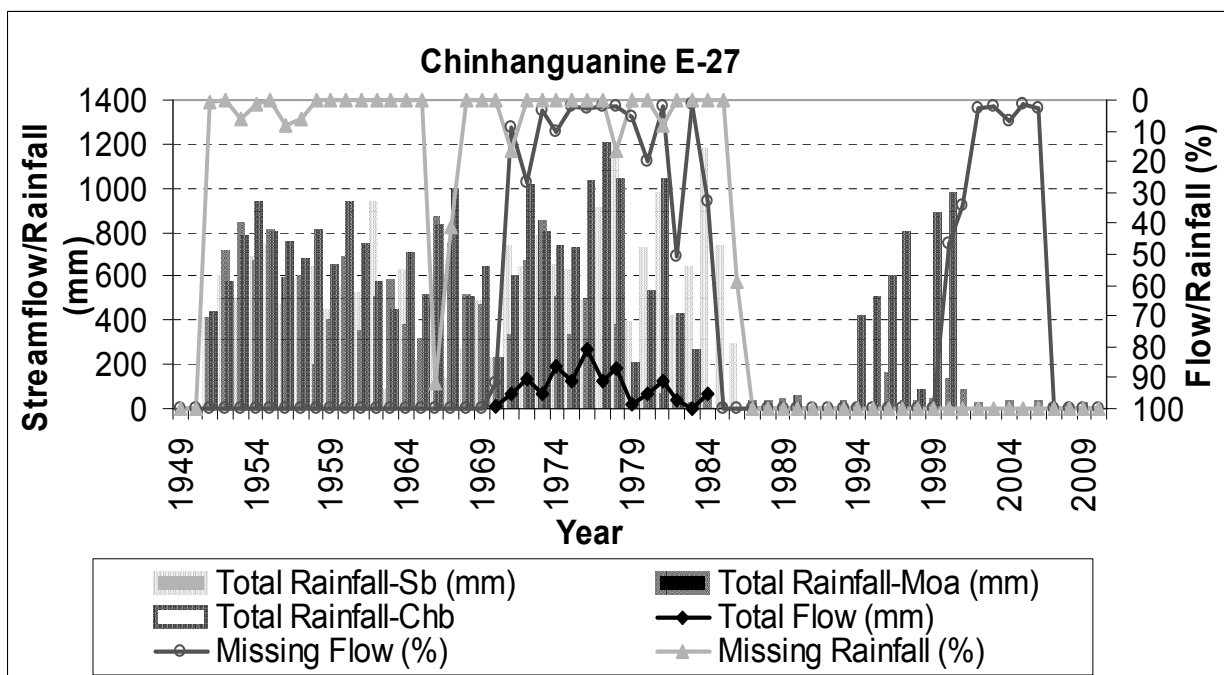


Figure 3.8 Rainfall and flow data of the represented station (E-27)

#### **3.1.2.4 Magude gauging station**

The Magude gauging station (E-43) is located downstream of the Chinhanganine gauging station E-27. Observed daily streamflow data is available from this station for the period November 1952 to May 2008. The drainage area is 37500 km<sup>2</sup>. The record has missing data, which amounts to approximately 16.6% of the observed period. The time series of streamflow data (April 1955 to January 1961, November 1964 to January 1997 and July 1997 to May 2008) were linked, in order to generate the FDC (Copestake and Young, 2008). After 1988, the streamflow seems to be lower, this can be explained by land use, abstractions and flow regulation and it is not caused by rainfall. The quality of the streamflow data at Magude appears to be better compared to other stations. The reasonable time series or period of data was selected from Figure 3.9, which was used to generate the FDC. FDC for the Magude (E43) gauging station is contained in Figure 7.4 in Appendix 1.

The Magude gauging station is situated downstream of the Sabie rainfall station. The Chobela and Macia rainfall stations are located in the same Catchment. Figure 3.10 show that the rainfall and flow data are well-distributed in all surrounding stations, in spite of having some gaps from 1983 up to 1994 at the Chobela raingauge station. The Magude gauging station is surrounded by Sabie raingauge (upstream), Chobela and Macia raingauges (downstream), respectively. The elevation of the rainfall station is approximately 18 meters. In the Magude gauging station area, there is no rainfall station with a significant period of record. Therefore, the Chobela rainfall station was used because it is the closest station, less than ten (10) km from Magude, and this rainfall station was commissioned in 1951. Flow data from 1951 to 2000 was used in this study. The highest and lowest values of the rainfall are 1202.4 mm (1977) and 200.5 mm (1979), respectively. Periods of missing flow data were from 1961 to 1964 and 1991 to 1997. The highest and lowest values of the flow data are 241.5 mm (1955) and 4.3 mm (1982), respectively (Figure 3.10).

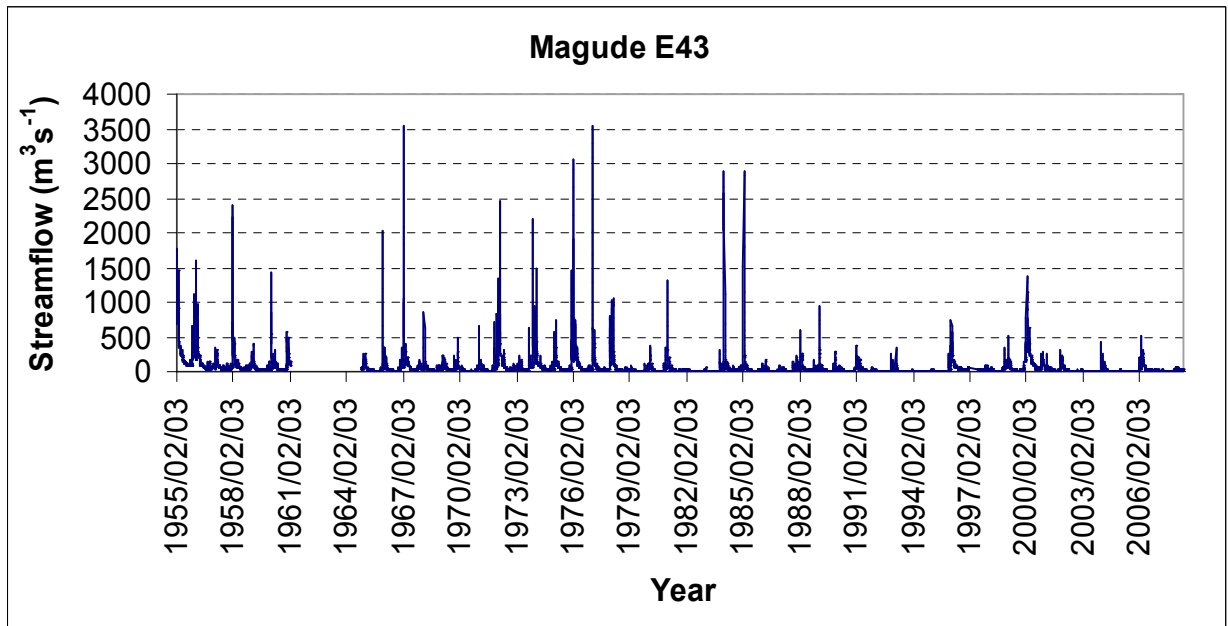


Figure 3. 9 Daily average discharge at Magude gauging station (E-43)

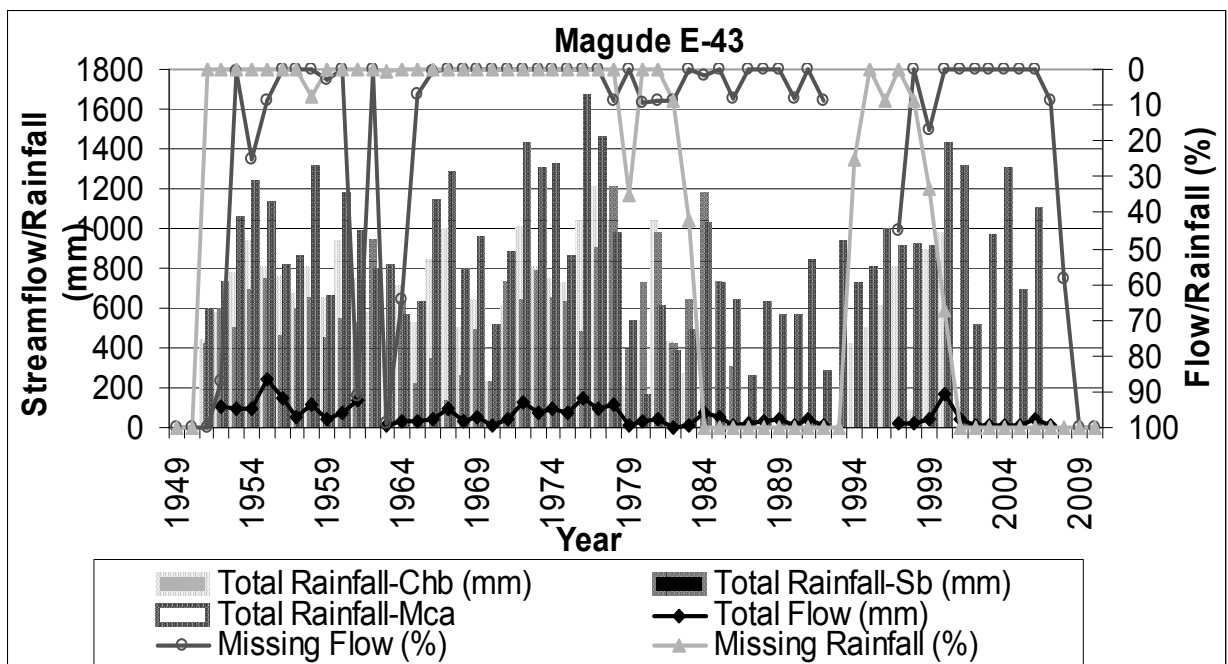


Figure 3. 10 Rainfall and flow data of the represented station (E- 43)

### 3.1.2.5 Chobela gauging station

The Chobela gauging station (E-44) is situated downstream of the Magude gauging station. Observed daily streamflow data is available for this station for the period January 1951 to

May 2005. The drainage area is 37600 km<sup>2</sup>. The linking of short time series in the analysis was applied to this data series (December 1957 to September 1962, January 1968 to August 1981, October 1982 to 1988 and October 1993 to May 2005), (Copestake and Young, 2008). The missing flow data amounts to approximately 28% and the suspect data are relatively few. The period of data used in the analysis was selected from Figure 3.11 and included December 1957 to September 1962, January 1968 to August 1981, October 1982 to 1988 and October 1993 to May 2005, which was used to generate the FDC. The FDC for the Chobela (E-44) gauging station is shown in Figure 7.5 in Appendix 1.

The Chobela rainfall station is located downstream of the Magude rainfall station. The distribution of rainfall data in all three stations seems to be good, since their establishment. The exception is the Chobela rainfall station, which has missing data from 1984 to 1994 (almost 10 years). The Chobela and Macia rainfall stations are located in the same Catchment. The Chobela gauging station is surrounded by Sabie raingauge (upstream), Chobela and Macia raingauges (downstream), respectively. The altitude of the Chobela rainfall stations is approximately 15 meters. In this study, flow data from 1951 to 2000 was used. Periods of missing flow data were from 1960 to 1968 and 1986 to 1993. The highest and lowest values of the rainfall are 1202.4 mm (1977) and 200.5 mm (1979), respectively. The highest and lowest values of the flow data are 396.2 mm (1998) and 18.8 mm (1983), respectively (Figure 3.12).

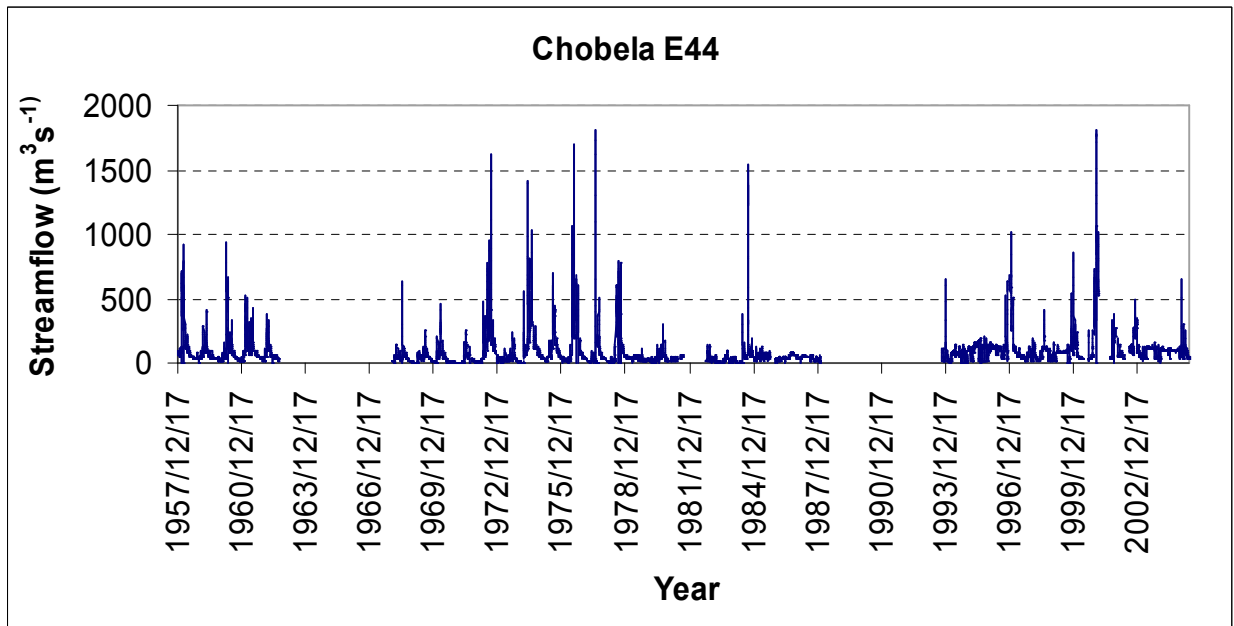


Figure 3. 11 Daily average discharge at Chobela gauging station (E-44)

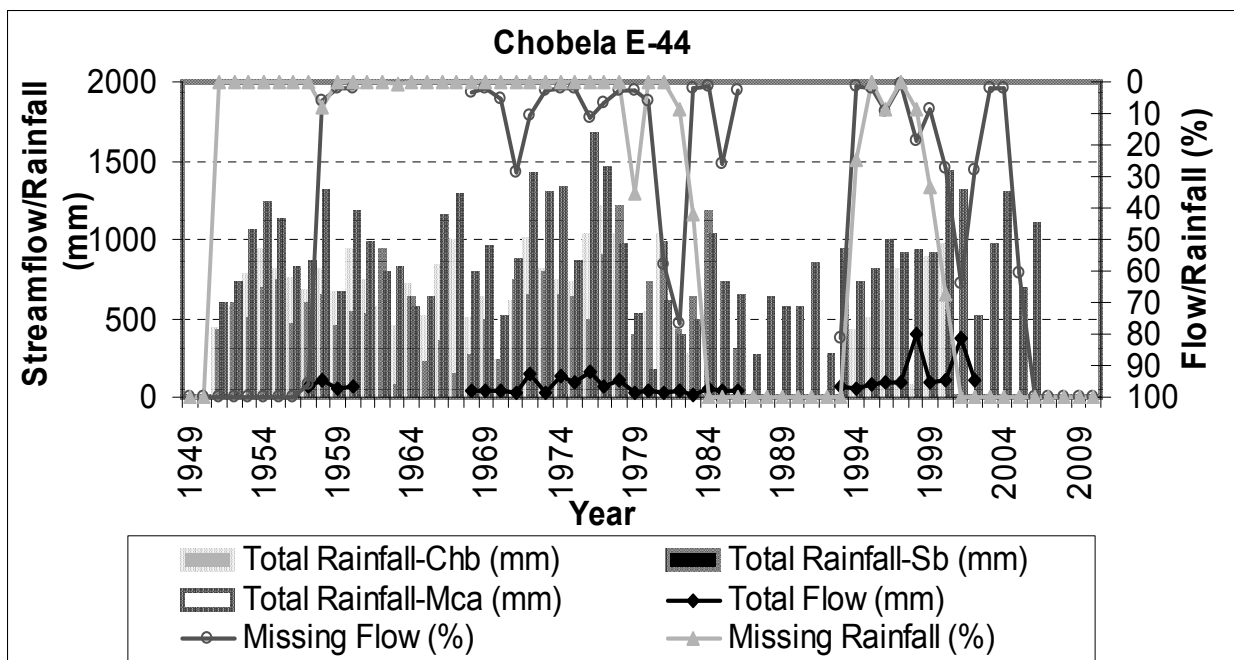


Figure 3. 12 Rainfall and flow data of the represented station (E-44)

### 3.1.2.6 Incoluane gauging station

The Incoluane gauging station (E-45) is located downstream of the Chobela gauging station. Observed daily streamflow data is available from this station for the period January 1956 to

September 1974. The drainage area is 42942 km<sup>2</sup>. The time series were linked to create a long time series from October 1956 to February 1960 and March 1969 to September 1974 (Copestake and Young, 2008). The flow at the Incoluane gauging station is constant from June 1961 to February 1969, indicating suspect data during this period. Missing streamflow data amounts approximately 64.3% of the record. The period of data used in the analysis (October 1956 to February 1960 and March 1969 to September 1974) was selected from Figure 3.13, which was used to generate the FDC. FDCs for the Incoluane (E-45) gauging stations are not shown in Appendix 1 as the streamflow data was not reliable enough to be used for further analysis in this study.

The Chobela and Macia rainfall stations are located upstream of the Incoluane gauging station and they are very close to each other. The distribution of rainfall data in all three stations seems to be good, since their establishment. The exception is the Chobela rainfall station, which showed missing data from 1984 to 1994 (almost 10 years). The Macia and Chobela rainfall stations are located in the same catchment. The Incoluane gauging station is surrounded by Chobela and Macia raingauges (upstream), and Manhica rainauge (downstream), respectively. The elevation of the Macia rainfall stations is approximately 56 meters. The Macia rainfall station was commissioned in 1951. For this study, flow data from 1969 to 1974 was selected. The highest and lowest values of the rainfall are 1664.8 mm (1976) and 155.8 mm (1980), respectively. The Incoluane gauging station was established in 1956. In this study, the data from 1956 to 1974 was selected. However, there are some gaps from 1960 to 1969. The highest and lowest values of the flow data are 277.2 mm (1974) and 44.6 mm (1971), respectively (Figure 3.14).

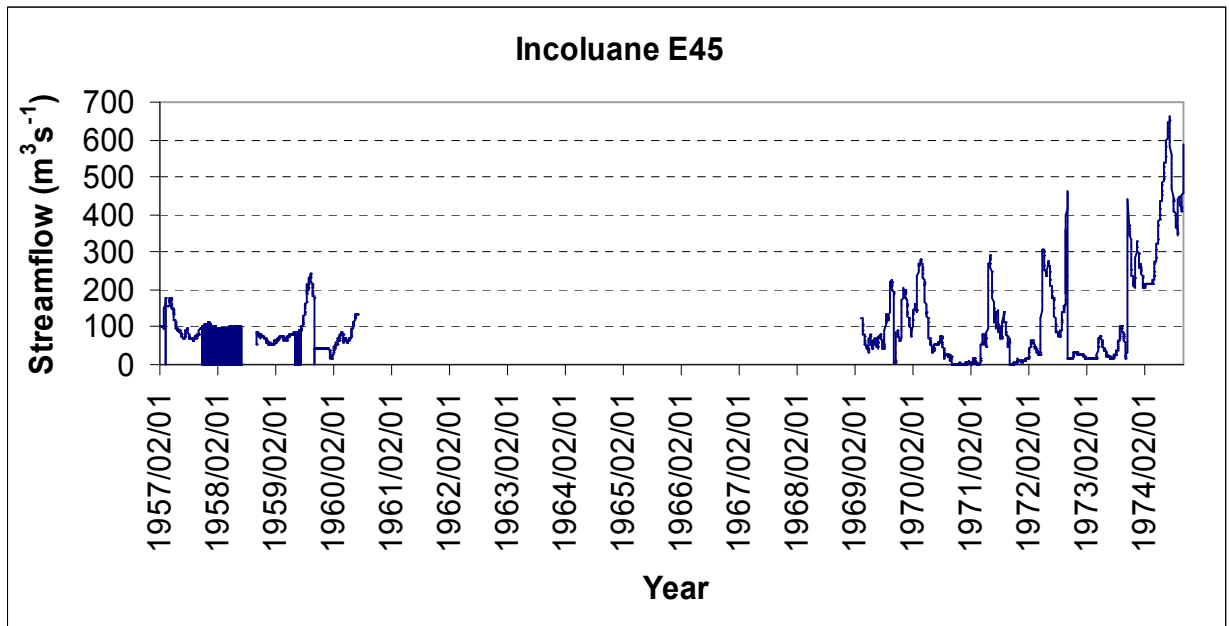


Figure 3. 13 Daily average discharge at Incoluane gauging station (E-45)

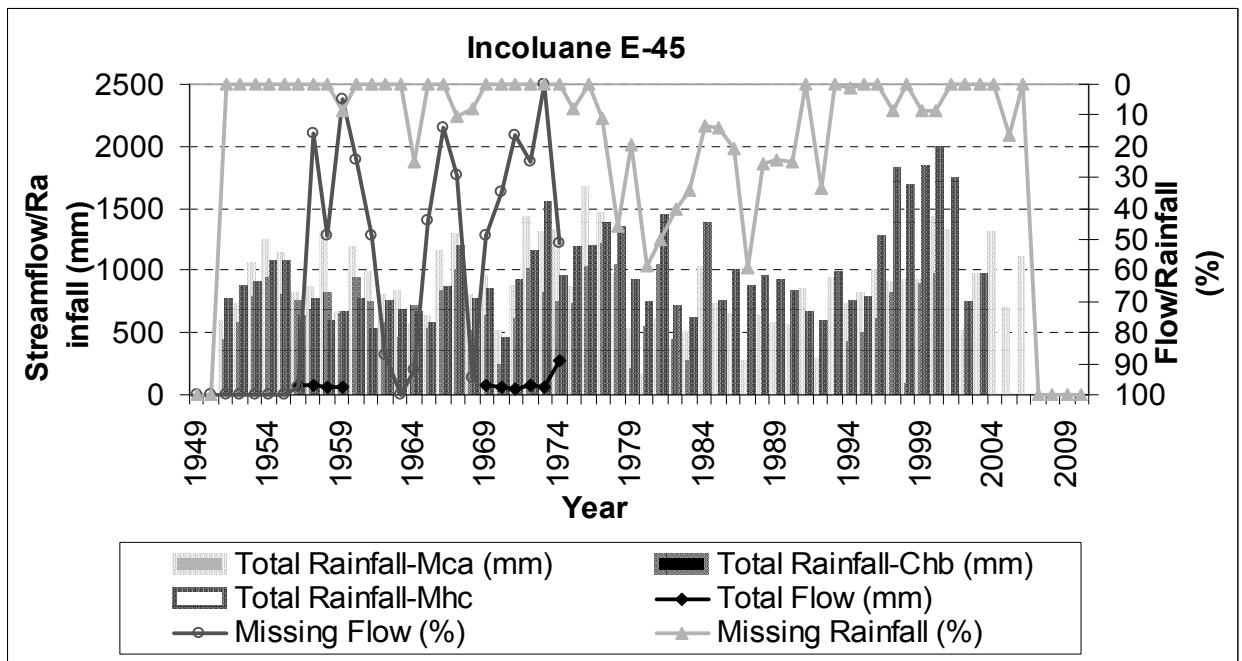


Figure 3. 14 Rainfall and flow data of the represented station (E-45)

The selected gauging and rainfall stations all have more than ten years of the record. The longest record of the flow data was registered in Ressano Garcia (57 years) and followed by Magude (56 years) gauging stations. The station at the highest elevation is the Ressano Garcia with 130 meters and the lowest elevation is 15 meters at Chobela rainfall stations. In terms of topography, the Mozambican part of the Inkomati River Catchment is a floodplain region. The Incoluane gauging station has the largest catchment area with (42 942 km<sup>2</sup>).

In this study, missing rainfall and flow data were the biggest constraint in the analysis of the selected stations. The reason of these missing data in the time-series might have been caused by several reasons, including the temporary absence of observers, the cessation of measurement or absence of observations, poor management of data related to water resources and limited financial resources to carry on with the project.

For most of the data used, there is a good correspondence between rainfall and streamflow, therefore where there are high values of precipitation there is a notable increase of streamflow values. During the dry season, there is significant reduction of streamflow which is exacerbated by the land use, abstractions and flow regulation in Xinavane sugar cane plantation.

Table 3.4 provides a summary of the gauging stations analysis and an assessment of data for each station on the Mozambique side. Ressano Garcia E-24, Machatuine E-26, Bobole E-29, Moamba Major E-396 and Sabie E-413 were excluded from further analysis because the data are not reliable enough to be used in this study.

Table 3. 4 Summary of Mozambican gauging stations analysis and assessment of data

Stations	Record period	Reliable data	Comments
Moamba E-22	1954 - 2009	Useful data	
R.Garcia E-23	1949 - 2009	Useful data	
R.Garcia E-24	1987 - 1999	Not reliable	Suspect data
Machatuine E-26	1997 - 2008	Not reliable	Short record
Chinhanguanine E-27	1983 - 2006	Useful data	
Bobole E-29	2001 - 2006	Not reliable	Missing data
Magude E-43	1955 - 2008	Useful data	
Chobela E-44	1957 - 2005	Useful data	
Incoluane E-45	1957 - 1974	Not reliable	Suspect and short record
M. Major E-396	1957 - 1974	Not reliable	short record
Sabie E-413	1999 - 2000	Not reliable	short record

### 3.1.3 Assessment and reliability of South African observed flow data

On the South African side of the Inkomati River Catchment, eight flow gauging stations were selected from the Sabie/Sand, the Crocodile and the Komati sub-catchments. The data measured at these stations are mean daily flow data and all of the stations are still operating since their establishment. The selected flow gauging stations are Queens River/Sassenheim (X2H008), Noordkaap River/Bellevue (X2H010), Suidkaap River/Glenthorpe (X2H024), Suartkoppiespruit/Kindergoed (X2H047), Nsikazi River/Kruger National Park (X2H072), Sabie River/Sabie (X3H001), White Water River/ Ethna (X3H007), Marite River/Injaka (X3H011), Mac- Elands River/Dawsonsspruit (X2H012) and Mac River/Geelhoutboom (X3H003). The amount of missing data is not significant, compared with the Mozambican gauging stations. Most of these gauging stations have good streamflow data. The Kruger National Park (X2H072), Ethna (X3H007) and Injaka (X3H011) gauging stations were

excluded because the data was not reliable for analysis. The time series of the streamflow has been plotted in Figures 3.15 to 3.22.

### 3.1.3.1 Sassenheim gauging station

The Sassenheim (X2H008) gauging station is located on the Queens River. Observed daily streamflow data is available from this station for the period February 1948 to January 2006. The unreliable/missing flow data amounts to approximately 2.83% of the observed period and the total catchment area is 180 km<sup>2</sup>. This station records approximately 2.1% of the total discharge of Crocodile River. The reasonable time series or period of data that was considered for the Sassenheim (X2H008) gauging station was determined from Figure 3.15. The time series (February 1948 to January 2006) was then used to generate the FDC for the station (see Figure 7.6 in Appendix 1).

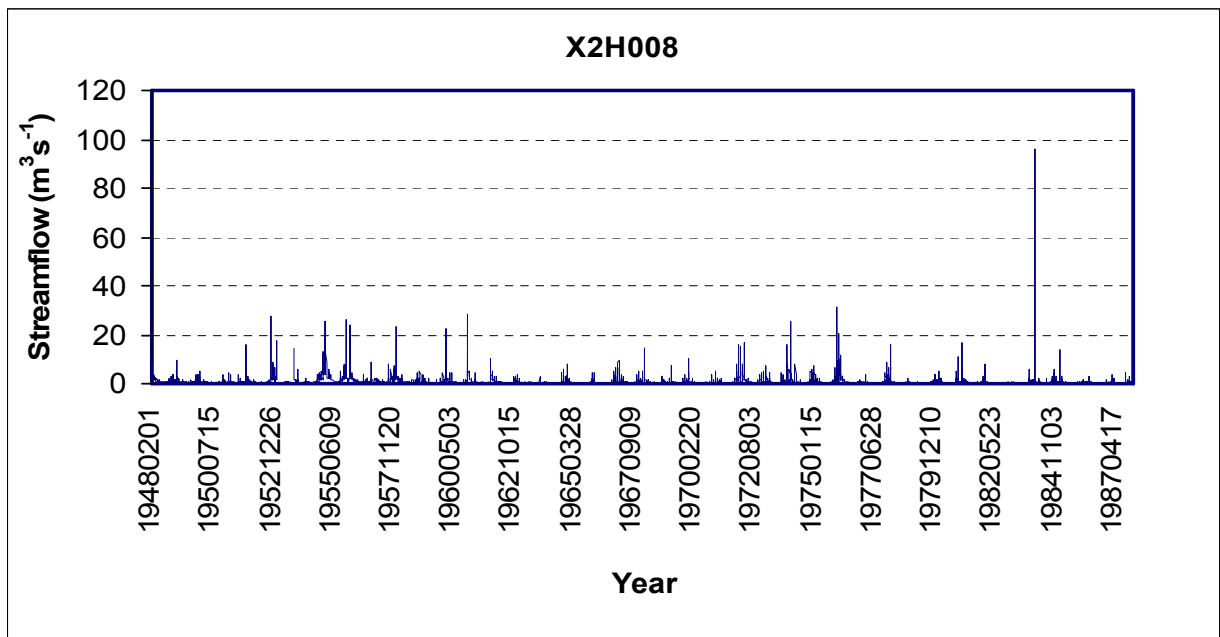


Figure 3. 15 Daily average discharge at Sassenheim gauging station (X2H008)

### 3.1.3.2 Bellevue gauging station

The Bellevue (X2H010) gauging station is located on the Noordkaap River. Observed daily streamflow data is available from this station for the period February 1948 to January 1987.

The unreliable/missing flow data amounts to approximately 3.73% of the record and the total catchment area is 126 km<sup>2</sup>. This station records approximately 2.5% of the total discharge of Crocodile River. The reasonable time series or period of data that was considered for the Bellevue (X2H010) gauging station was determined from Figure 3.16. The time series (February 1948 to January 1987) was then used to generate the FDC for the station (see Figure 7.7 in Appendix 1). From 1970's there is significant reduction of streamflow, particularly in dry months, this might be explained by land use (forest increase), abstractions and flow regulation.

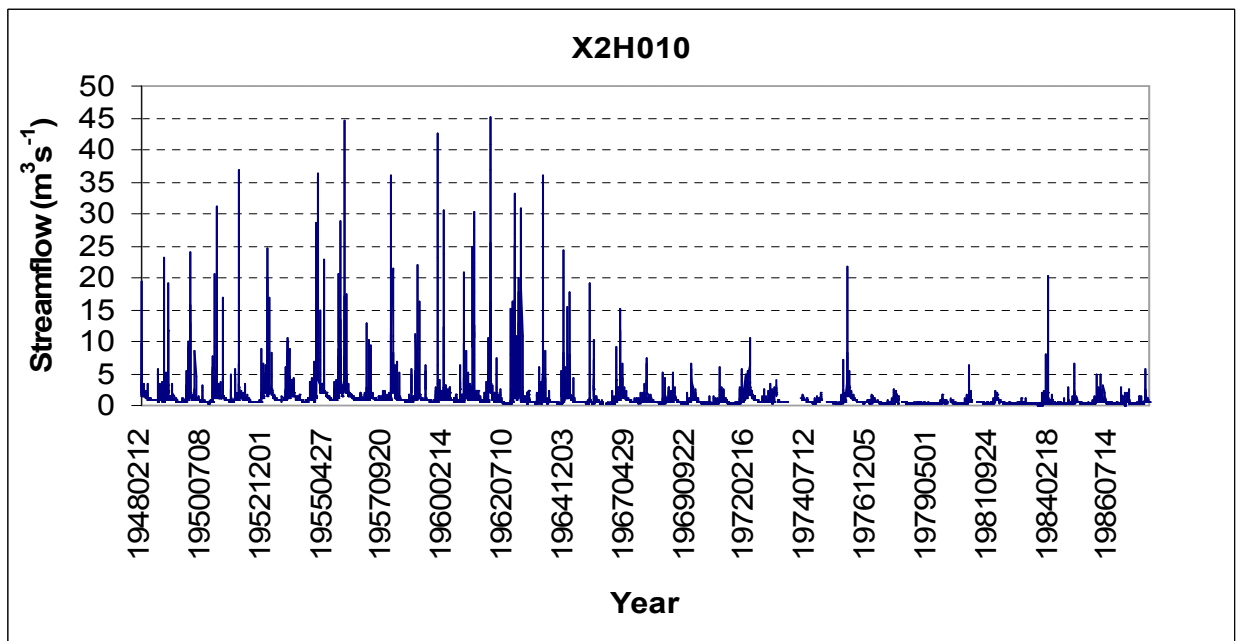


Figure 3. 16 Daily average discharge at Bellevue gauging station (X2H010)

### 3.1.3.3 Glenthorpe gauging station

The Glenthorpe (X2H024) gauging station is located on the Suidkaap River. Observed daily streamflow data is available from this station for the period September 1964 to January 2006. The unreliable/missing flow data amounts to approximately 0.64% and the total Catchment area is 80 km<sup>2</sup>. This station measures about 1.8% of the total discharge of Crocodile River. The reasonable time series or period of data that was considered for the Glenthorpe (X2H024) gauging station from Figure 3.17. The time series (September 1964 to January 2006) was then used to generate the FDC for the station (see Figure 7.8 in Appendix 1).

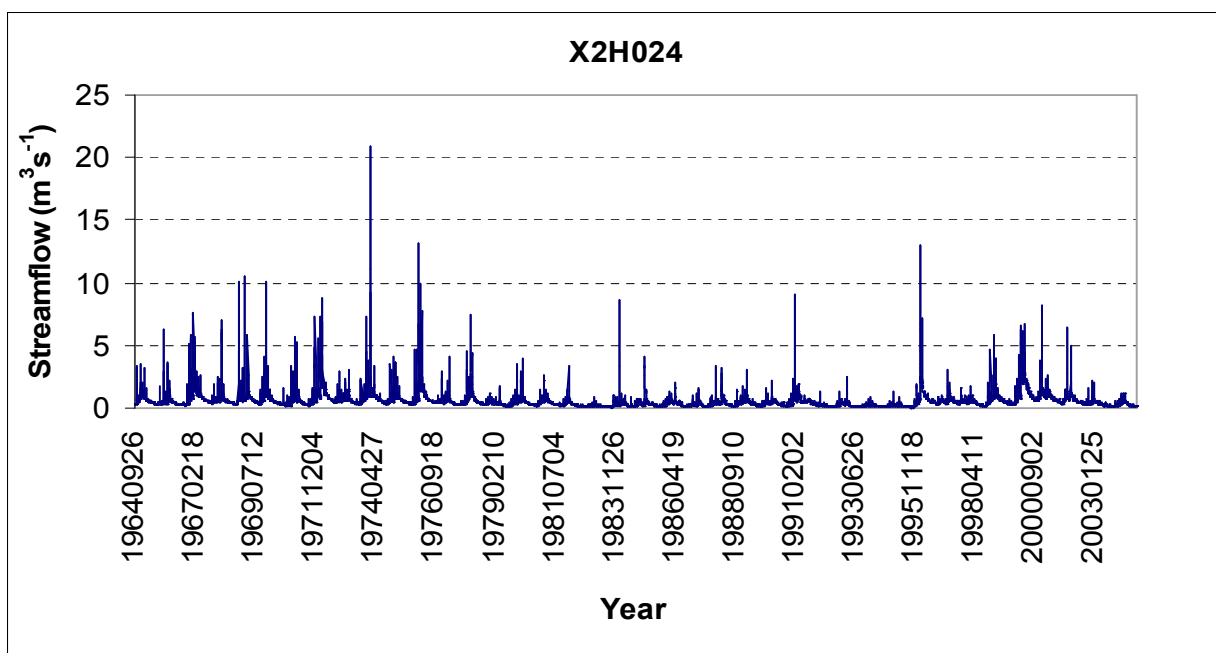


Figure 3. 17 Daily average discharge at Glenthorpe gauging station (X2H024)

### 3.1.3.4 Kindergoed gauging station

The Kindergoed (X2H047) gauging station is located before the confluence with Elands River and it is used to study the impact of forestry on the catchment. Observed daily streamflow data is available from this station for the period October 1985 to January 2006. The unreliable/missing flow data amounts to approximately 2.13% of the record and the total catchment area is 110 km<sup>2</sup>. This station measures about 1.1% of the total discharge of Crocodile River. The reasonable time series or period of data that was considered for the Kindergoed (X2H047) gauging station was determined from Figure 3.18. The time series was (October 1985 to January 2006) then used to generate the FDC for the station (see Figure 7.9 in Appendix 1).

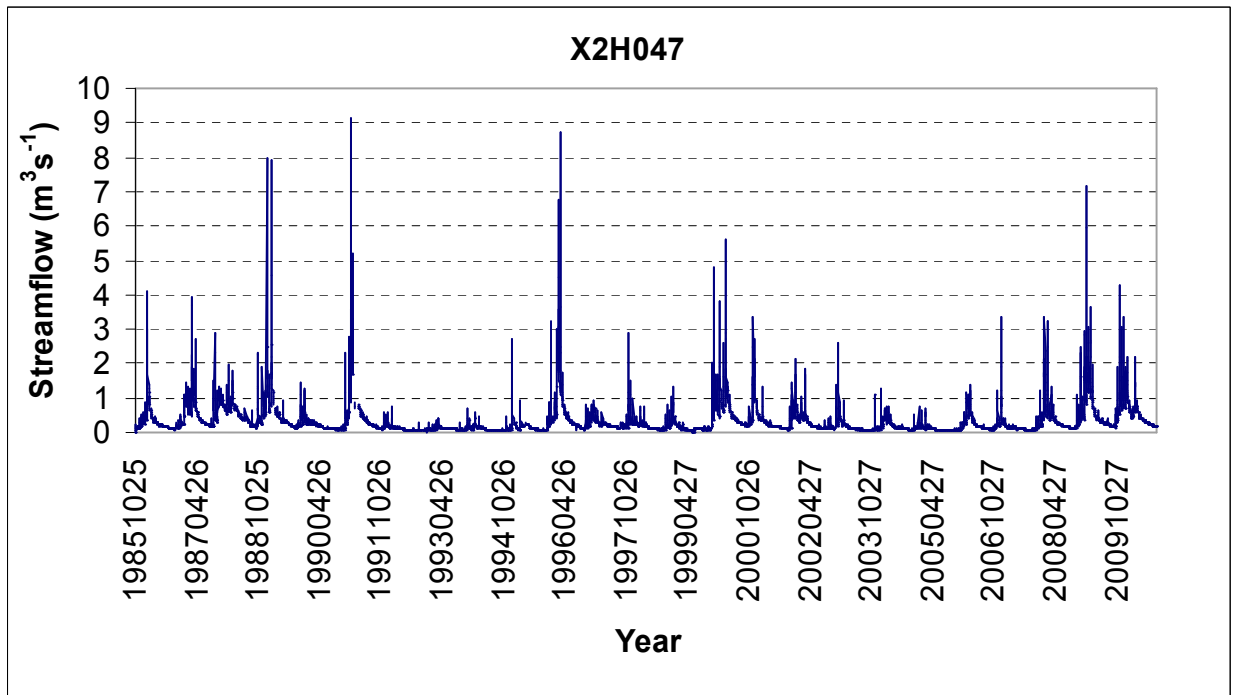


Figure 3. 18 Daily average discharge at kindergoed gauging station (X2H047)

### 3.1.3.5 Kruger National Park gauging station

The Kruger National Park (X2H072) gauging station is located on theNsikazi River. Observed daily streamflow data is available from this station for the period December 1989 to August 2009. The unreliable/missing flow data amounts to approximately 50% of the record and the total catchment area is  $64 \text{ km}^2$ . The reasonable time series or period of data that was considered for the Kruger National Park (X2H072) gauging station was determined from Figure 3.19. The flow data was deemed to be unreliable and was not used in the analysis.

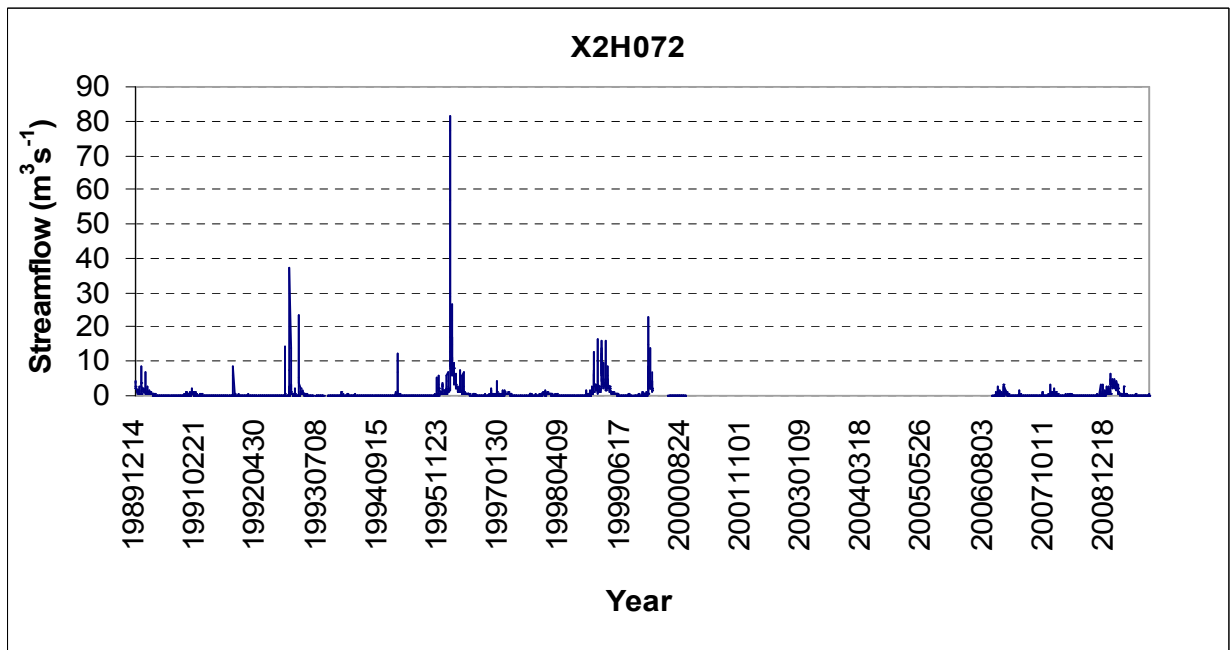


Figure 3. 19 Daily average discharge at Kruger National Park gauging station (X2H072)

### 3.1.3.6 Sabie gauging station

The Sabie (X3H001) gauging station is located in good downstream conditions of the River. Observed daily streamflow data is available from this station for the period March 1948 to March 2006. The unreliable/missing flow data amounts to approximately 1.75% of the record and the total catchment area is 174 km<sup>2</sup>. The reasonable time series or period of data that was considered for the Sabie (X3H001) gauging station was determined from Figure 3.20. The time series (March 1948 to March 2006) was then used to generate the FDC for the station (see Figure 7.10 in Appendix 1).

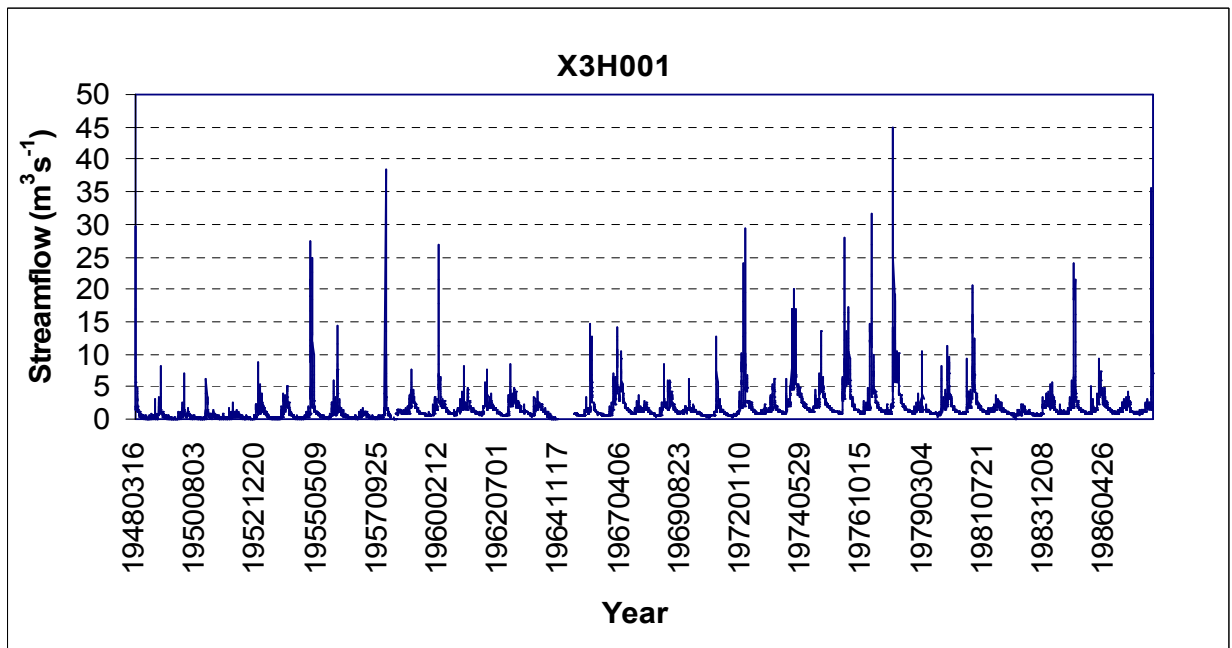


Figure 3. 20 Daily average discharge at Sabie gauging station (X3H001)

### 3.1.3.7 Ethna gauging station

The Ethna (X3H007) gauging station is located on the White Water River. Observed daily streamflow data is available from this station for the period November 1963 to November 1986. The flow data is unreliable because the rating has been exceeded and has also been changed over time. The total catchment area is 46 km<sup>2</sup>. The flow data was deemed to be unreliable and was not used in the analysis (see Figure 3.21).

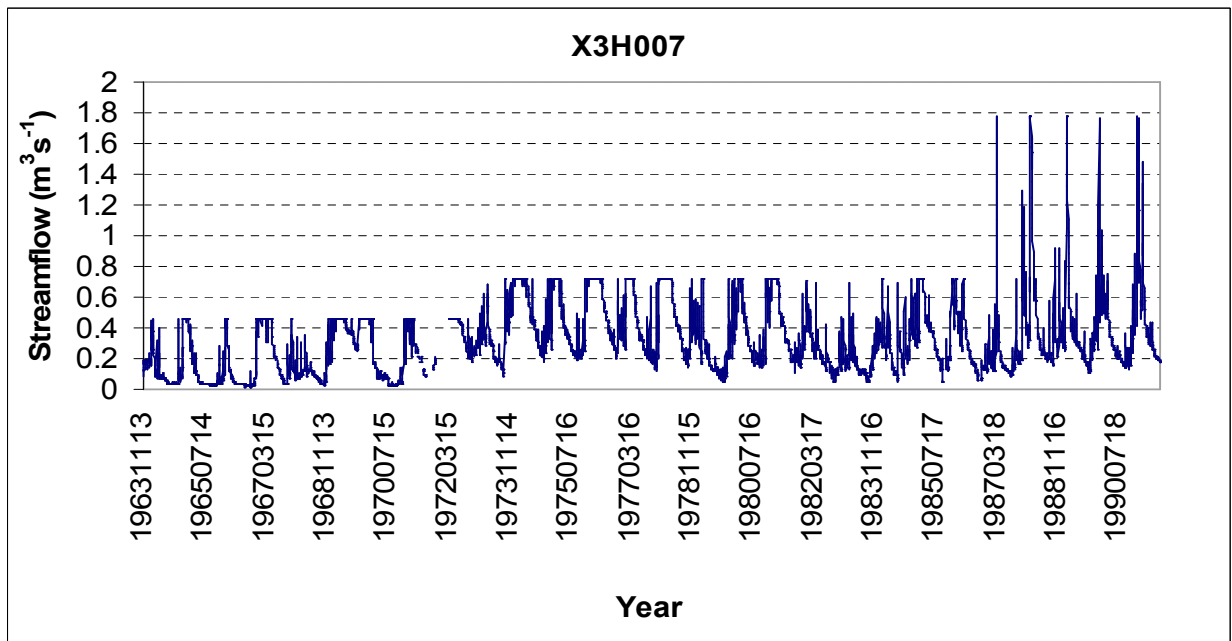


Figure 3. 21 Daily average discharge at Ethna gauging station (X3H007)

### 3.1.3.8 Injaka gauging station

The Injaka (X3H011) gauging station is located on the Marite River. Observed daily streamflow data is available from this station for the period November 1978 to December 1999. The unreliable/missing flow data amounts to approximately 11.19% of the record and the total catchment area is 212 km<sup>2</sup>. This station was excluded from further analysis because the flow data was deemed to be not reliable enough and the probability of exceedance of the FDC was not reaching 100%.

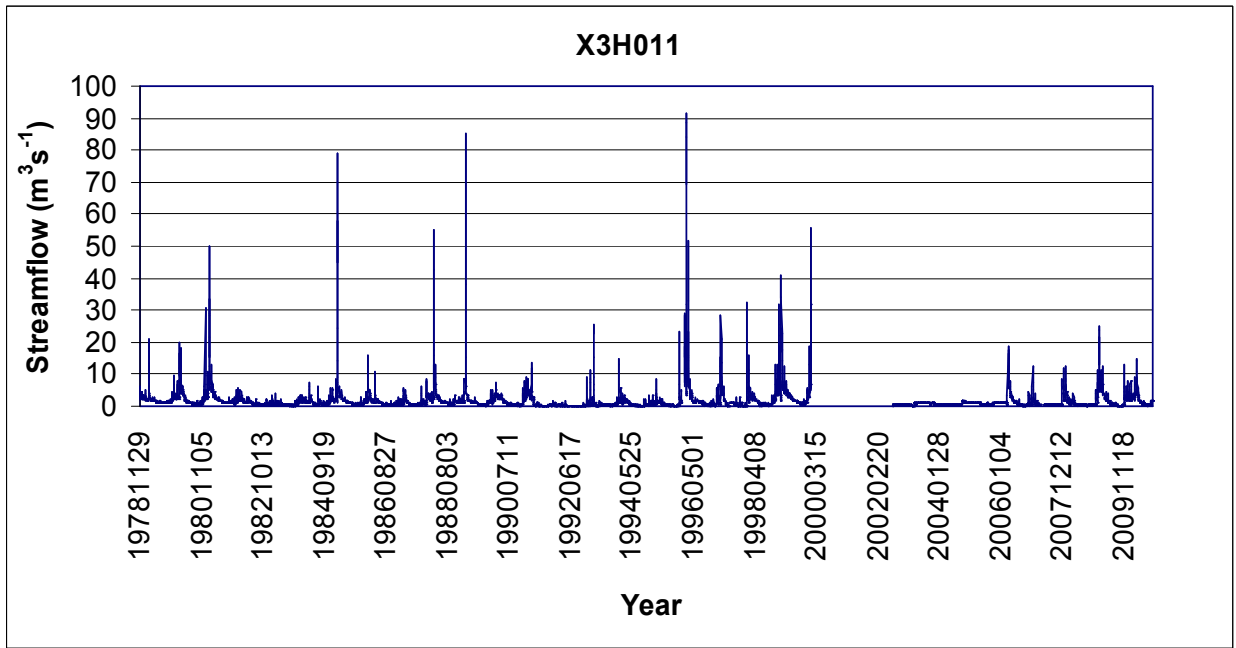


Figure 3. 22 Daily average discharge at Injaka gauging station (X3H011)

### 3.1.3.9 Dawsonsspruit gauging station

The Dawsonsspruit (X2H012) gauging station is located before the confluence with the Elands River. Observed daily streamflow data is available from this station for the period October 1956 to January 2006. The unreliable/missing flow data amounts to approximately 1.84% of the record and the total catchment area is 91 km<sup>2</sup>. This station measures about 1% of the total discharge of Crocodile River. The reasonable time series or period of data (October 1956 to January 2006) that was considered for the Dawsonsspruit (X2H012) gauging station was determined from Figure 3.23. The time series was then used to generate the FDC for the station (see Figure 7.11 in Appendix 1).

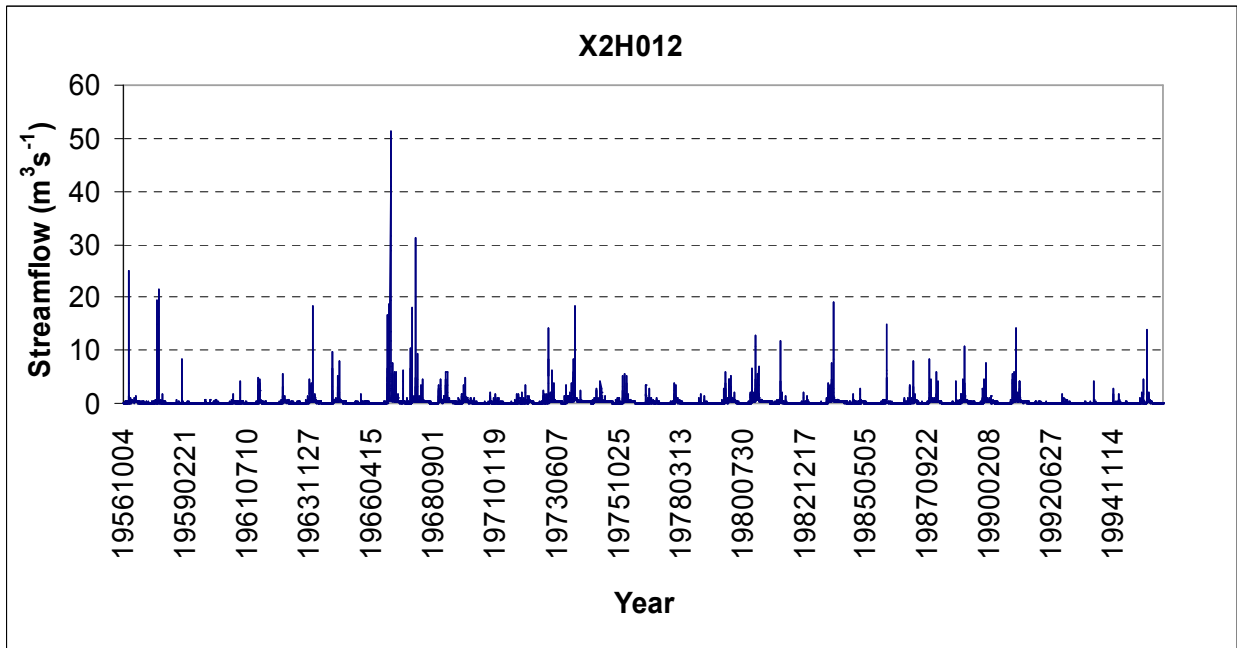


Figure 3. 23 Daily average discharge at Dawsonsspruit gauging station (X2H012)

### 3.1.3.10 Mac-Mac River gauging station

The Geelhoutboom (X3H003) gauging station is located on the Mac-Mac River. Observed daily streamflow data is available from this station for the period March 1948 to March 2006. The unreliable/missing flow data amounts to approximately 0.13% of the record and the total catchment area is 52 km<sup>2</sup>. The reasonable time series or period of data (March 1948 to March 2006) that was considered for the Geelhoutboom (X3H003) gauging station was determined from Figure 3.24. The time series was then used to generate the FDC for the station (see Figure 7.12 in Appendix 1).

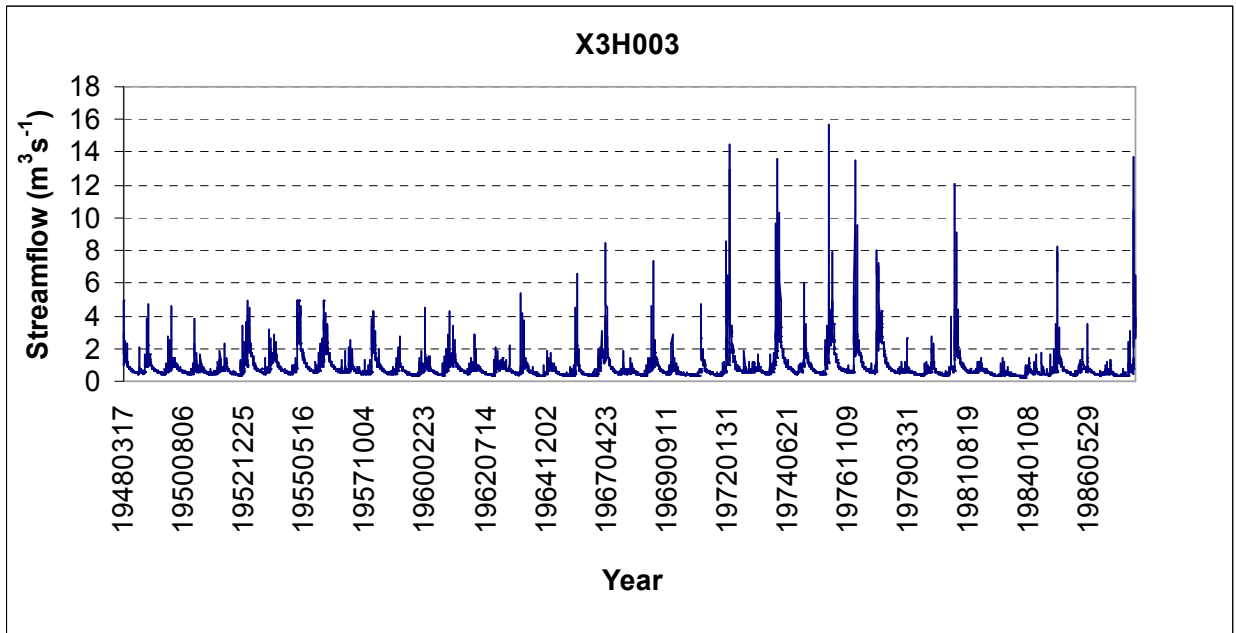


Figure 3. 24 Daily average discharge at Geelhoutboom gauging station (X3H003)

Table 3.5 provides a summary of the gauging stations analysis and an assessment of data for each station on the South African side. Kruger National Park (X2H072), Ethna (X3H007) and Injaka (X3H011) were excluded from further analysis because the data were deemed to be not reliable enough to be used in this study. The Incoluane (E-45) gauging station on the Mozambican side was also excluded for the same reason.

Table 3. 5 Summary of South African gauging stations analysis and assessment of data

<b>Stations</b>	<b>Record period</b>	<b>Reliable data</b>	<b>Comments</b>
Queens River X2H008	1948-2005	Useful data	
Noordkaap River X2H010	1948-2005	Useful data	
Dawsonsspruit X2H012	1952-2005	Useful data	
Suidkaap River X2H024	1964-2005	Useful data	
Suart Koppesspruit X2H047	1985-2005	Useful data	
Nsikazi River X2H072	1989-2002	Not reliable	Suspect data
Sabie River X3H001	1948-2005	Useful data	
Mac-Mac River X3H003	1948-2005	Useful data	
White Water River X3H007	1963-1991	Not reliable	Suspect data
Marite River X3H011	1978-2005	Not reliable	Suspect data

### 3.2 Determination of Catchment Physical Parameters

In this study, a GIS was used to obtain the river network from a digital elevation model (DEM) and to extract the important catchment parameters that affect streamflow. The Arc View GIS 3.2 spatial analyst tool (Patterson, 1997) was used to estimate physical parameters. A digital elevation model (DEM) for Mozambique was generated with a resolution of 90x90 m, downloaded from the USGS website (Patterson, 1997). From the DEM, the following parameters were extracted: the drainage area (A) in square kilometers (km<sup>2</sup>), the hypsometric fall (H) in meters (m) and the length of the main river course from the divide of the catchment to the gauging station in kilometers (Mimikou and Kaemaki, 1985a). The mean annual precipitation (P) in millimeters (mm) was calculated from monthly rainfall in the Mozambican side of the Inkomati River Catchment (hydro-meteorological data). The extracted parameters are illustrated in the results chapter.

### 3.2.1 Mean annual precipitation

In this study, the Thiessen Polygon method was applied to estimate the mean annual precipitation, because a single point precipitation measurement is quite often not representative of the volume of precipitation falling over a given catchment area. Therefore, a dense network of point measurements can provide a better representation of the true volume over a given area (Fiedler, 2003; Bayraktar *et al.*, 2005; Al-Hallaq and Elaish, 2008).

The Arc View 3.2 Areal-Rain extension (Berk, 1988) was used for the creation of the Thiessen polygon. The Inkomati River Catchments' average depths were computed as shown in Tables 4.1 and 4.2 in the Results chapter. To estimate the mean annual precipitation, Equation 3.1 was used:

$$MAP = \frac{P_1 A_1 + P_2 A_2 + P_3 A_3 + \dots + P_n A_n}{A_1 + A_2 + A_3 + \dots + A_n} = \frac{\sum_{i=1}^n P_i A_i}{\sum_{i=1}^n A_i} \quad \text{Equation (3.1)}$$

where

- $MAP$  = mean areal precipitation, or the weighted average (mm),
- $P_i$  = MAP of the station located at the centroid of the Polygon= $i$ , and
- $A_i$  = areas of the  $i$ -th polygon (km<sup>2</sup>).

The Thiessen polygons generated for the area are displayed in Figure 3.25

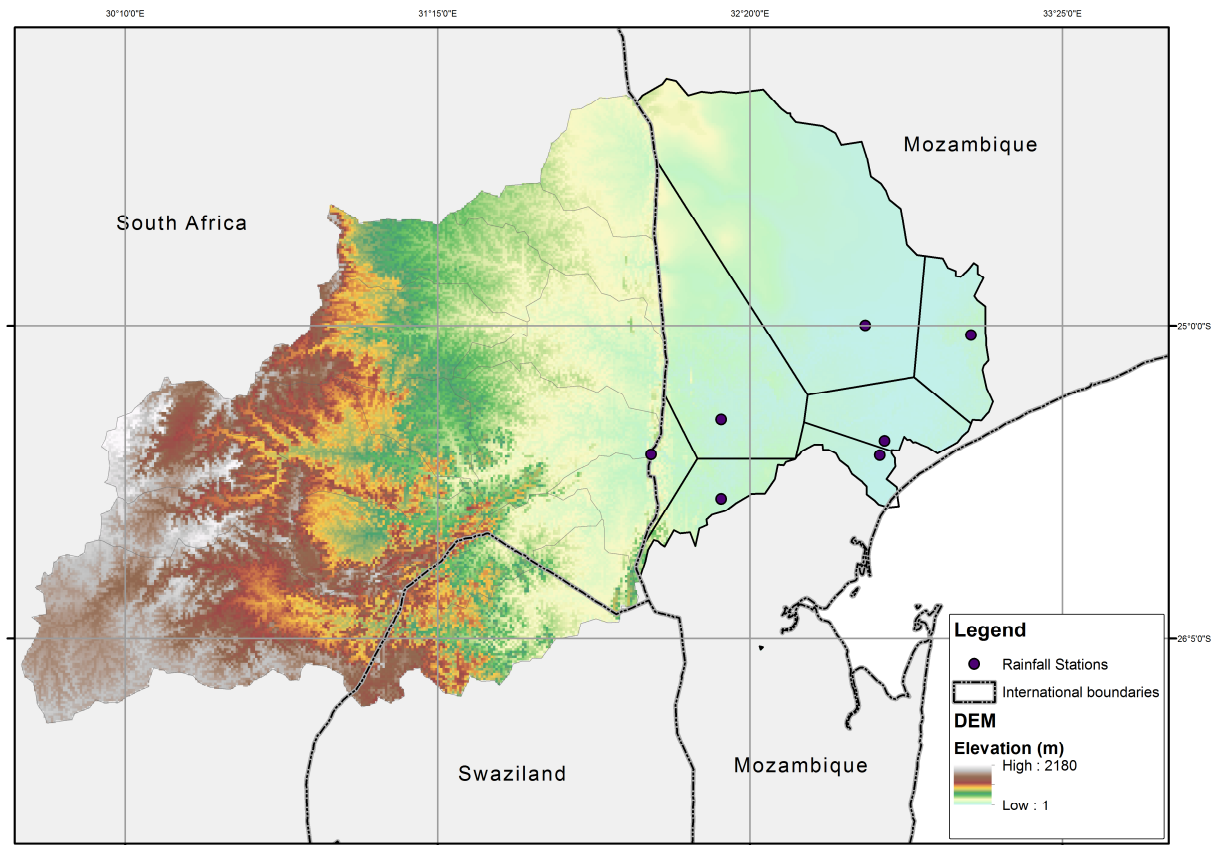


Figure 3. 25 Map of Inkomati River Catchment showing the Thiessen polygon method

### 3.2.2 Drainage area

Drainage area is the most important catchment parameter that affects streamflow discharge (Hussein and Raman, 2010). There is a close relationship between the size of the catchment and the discharge. The discharge volume from a catchment can be related to the contributing area (Hussein and Raman, 2010). Sub-catchment boundaries can be determined, using topographical maps or DEMs. In this study, the stream gauging stations were taken as outlet points and their catchments were determined as contributing drainage areas to those gauges (Rojanamon *et al.*, 2009). After digitization, sub-catchment polygons were used to extract the necessary information from either the DEM or other spatial data (Rojanamon *et al.*, 2009).

### **3.2.3 Hypsometric fall**

The hypsometric fall is defined as the difference between the highest point value (upstream elevation) and the lowest point (downstream elevation) in the catchments or sub-catchments close to the selected gauging station (Mimikou and Kaemaki, 1985a). In this study, the hypsometric fall was calculated from upstream, to the outlet gauge point, with the upstream elevation taken at the catchment divide, from where the main river starts (Rojanamon *et al.*, 2009).

### **3.2.4 River length**

The DEM was used to create an interconnected river network. The flow from one cell (pixel) at higher altitude to an adjacent cell having the lowest altitude of the surrounding 8 creates a grid or raster of flow direction. The accumulation of flow from pixel to pixel moving down slope allows the generation of a raster of flow accumulation. The areas of highest flow accumulation define the river course. The length of the main rivers was calculated from the flow accumulation raster by using the longest stream branch in the sub catchments (Mimikou and Kaemaki, 1985a).

## **3.3 Derivation of Flow Duration Curve for the Gauged Sites**

A FDC is defined as a graph of the streamflow of the river ( $\text{m}^3 \cdot \text{s}^{-1}$ ) plotted against the frequency of exceedance (%) (Viola *et al.*, 2010). FDCs were derived from observed daily streamflow data in the Inkomati River Catchment. The construction and interpretation of FDC is provided by many sources and the calculations were done, using the available record period of reliable data (Ganora *et al.*, 2009). The probability of exceedance in percentage (%) was calculated using Equation 2.1.

For the estimation of hydropower, 50%, 75% and 90% percentiles of non-exceedance are generally considered (Kusre *et al.*, 2010). For this study, eight levels of percentile flows have been considered.

### 3.4 Development of Regional Flow Duration Frequency Curves

The objective of Multiple Regression analysis (MRA) is to develop a prediction equation, relating a variable to independent predictor variables. MRA can lead to significant increases in prediction accuracy and the ability to measure the effect of each independent variable on the dependent variable (McCuen, 1993). Regression is used for the purpose of obtaining the relation between variables, while regression analysis is used to represent this relation via mathematical functions. The regression equation is the result of the function defined by the regression analysis. This equation includes the dependent variable (response) and the independent variables (predictors) that define the dependent variable (Corston and Colman, 2003).

Before starting the regression analysis, appropriate relationships in the model should be considered and selected, so that the model can be built up from these. It is firstly necessary to investigate which kind of relations exist between the dependent and independent parameters (McCuen, 1993). The relationship between the response and predictors can be linear or non-linear, for example, exponential, power, logarithmic, quadratic and cubic equations. To obtain the FDC, the discharge  $Q$  was plotted against the percent of time  $D$  during the period of the record in which the particular discharge is equalled or exceeded (Niadas, 2005).

Various models of FDCs have been developed in different studies. For example, (Alejandrino and McNally, 1983) proposed an exponential model for daily FDC in the Philippines. (Mimikou and Kaemaki, 1985b) proposed the use of a cubic model for monthly FDC in the Western and Northwestern regions of Greece. (Franchini and Suppo, 1996) proposed the use of an exponential equation for calculating average daily discharge in a Limestone area of the Molise in Italy. (Yu *et al.*, 2002) found that the cubic model fitted the daily FDC in the upstream catchments of the Cho-Shuei Creek in central Taiwan. From these studies, different results were found.

According to (Mimikou and Kaemaki, 1985a), the calibration of the FDC of all eleven gauging stations (South Africa and Mozambique) was done, using various mathematical models or Equations as follows:

$$Q = a \exp(-bD) \quad \text{Equation (3.2)}$$

$$Q = aD^{-b} \quad \text{Equation (3.3)}$$

$$Q = a - b \ln D \quad \text{Equation (3.4)}$$

$$Q = a - bD + cD^2 \quad \text{Equation (3.5)}$$

$$Q = a - bD + cD^2 - dD^3 \quad \text{Equation (3.6)}$$

where

$Q$  = average daily discharge per unit area of the catchment ( $\text{m}^3 \cdot \text{s}^{-1} \cdot \text{km}^{-2}$ ),  
 $D$  = corresponding time of exceedance (%), and  
 $a, b, c, d$  = constants.

Equations 3.2; 3.3; 3.4; 3.5 and 3.6 are referred to as exponential, power, logarithmic, quadratic and cubic models, respectively.

### 3.4.1 Statistical analysis

In this study, the SPSS software Version 18 (Corston and Colman, 2003) and the Stata software Version 11 as applied by (Berk, 1988; Kennedy, 2003; Kutner *et al.*, 2004) were used in the regression analysis of all thirteen gauging stations (4 in Mozambique listed in Table 3.4 and 6 in South Africa listed in Table 3.3, and different types of relationships and appropriate predictor variables were investigated (Corston and Colman, 2003). SPSS 18 and Stata 11 are software packages used for entering, manipulating and summarizing data and for conducting statistical analyses (Corston and Colman, 2003). The analysis was performed, starting from the discharge as a dependent parameter. Independent parameters considered included the probability of time exceedance, the mean annual precipitation, the drainage area, the hypsometric fall and the length of the main river or the longest river in the sub-catchments. Equations 3.2 to 3.6 were applied in the calibration to select the best fitting model for all the gauging stations.

### 3.4.2 Regional Model

The application of the regionalized regression relationships to estimate the FDCs at ungauged sites in different geographic regions throughout the world, could be one of the steps that could be used to solve problems related to the scarcity of observed streamflow data, or generally, at sites where data is not sufficient (Castellarin *et al.*, 2004).

The morphoclimatic characteristics of catchments have been used in the regionalisation of FDCs. Regionalisation is therefore one of the methods to transfer hydrological information from gauged sites to ungauged sites (Mimikou and Kaemaki, 1985a; Rojanamon *et al.*, 2007).

The hydrological regionalisation has been undertaken by plotting contours of equal value of some numerical measure of the hydrological characteristics. The data can be transferred from one gauged site to an ungauged site of interest, or by explaining analytically the spatial variation of some parameters of the hydrological characteristic at various measuring sites (Kusre *et al.*, 2010).

The regionalisation approach plotted the spatial variation of the parameters, for example ***a*** and ***b***, in the power model in Equation 3.3, and regression analyses was performed at all stations (Mimikou and Kaemaki, 1985a). Four regression equations were tested based on a study reported in literature (Mimikou and Kaemaki, 1985a) in order to model estimate the parameters (***a***, ***b***, ***c*** and ***d***) at ungauged sites. The equations used were the following:

$$V = b_0 + b_1 P + b_2 A + b_3 L + b_4 H \quad \text{Equation (3.7)}$$

$$V = b_0 P^{b_1} (A/L)^{b_2} H^{b_3} \quad \text{Equation (3.8)}$$

$$V = b_0 P^{b_1} A^{b_2} (H/L)^{b_3} \quad \text{Equation (3.9)}$$

$$V = b_0 P^{b_1} A^{b_2} H^{b_3} L^{b_4} \quad \text{Equation (3.10)}$$

where

$V$  = dependent variable representing ***a***, ***b***, ***c***, ***d***,

$P$  = mean annual precipitation (mm),

$H$  = hypsometric fall (m),  
 $A$  = drainage area (km<sup>2</sup>),  
 $L$  = length of the main river (km), and  
 $b_0, b_1, b_2, b_3, b_4$  = regressions constants.

MRA was performed according to standard statistical methods. For example, Equations 3.7 to 3.10 were used to estimate the two parameters  $a$  and  $b$  of the power model in Equation 3.3 at each station in order to find the best prediction model, which expresses those parameters in terms of Precipitation ( $P$ ), Area ( $A$ ), Hypsometric fall ( $H$ ) and Length of the river ( $L$ ).

The Mac-Mac River (X3H003) and R.Garcia E-23 on the South African and Mozambican sides, respectively were not used for the calibration procedure. However, they were selected for independent verification of the methodology because both of them are located upstream of the catchment on both sides and the border and they represent a range of catchment sizes with the Mac-Mac River (X3H003) and R.Garcia (E-23) are small (154 km<sup>2</sup>) and big (21200 km<sup>2</sup>) catchments, respectively. The accuracy of the regional model was verified from the data of the estimated flow duration, using the Root Mean Square Error ( $RMSE$ ), shown in Equation 3.11.

$$RMSE = N^{-1} \left[ \sum_{i=1}^N \left( \frac{Q_i - \hat{Q}_i}{Q_i} \right)^2 \right]^{1/2} \quad \text{Equation (3.11)}$$

where

$Q_i$  = observed discharge (m<sup>3</sup>.s<sup>-1</sup>),  
 $\hat{Q}_i$  = estimated discharge (m<sup>3</sup>.s<sup>-1</sup>),  
 $i$  = ranges from 1 to  $N$ ,  
 $N$  = number of data points, and  
 $RSME$  = root mean square error (%).

### **3.4.3 Determination of hydro-potential for Small Hydropower Plants**

Small hydropower plants are the most important renewable source for the production of the electric power. In order to determine the power potential at a given site, under conditions where the daily or monthly flow data and head at the site are available, the plant efficiency, specific weight of water and flows must be known (Ramachandra *et al.*, 2004).

This chapter has described the methodology used in this study and included information about the assessment and reliability of observed flow and rainfall data on both sides of the international boundary between Mozambique and South Africa. The following chapter contains the details of the application and the results from the application of the above methodology.

## 4. RESULTS

The results for the determination of physical catchment parameters using Geographical Information Systems (GIS) at the selected sites, the derivation of Flow Duration Curves (FDCs) for the gauged sites, the development of regional flow frequency curves using the multiple regressions analysis (MRA), and the estimation of hydro-potential for Small Hydropower Plants (SHPs) are presented in this chapter.

### 4.1 Determination of Catchment Physical Parameters

Using GIS, several morphoclimatic characteristics of the drainage basins in the selected Mozambican and South African gauging stations were extracted, as summarised in Table 4.1. In general, the drainage area and length of the main rivers on the Mozambican sub-catchments have high values (up to 42 942 km<sup>2</sup> and 109 km, respectively), compared with the values on the South African side (up to 398 km<sup>2</sup> and 34 km, respectively). The hypsometric falls and mean annual precipitation have relatively low values (674 m and 872 mm) on the Mozambican side, compared with the values on the South African side (1040 m and 1294 mm).

Table 4.1 Morphoclimatic characteristics for the Mozambique and South Africa catchments

Station Name	Station ID	Area (km <sup>2</sup> )	Hypsometric. Fall (m)	MAP (mm)	Length (km)
Moamba	E-22	21850	208	571	42
R.Garcia	E-23	21200	674	460	90
Chinhanguanine	E-27	31073	52	574	40
Magude	E-43	37500	393	693	102
Chobela	E-44	37600	408	694	109
Incoluane	E-45	42942	370	872	90
Queens River-Sassenheim	X2H008	180	820	820	10
Noordkaap River-Bellevue	X2H010	127	740	845	20
Suidkaap River-Glenthorpe	X2H024	82	780	814	9
Suarkoppiesspruit-Kindergoed	X2H047	349	760	796	29
Nsikazi River-Kruger National Park	X2H072	249	440	721	32
Sabie River-Sabie	X3H001	230	980	1241	22
White waters River-Ethna	X3H007	61	720	1178	12
Dawson Spruit	X2H012	398	200	871	29
Mac-Mac River- Geelhoutboom	X3H003	154	440	1294	13

## 4.2 Derivation of Flow Duration Curve for the Gauged Sites

FDCs are used to compare the flow regimes of different rivers (Patel, 2007). The construction of the flow duration curves was based on ranking the daily discharge data and the frequency of exceedance was calculated for each value. The percentage of time that any discharge is exceeded can be estimated from the plotted graphs as contained in Figures 7.1 to 7.12 in Appendix 1.

The flow estimates for various levels of probability of exceedance and the flow quantiles for all selected gauging stations are presented in Table 4.2 and Figure 4.1. These results indicate that all the Mozambican gauging stations have high flows for almost all exceedance levels from 10% to 95%. The high and low flow values are represented in the flow duration intervals (0-10%) and (90-100%), which generally indicate floods and drought events, respectively. Table 4.2 contains a summary of the streamflow quantiles for the eight flow duration intervals and the catchment areas of all gauging stations. The results indicate that the Incoluane gauging station E-45 has the largest total drainage area (42 942 km<sup>2</sup>) and the streamflow values are also larger than other interval levels, except level D=95% with 1.1 m<sup>3</sup>s<sup>-1</sup>. Gauging stations X2H072 and X3H007 have the lowest streamflow values and their drainage areas are relatively smaller (249 and 61 km<sup>2</sup>, respectively).

Table 4. 2 Flow estimates for various levels of probability of exceedance (D) (%)

Station	Area (km <sup>2</sup> )	Flow (m <sup>3</sup> .s <sup>-1</sup> )							
		10%	25%	50%	60%	75%	80%	90%	95%
E-22	21850	141.5	69.6	28.8	17.3	5.7	3.4	0.0	0.0
E-23	21200	142.8	63.3	24.5	14.6	5.6	3.8	1.0	0.7
E-27	31073	269.2	124.4	46.5	33.8	19.3	14.6	5.7	3.2
E-43	37500	118.5	45.7	17.2	11.4	5.6	4.6	3.1	1.9
E-44	37600	212.8	74.2	36.4	29.2	18.6	15.5	7.8	4.2
E-45	42942	307.5	203.2	68.7	51.5	23.7	16.2	7.3	1.1
X2H008	180	1.4	0.7	0.3	0.2	0.1	0.1	0.1	0.0
X2H010	127	1.8	1.0	0.7	0.5	0.4	0.4	0.2	0.0
X2H024	82	1.0	0.6	0.4	0.3	0.2	0.2	0.2	0.1
X2H047	349	0.7	0.4	0.2	0.1	0.1	0.1	0.1	0.0
X2H072	249	0.6	0.1	0.0	0.0	0.0	0.0	0.0	0.0
X3H001	230	3.2	1.8	1,1	0.9	0.6	0.5	0.2	0.0
X3H007	61	0.7	0.4	0.3	0.2	0.1	0.0	0.0	0.0
X3H011	154	3.2	1.6	0.8	0.6	0.4	0.3	0.0	0.0

The FDCs for all selected gauging stations are presented in Figure 4.1. The results in Figure 4.1 indicate that the curves lie close to each other and are grouped for the Mozambican and South African stations. The biggest differences can be seen in the area of extreme low flows, which are exceeded more than 90% of the time, and high flows, which are exceeded less than 5% of the time.

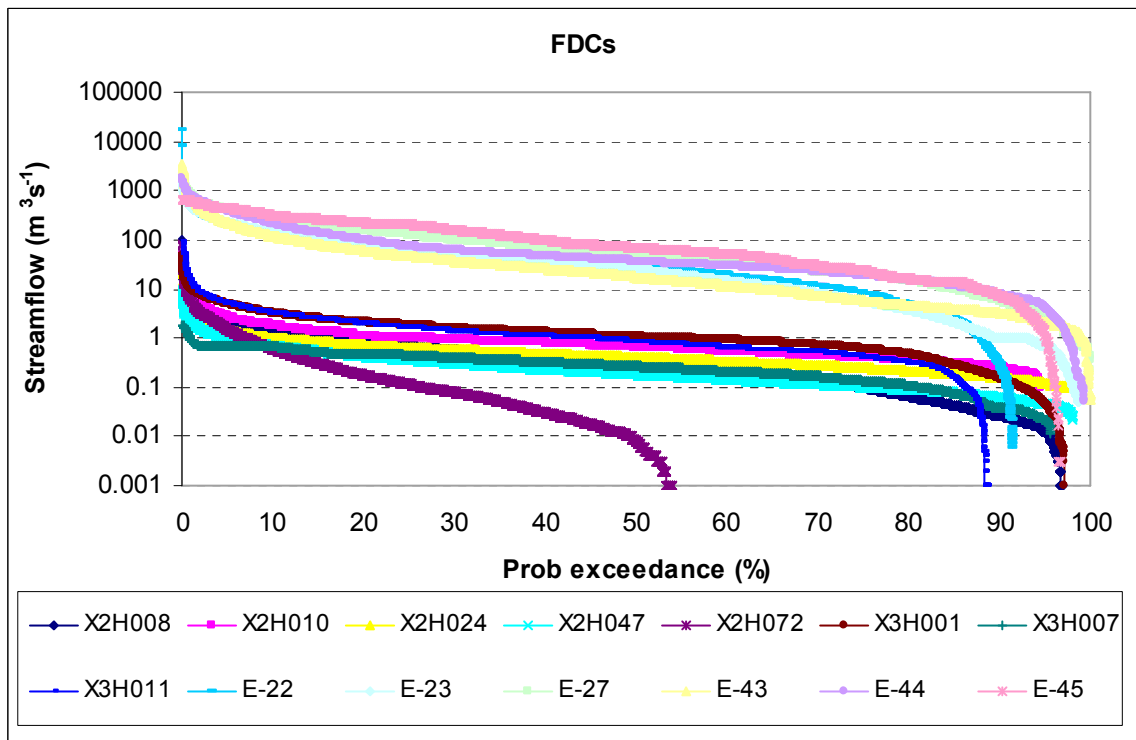


Figure 4. 1 Superimposed daily Flow Duration Curves for all selected flow gauges

Figure 4.1 indicates that approximately 10% of all days have zero flows. If the slope of the low flow part (drought) of the FDC is flat, groundwater/subsurface flow contribution is normally significant and low flows are sustainable. The shape of the FDC can be an indication of hydrogeological conditions in the catchment.

### 4.3 Regionalisation using the Multiple Regressions Technique

The objective of this section, therefore, was to identify a reasonable model of FDCs for the Inkomati River Catchment. The curve can be fitted using five mathematical models, namely, logarithmic, quadratic, cubic, power and exponential. By using regression analysis, the models in Equations 3.2 to 3.6 were fitted to each set of paired values of discharge (Q)

versus the time probability of exceedance. After fitting the five models, the best fitted model (observed minus the estimated data is minimum).

#### 4.3.1 Calibration of the flow duration curves

Various mathematical models were used for the calibration of the FDCs at gauging stations. The calibration results at each station are presented in this section. The average coefficient of determination ( $R^2$ ) was good in all models and the mean standard error showed the lowest values. The results are summarised in Tables 4.3. The power model was therefore selected for use in the regionalisation of the FDC models because it showed highest average value of  $R^2$  and seven times than other models.

Table 4.3 Coefficient of determination ( $R^2$ ) and Mean Square Error (MSE) for five mathematical models

Station	Exponential		Power		Logarithmic		Quadratic		Cubic	
	$R^2$	MSE ( $m^3.s^{-1}$ ) <sup>2</sup>	$R^2$	MSE ( $m^3.s^{-1}$ ) <sup>2</sup>	$R^2$	MSE ( $m^3.s^{-1}$ ) <sup>2</sup>	$R^2$	MSE ( $m^3.s^{-1}$ ) <sup>2</sup>	$R^2$	MSE ( $m^3.s^{-1}$ ) <sup>2</sup>
E-22	0.82	55.89	0.88	45.49	0.80	52.63	0.54	79.82	0.64	70.36
E-27	0.89	66.55	0.87	70.84	0.90	54.44	0.68	0.96	0.98	26.48
E-43	0.84	71.29	0.87	62.97	0.59	106.7	0.34	135.5	0.81	72.22
E-44	0.92	50.07	0.84	72.05	0.84	63.07	0.61	48.99	0.99	19.48
X2H008	0.78	0.72	0.92	0.42	0.71	0.73	0.80	0.60	0.86	0.51
X2H010	0.81	1.05	0.90	0.77	0.58	1.39	0.69	1.19	0.79	0.99
X2H024	0.76	0.42	0.97	0.16	0.80	0.30	0.84	0.26	0.89	0.22
X2H047	0.81	0.24	0.93	0.14	0.83	0.18	0.90	0.15	0.93	0.12
X3H001	0.82	1.15	0.93	0.72	0.85	0.82	0.90	0.68	0.95	0.49
X2H012	0.82	0.50	0.97	0.22	0.37	0.91	0.49	0.82	0.59	0.74
Average	0.83	24.8	0.91	25.4	0.73	21.8	0.68	26.9	0.84	19.2

At the Moamba gauging station E-22, the relationship between the discharge and the probability of exceedance was analyzed by applying Equations 3.2 to 3.6. The results showed that the power, exponential and logarithmic models have the best fit ( $R^2=88\%$ ,  $R^2=82\%$  and  $R^2=80\%$ ), followed by the cubic and quadratic models ( $R^2=64\%$  and  $R^2=54\%$ , respectively). All of the models are a good fit, with coefficients of determination  $R^2$  ranging from 54% to 88%. The lowest MSE=45.49 was indicated in the power model. The high and low flows were well-estimated. The results for the power model are shown in Figure 4.2.

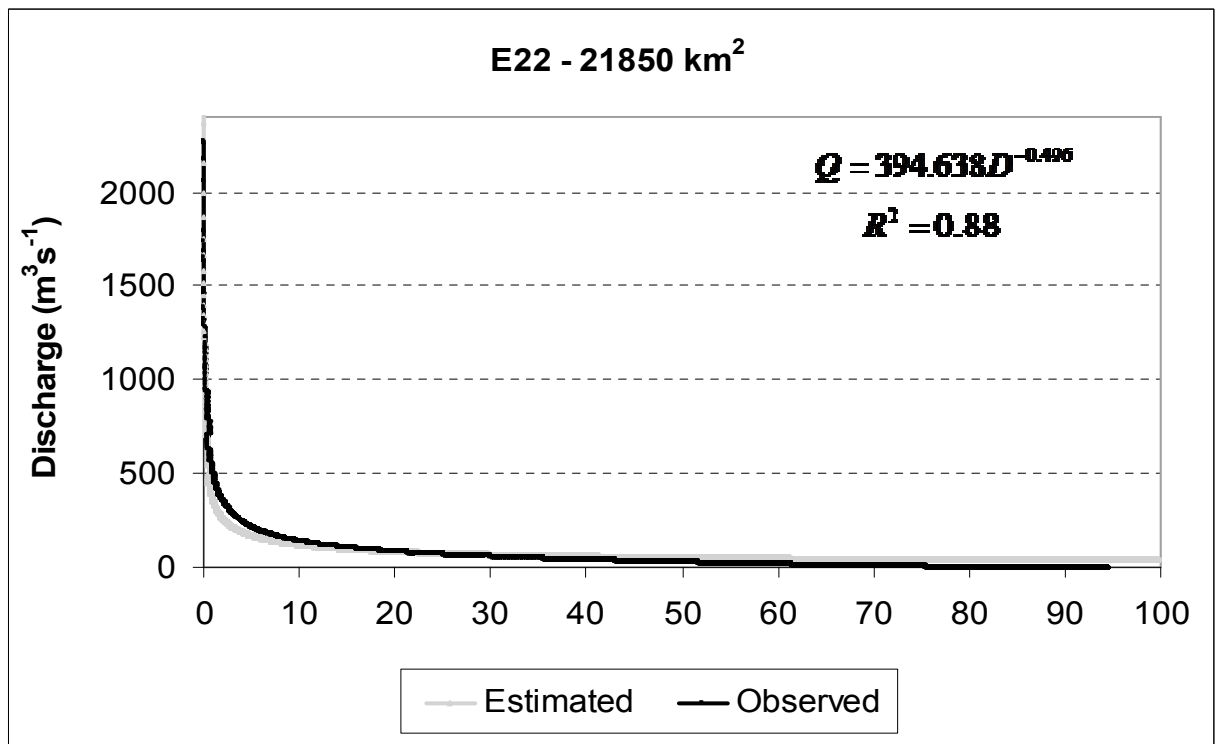


Figure 4. 2 Daily Flow Duration Curves of observed and estimated flow data for (E-22)

The relationship between the dependent (flow) and independent (probability of exceedance) variables at the Chinhanguanine gauging station E-27 was determined, using Equations 3.2 to 3.6. The results of the analysis showed that all of the models had good fits, with coefficients of determination ( $r^2$ ) ranging from 68% to 98%. The cubic and logarithmic models have the best fit ( $R^2=98\%$  and  $R^2=90\%$ , respectively), followed by the exponential, power and quadratic models ( $R^2=89\%$ ,  $R^2=87\%$  and  $R^2=68\%$ , respectively). The MSE=54.44 was indicated in the logarithmic model. The high flows were under-estimated and the low flows over-estimated. The results for the power model are illustrated in Figure 4.3.

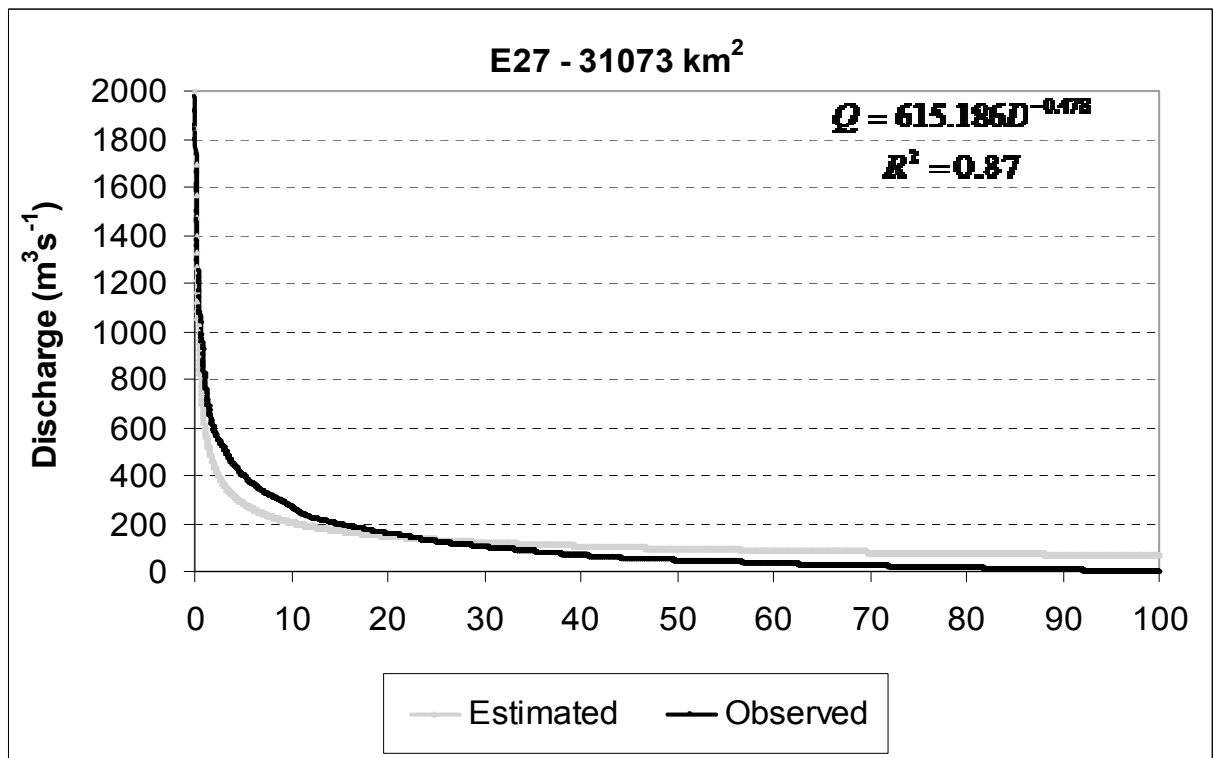


Figure 4.3 Daily Flow Duration Curves of observed and estimated flow data for (E-27)

The relationship between discharge (dependent) and the probability of exceedance (independent) at the Magude gauging station E-43 was regressed by using Equations 3.2 to 3.6. The results of the analysis showed that the power, exponential and cubic models had good fits, with coefficients of determination  $R^2$  ranging from 81% to 87%. The power, exponential and cubic models resulted in the best fits ( $R^2=87\%$ ;  $R^2=84\%$  and  $R^2=81\%$ , respectively), followed by the logarithmic and quadratic models ( $R^2=59\%$  and  $R^2=34\%$ ). The  $MSE=62.97$  was indicated in the power model. The high and low flows were well-estimated. The results for the power model are shown in Figure 4.4.

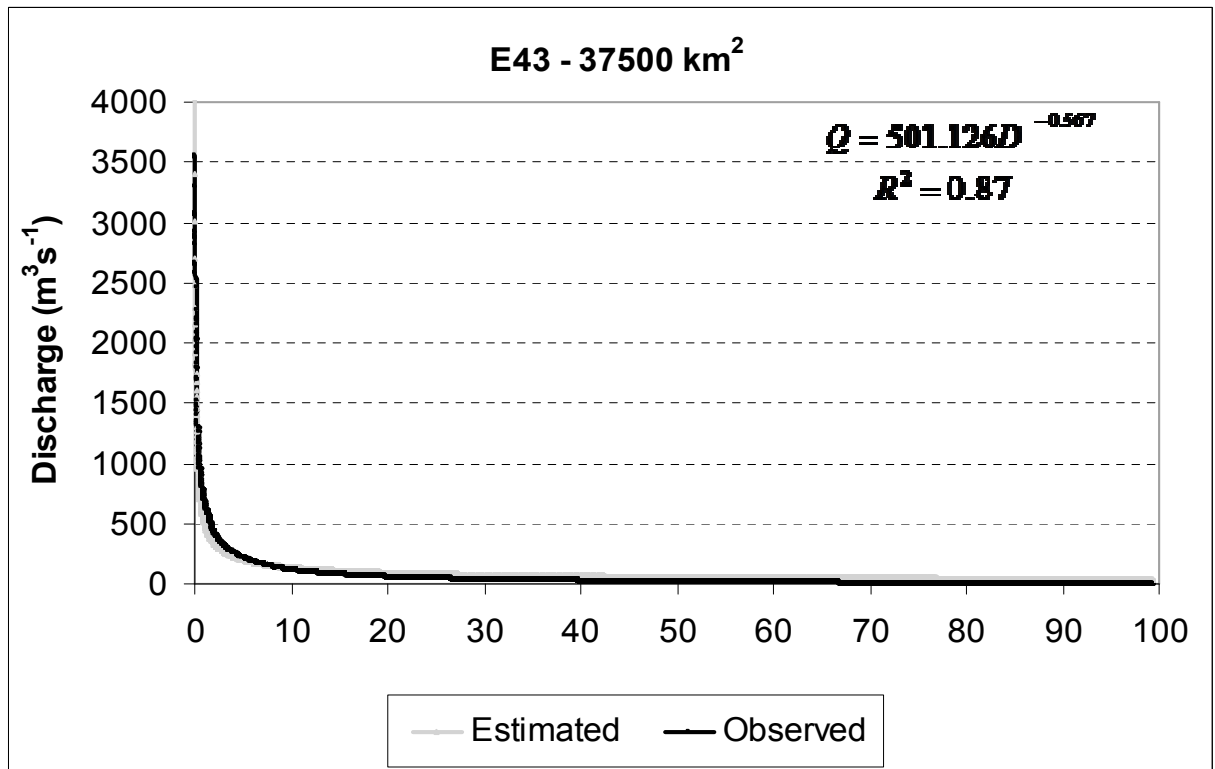


Figure 4. 4 Daily Flow Duration Curves of observed and estimated flow data for (E-43)

The relationship between the discharge and the probability of exceedance at the Chobela gauging station E-44 was regressed by using Equations 3.2 to 3.6. The results of the analysis showed that all of the models had good fits, with coefficients of determination  $R^2$  ranging from 61% to 99%. The cubic and exponential models have the best fit ( $R^2=99\%$  and  $R^2=92\%$ ), followed by the power, logarithmic and quadratic models ( $R^2=84\%$ ,  $R^2=84\%$  and  $R^2=61\%$ , respectively). The MSE= 50.07 was observed in the exponential model. The high flows were under-estimated and the low flows over-estimated. The results for the power model are shown in Figure 4.5.

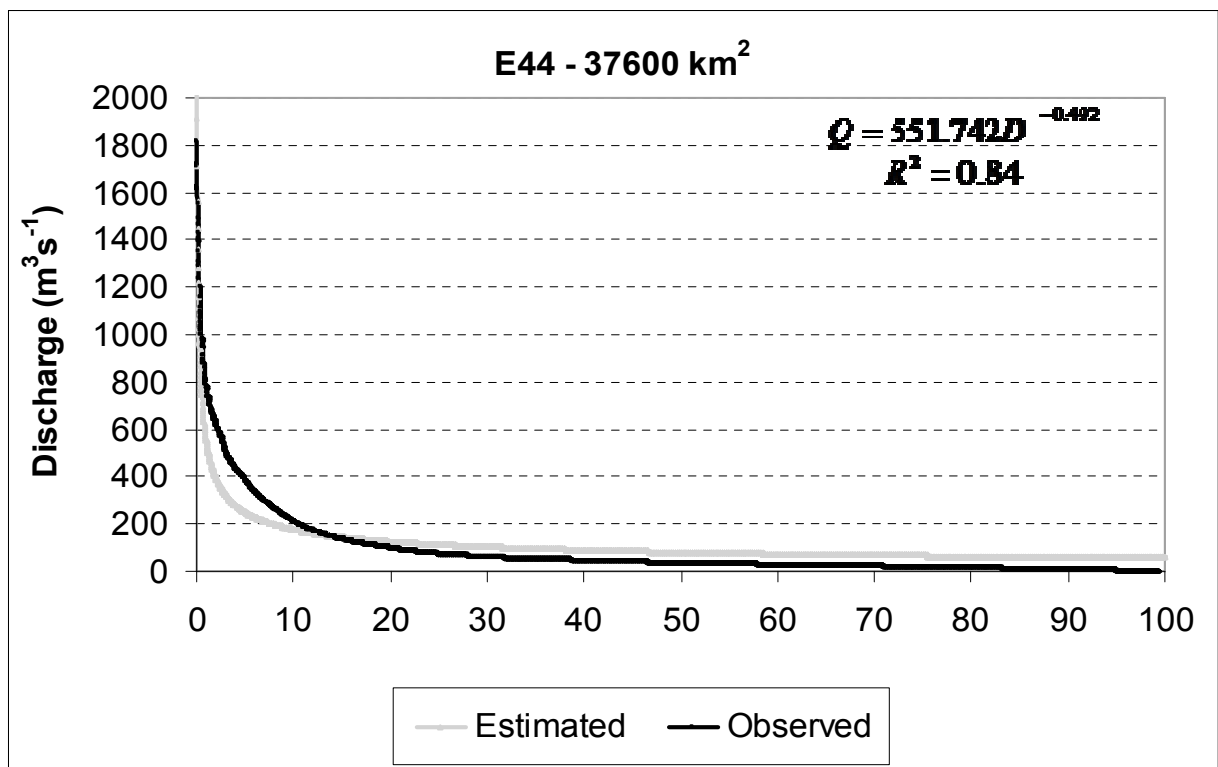


Figure 4. 5 Daily Flow Duration Curves of observed and estimated flow data for (E-44)

At the Queens River gauging station X2H008, the relationship between the discharge and the probability of exceedance was regressed by applying Equations 3.2 to 3.6. The results showed that the power and cubic models had the best fit ( $R^2=92\%$  and  $R^2=86\%$ ), followed by the quadratic, exponential and logarithmic models ( $R^2=80\%$ ;  $R^2=78\%$  and  $R^2=71\%$ , respectively). The models had good fits, with coefficient of determination  $R^2$  ranging from 71% to 92%. The MSE=0.42 was shown in the power model. The high and the low flows were well-estimated. The results for the power model are illustrated in Figure 4.6.

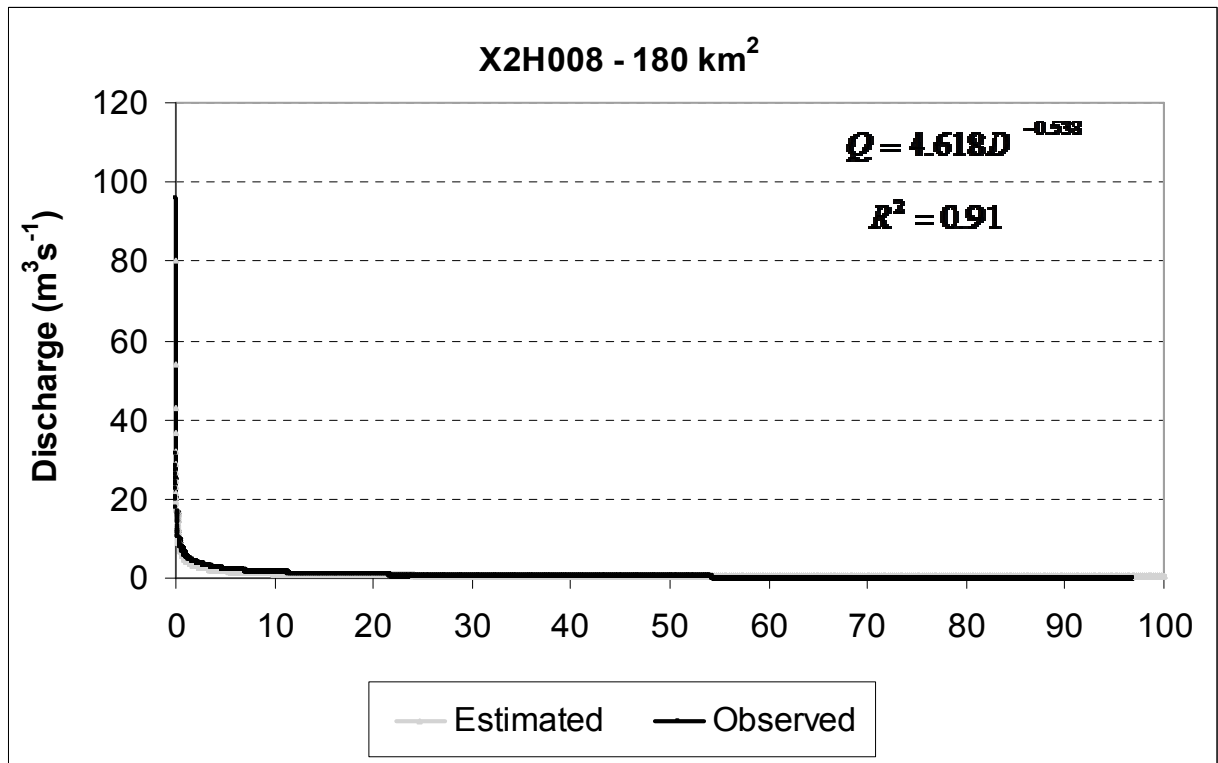


Figure 4.6 Daily Flow Duration Curves of observed and estimated flow data for (X2H008)

At the Noordkaap River gauging station X2H010, the relationship between the discharge and the probability of exceedance was regressed by using Equation 3.2 to 3.6. The results found in this analysis showed that the power and exponential models had the best fit ( $R^2=90\%$  and  $R^2=81\%$ ), followed by the cubic, quadratic and logarithmic models ( $R^2=79\%$ ;  $R^2=69\%$  and  $R^2=58\%$ , respectively). The models had good fits, with coefficient of determination  $R^2$  ranging from 58% to 90%. The  $MSE=0.77$  was found in the power model. The high and the low flows were well-estimated. The results for the power model are shown in Figure 4.7.

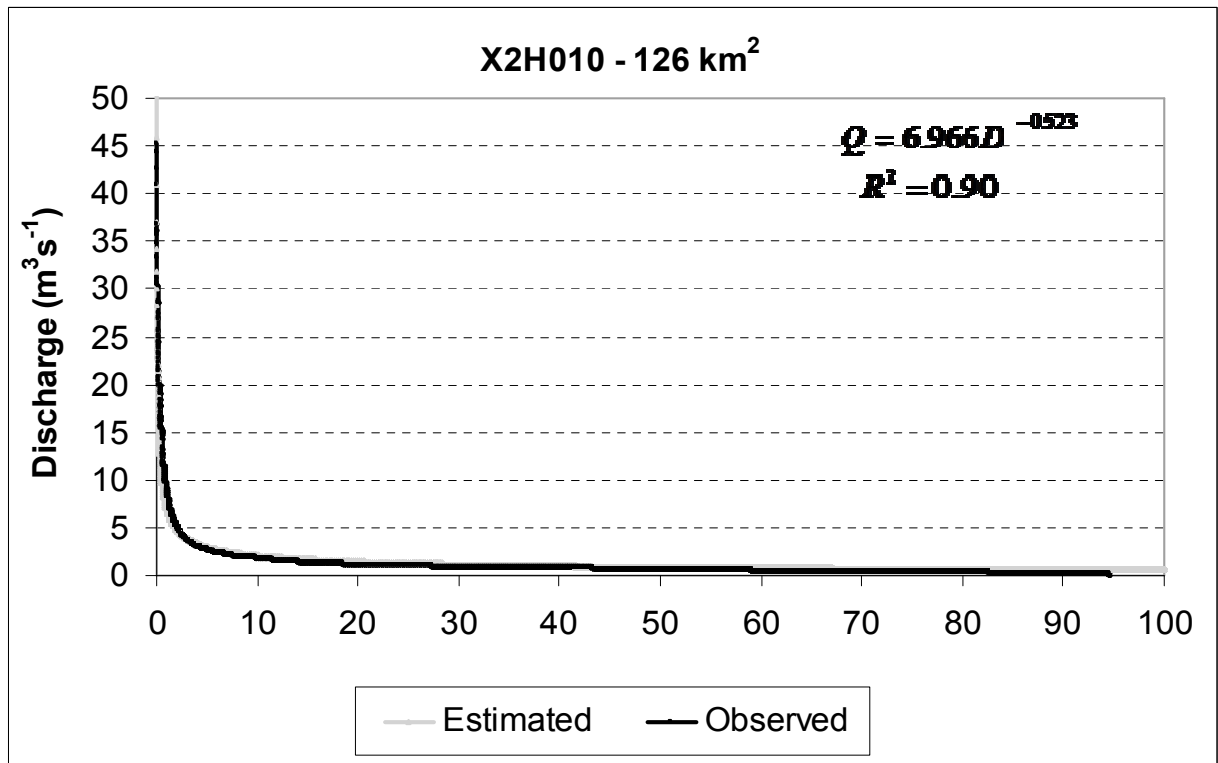


Figure 4.7 Daily Flow Duration Curves of observed and estimated flow data for (X2H010)

The relationship between the discharge and the probability of exceedance at the Suidkaap River gauging station X2H024 was regressed by using Equations 3.2 to 3.6. The results of the analysis show that all of the models are a good fit, with coefficients of determination  $R^2$  ranging from 76% to 97%. The power, cubic and quadratic models have the best fits ( $R^2=97\%$ ;  $R^2=89\%$  and  $R^2=84\%$ ), followed by the logarithmic and exponential models ( $R^2=80\%$  and  $R^2=76\%$ , respectively). The power model indicated that the  $MSE=0.16$ . The high flows and the low flows were well-estimated. Figure 4.8 illustrates the results of the power model.

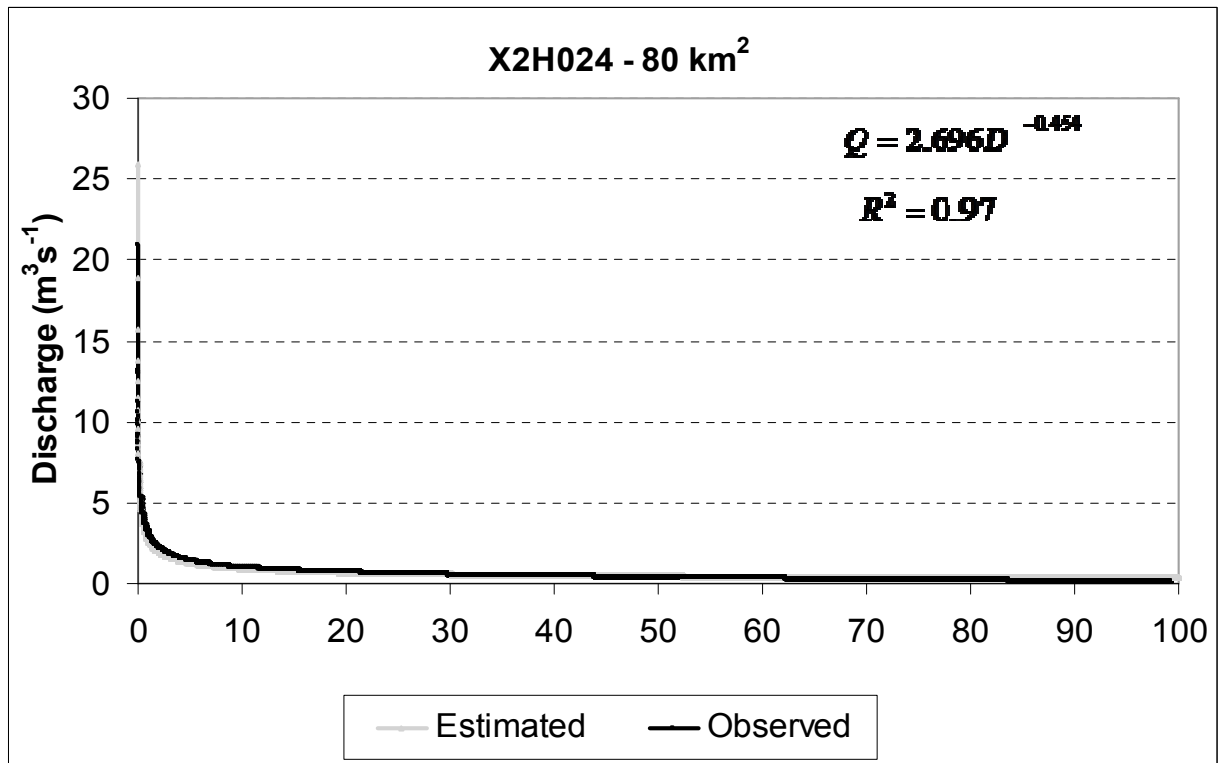


Figure 4. 8 Daily Flow Duration Curves of observed and estimated flow data for (X2H024)

The relationship between the discharge and the probability of exceedance at the Suartkoppiespruit gauging station X2H047 was regressed by using Equations 3.2 to 3.6. The results of analysis showed that all of the models are a good fit, with coefficients of determination  $R^2$  ranging from 81% to 93%. The power, cubic and quadratic models have the best fit ( $R^2=93\%$ ;  $R^2=93\%$  and  $R^2=90\%$ ), followed by the logarithmic and exponential models ( $R^2=83\%$  and  $R^2=81\%$ , respectively). The  $MSE=0.12$  was found in the cubic model. The high flows were under-estimated and the low flows over-estimated. The results for the power model are illustrated in Figure 4.9.

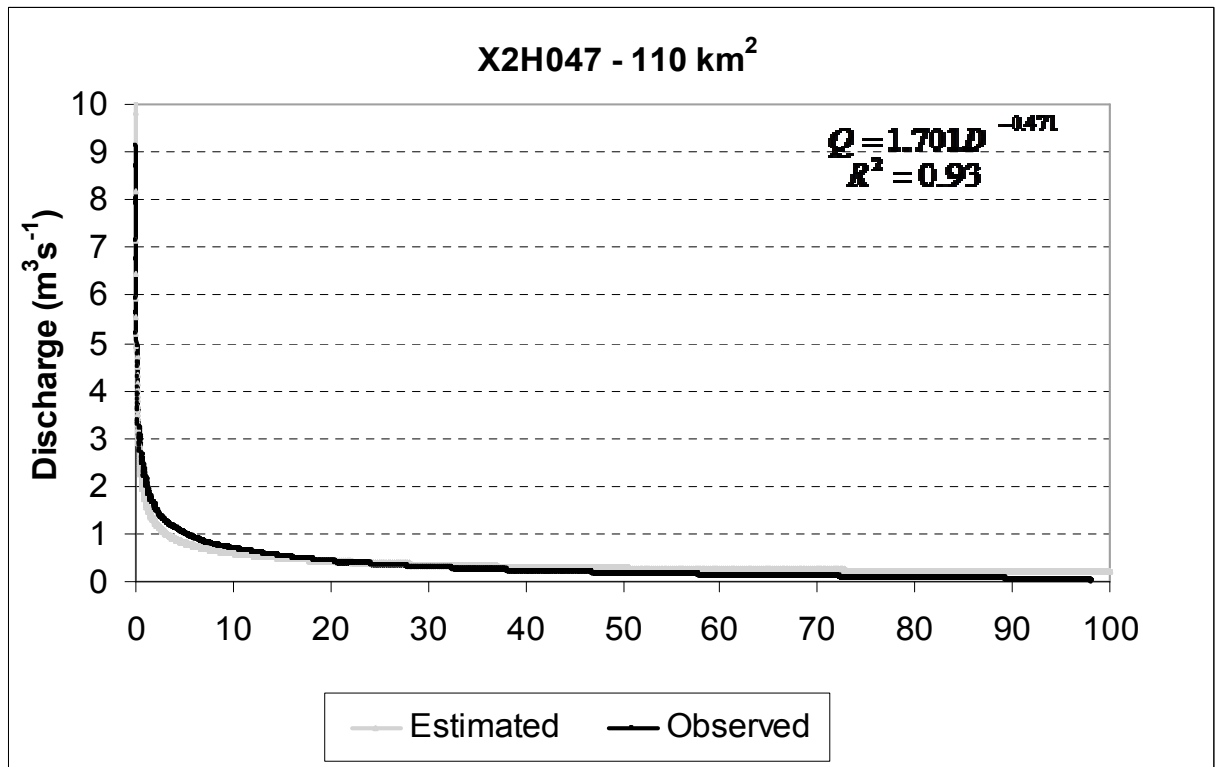


Figure 4.9 Daily Flow Duration Curves of observed and estimated flow data for (X2H047)

The relationship between the discharge and the probability of exceedance at the Sabie River gauging (Station X3H001) was regressed by using Equations 3.2 to 3.6. The results of analysis show that all of the models are a good fit, with coefficients of determination  $R^2$  ranging from 82% to 95%. The cubic, power and quadratic models have the best fit ( $R^2=95\%$ ;  $R^2=93\%$  and  $R^2=90\%$ , respectively), followed by the logarithmic and exponential models ( $R^2=85\%$ ;  $R^2=82\%$  and  $R^2=82\%$ , respectively). The  $MSE=0.49$  was shown in the cubic model. The high flows were under-estimated. The median and low flows were well-estimated. The results of the power model are illustrated in Figure 4.10.

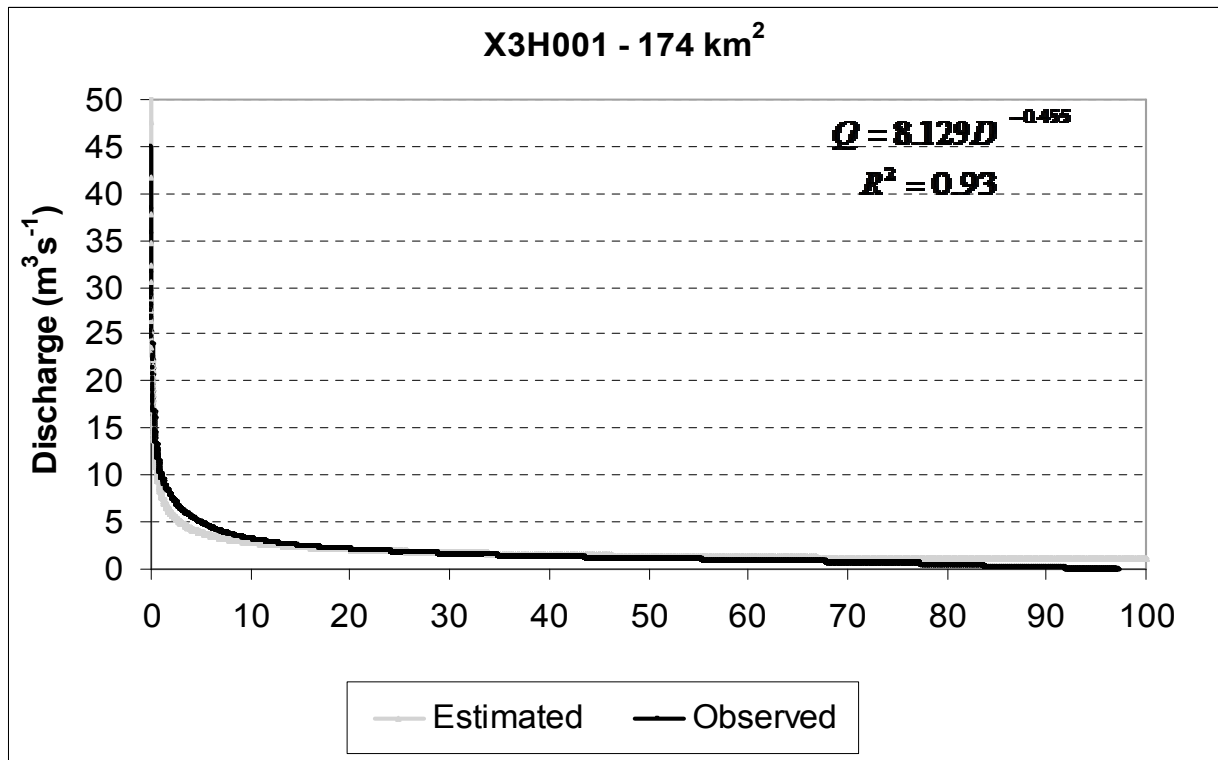


Figure 4. 10 Daily Flow Duration Curves of observed and estimated flow data for (X3H001)

The relationship between the discharge and the probability of exceedance at the Dawsonsspruit gauging (Station X2H012) was regressed by using Equations 3.2 to 3.6. The results of the analysis show that the power and exponential and cubic models are a good fit, with coefficients of determination  $R^2$  ranging from 59% to 97%. The power, exponential, and cubic models have the best fit ( $R^2=97\%$ ;  $R^2=82\%$  and  $R^2=59\%$ , respectively), followed by the quadratic and logarithmic models ( $R^2=49\%$ ;  $R^2=37\%$ , respectively). The  $MSE=0.22$  was found in the power model. The high flows were under-estimated. The median and low flows were well-estimated. The results of the power model are illustrated in Figure 4.11.

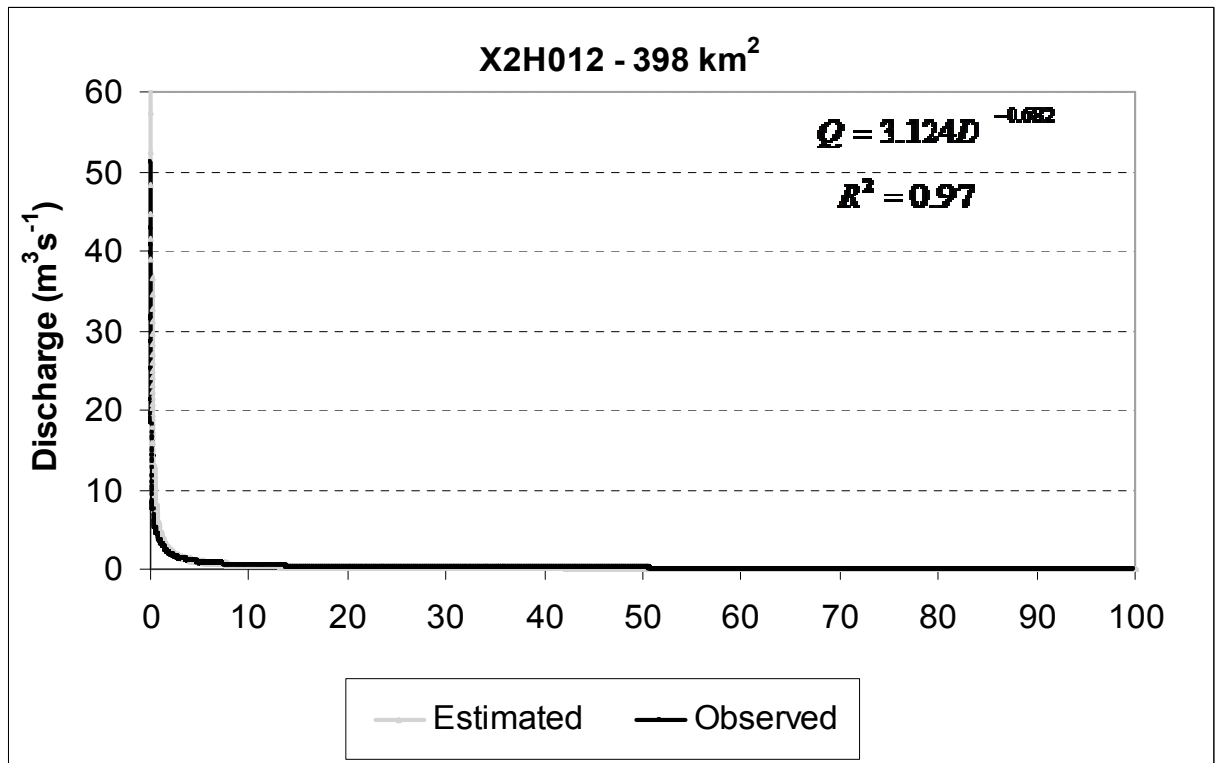


Figure 4. 11 Daily Flow Duration Curves of observed and estimated flow data for (X2H012)

The results of the regression analysis in the calibration of flow duration models for all gauging stations are summarized in Table 4.2. The average  $R^2$  at all stations of the exponential, power, logarithmic, quadratic and cubic models are 0.83, 0.91, 0.73, 0.68 and 0.84, respectively. The power model was the best-fitting (accurate) ( $R^2=91\%$ ) followed by the cubic model ( $R^2=84\%$ ). It was found that the power model in Equation 3.3 had the best fit among ten gauging stations because it showed the highest average value of  $R^2$  and seven times. The lowest average value of  $MSE=19.2$  was shown in the cubic model.

#### 4.3.2 Regionalization of the flow duration curves

Using Equations 3.7 to 3.10, MRA was used to predict the calibrated parameters ( $a$  and  $b$ ) in Equation 3.3, using precipitation ( $P$ ), Area ( $A$ ), hypsometric fall ( $H$ ) and length of the river ( $L$ ) as potential predictor variables. The parameters and morphoclimatic data used in the Multiple Regression Analysis are shown in Table 4.4.

Table 4. 4 Parameters, morphoclimatic data used in the MRA

Name and station code	a	b	<i>P</i> (mm)	<i>A</i> (km <sup>2</sup> )	<i>H</i> (m)	<i>L</i> (km)
Moamba- E-22	394.6384	0.4964	571	21850	208	42
Chinhanguanine E-27	615.1862	0.4784	574	31073	52	40
Magude- E-43	501.1255	0.5674	693	37500	393	102
Chobela- E-44	551.74201	0.4924	694	37600	408	109
Queens River- X2H008	4.6176	0.5384	820	180	820	10
Noordkaap River- X2H010	6.9657	0.5234	845	127	740	20
Suidkaap River- X2H024	2.6958	0.4542	814	82	780	9
Suarkoppiesspruit- X2H047	1.7006	0.4711	796	349	760	29
Sabie River- X3H001	8.1293	0.4549	1241	230	980	22
Dawsonsspruit- X2H012	3.1244	0.6821	398	200	871	29

### 4.3.3 Estimation of the parameter *a*

Using Equation 3.7, a scatter matrix for parameter *a*, and the variables area (*A*), precipitation (*P*), length (*L*) and hypsometric fall (*H*) was drawn as shown in Figure 4.12. This indicates that parameter *a* is approximately linearly related to area and length, and poorly related to precipitation and hypsometric fall.

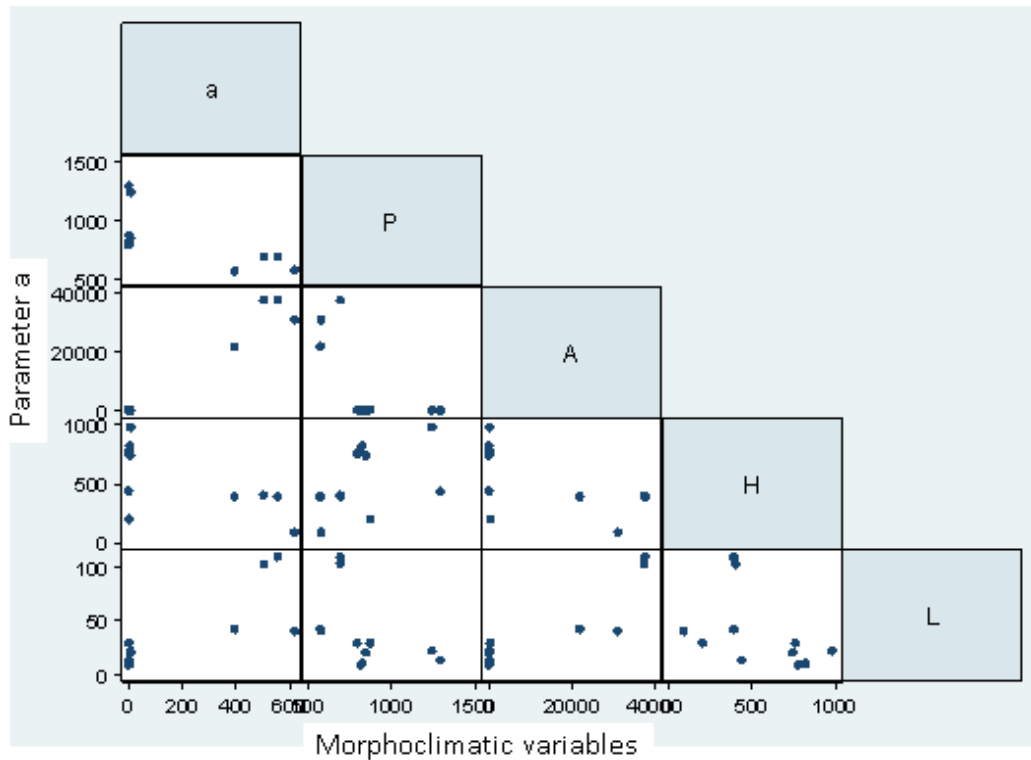


Figure 4. 12 Scatter matrix for variables  $a$ ,  $P$ ,  $A$ ,  $H$  and  $L$  for Model 3.7

However, the correlation matrix in Table 4.5 indicates that all variables are related to  $a$  at 5% significance level (all  $P$ -values  $< 0.05$ ). In other words, the probability that any of the predictors  $P$ ,  $A$ ,  $H$  and  $L$  has no effect in determining the regionalized value of the parameter  $a$  is less than the significance level of 0.05. Thus, each of the four predictors significantly affect the value of the parameter  $a$ .

Table 4. 5 Correlation matrix for variables  $a$ ,  $P$ ,  $A$ ,  $H$  and  $L$  for Model 3.7

(Note that the numbers in brackets are  $p$ -values. Here, a  $p$ -value indicates the probability that two variables are uncorrelated)

	<b>a</b>	<b>P</b>	<b>A</b>	<b>H</b>	<b>L</b>
<b>a</b>	1				
<b>P</b>	-0.6673 (0.0249)	1			
<b>A</b>	0.9797 (0.0000)	-0.6319 (0.0370)	1		
<b>H</b>	-0.6580 (0.0277)	0.4505 (0.1644)	-0.6075 (0.0474)	1	
<b>L</b>	0.7871 (0.0040)	-0.4595 (0.1551)	0.8867 (0.0003)	-0.4334 (0.1829)	1

Note that the correlation matrix indicates that the predictor variables are highly correlated:  $A$  and  $P$  ( $p$ -value=0.0370);  $H$  and  $A$  ( $p$ -value=0.0474) and  $L$  and  $A$  ( $p$ -value=0.0003).

Hence, there is possibly a problem of multi-collinearity, making some parameter estimates insignificant (Kutner *et al.*, 2004).

Fitting a linear regression model with  $a$  as the response variable, and the morphoclimatic variables as predictors, it was found that the regression model with Equation 3.7 with the equation is the following:

$$a = 92.7064 - 0.184P + 0.0200A - 0.0357H - 2.6783L, \text{ with } R^2 = 0.99 \text{ and } RMSE = 30.242.$$

However, the parameters estimate corresponding to the area ( $A$ ) ( $p$ -value  $< 0.0001$ ) and the length ( $p$ -value  $< 0.006$ ) are significantly different from zero. The best way of selecting significant predictors of  $a$  is to use step-wise regression, where the area ( $A$ ) and length ( $L$ ) were retained. The fitted model is:  $a = 54.8895 + 0.0209A - 2.8805L$ , with  $R^2 = 0.99$  and  $RMSE = 27.849$ . The root mean square error (RMSE) is expressed in  $\text{m}^3 \cdot \text{s}^{-1}$ .

A plot of the residuals versus fitted values in Figure 4.13 shows that residuals are randomly scattered around  $e=0$ . However, the variance seems to be constant. Although the model has a high coefficient of determination  $R^2$ , some estimated values of  $a$  are negative, namely for gauging stations X2H010, X2H047, X2H012 and X3H001.

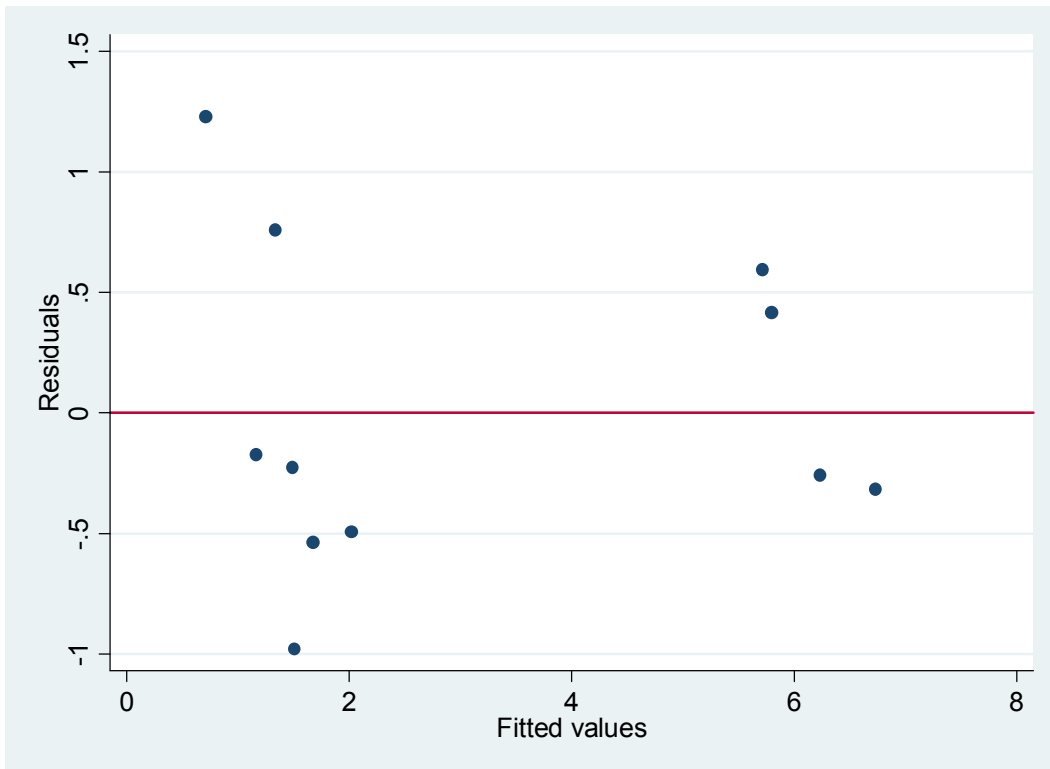


Figure 4. 13 Plotted graph of residual versus fitted values for model 3.7

When using Model 3.8  $a = b_0 P^{b_1} (A/L)^{b_2} H^{b_3}$ , the corresponding model on the log scale is:

$$\ln(a) = \ln(b_0) + b_1 \ln(P) + b_2 [\ln(A) - \ln(L)] + b_3 \ln(H)$$

The scatter matrix shown in Figure 4.14 reveals that the ratio of  $\ln(A/L)$  is approximately related to  $\ln(a)$ .

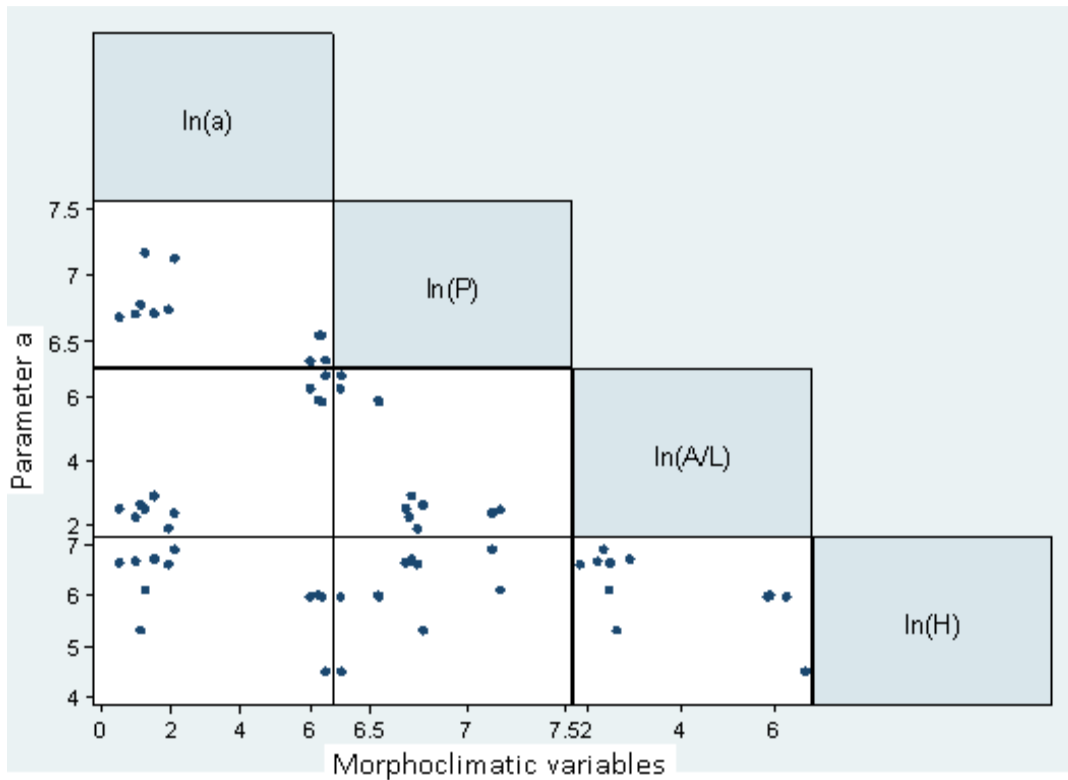


Figure 4. 14 Scatter matrix for the variables  $a$ ,  $P$ ,  $A$ ,  $H$  and  $L$  for Model 3.8

However, the correlation matrix in Table 4.6 indicates that  $\ln(a)$  is significantly correlated with two predictor variables;  $\ln(A/L)$  and  $\ln(P)$  at 5% significance level (Kutner *et al.*, 2004).

Table 4. 6 Correlation matrix for the variables  $a$ ,  $P$ ,  $A$ ,  $H$  and  $L$  for Model 3.8

	<b>la</b>	<b>IP</b>	<b>Al</b>	<b>IH</b>
<b>la</b>	1			
<b>IP</b>	-0.6964 (0.0173)	1		
<b>Al</b>	0.9644 (0.0000)	-0.7666 (0.0059)	1	
<b>IH</b>	-0.5476 (0.0812)	0.4929 (0.1234)	-0.6347 (0.0359)	1

Performing multiple regression with  $\ln(a)$  as the response variable, and  $\ln(P)$ ,  $\ln(L)$  and  $\ln(H)$  as predictor variables, resulted in:

$$\ln(a) = -11.0863 + 0.9667\ln(P) + 1.4438\ln(A/L) + 0.3741\ln(H), \quad \text{with } R^2 = 0.94 \quad \text{and} \\ RMSE = 0.72 .$$

However, it was found that only area by length  $\ln(A/L)$  is an important predictor of  $\ln(a)$  ( $p=0.001$ ). The model in step-wise regression is:  $\ln(a) = -1.6053 + 1.2538\ln(A/L)$ ; or  $a = e^{-1.6053}(A/L)^{1.2538}$  with  $R^2 = 0.93$  and  $RMSE = 0.70$ .

A plot of the residuals versus fitted values in Figure 4.15 shows that residuals are randomly scattered around  $e=0$ , and assumption of equal variance was not quite satisfied.

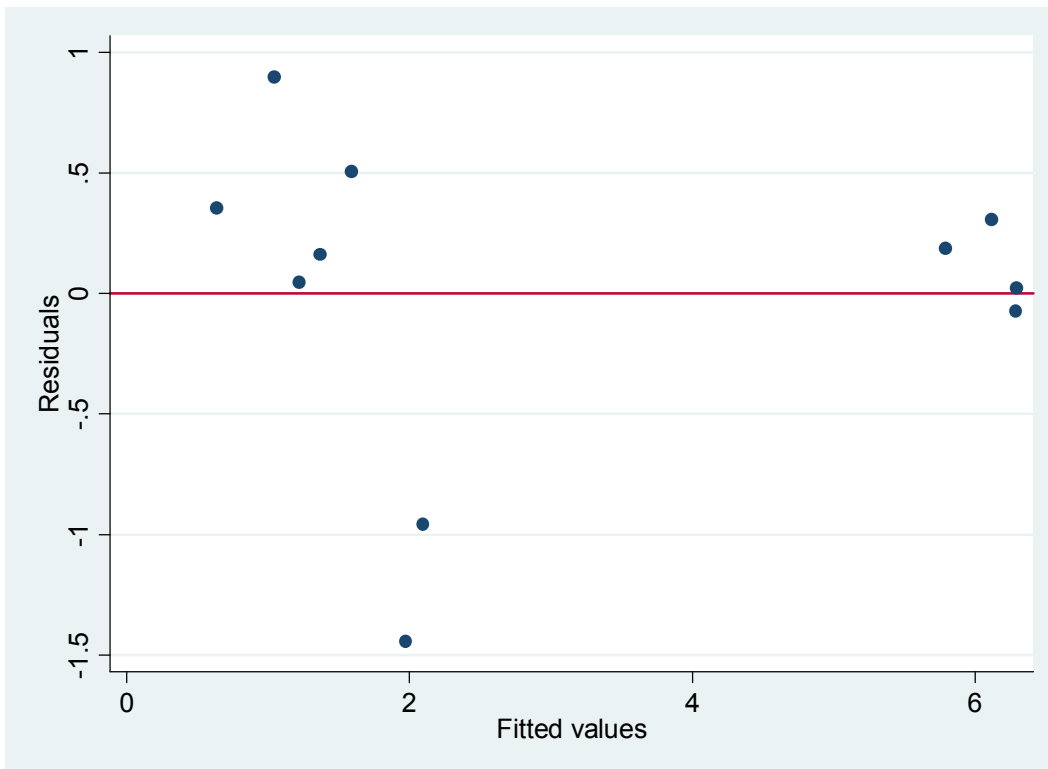


Figure 4. 15 Plotted graph of residual versus fitted values for model 3.8

Model 3.9 with equation  $a = b_0 P^{b_1} A^{b_2} (H/L)^{b_3}$  can be written in the log scale as  $\ln(a) = \ln(b_0) + b_1 \ln(P) + b_2 \ln(A) + b_3 [\ln(H) - \ln(L)]$ . The scatter matrix of the variables  $\ln(a)$ ,  $\ln(P)$ ,  $\ln(A)$ ,  $\ln(H)$  and  $\ln(H/L)$  is shown in Figure 4.16 and indicates that  $\ln(a)$  is positively and linearly related with  $\ln(A)$  and negatively linearly related with precipitation ( $P$ ) and ratio of hypsometric fall and length  $\ln(H/L)$ .

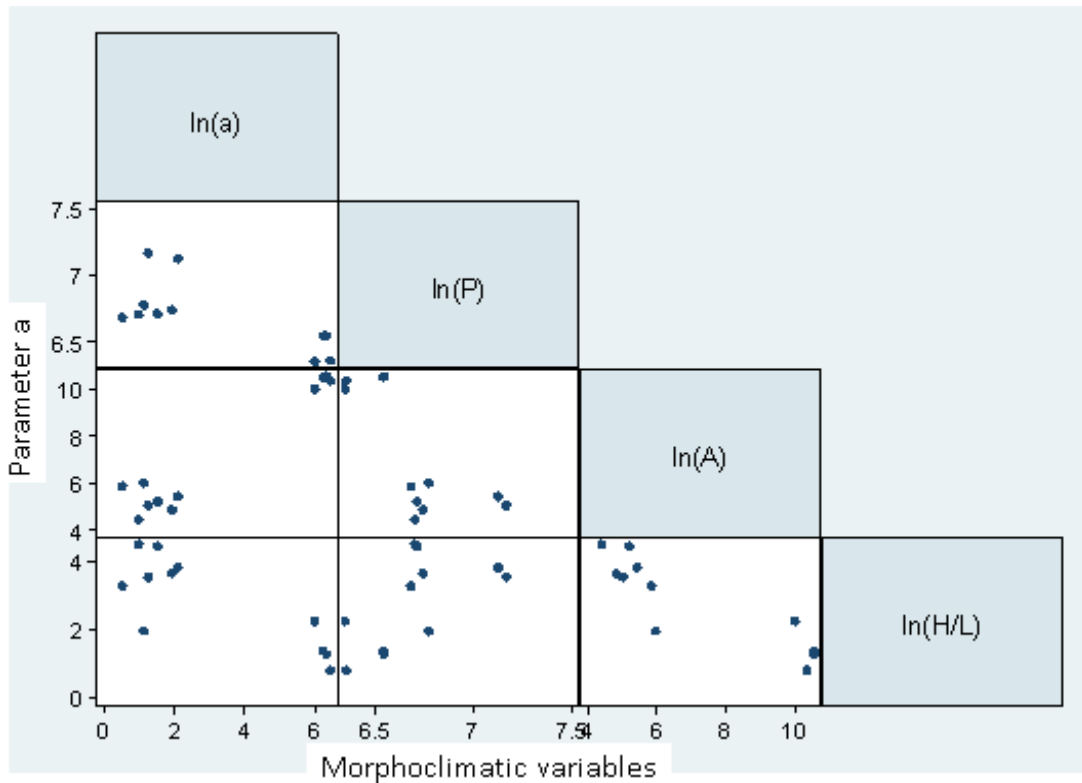


Figure 4. 16 Scatter matrix for the variables  $a$ ,  $P$ ,  $A$ ,  $H$  and  $L$  for Model 3.9

Indeed, the correlation matrix in Table 4.7 indicates that  $\ln(a)$  is significantly correlated with all the three predictor variables,  $\ln(P)$ ,  $\ln(A)$  and  $\ln(H/L)$  at the significance level of 5%.

Table 4. 7 Correlation matrix for variables  $a$ ,  $P$ ,  $A$ ,  $H$  and  $L$  for Model 3.9

	<b>la</b>	<b>IP</b>	<b>IA</b>	<b>HI</b>
<b>la</b>	1			
<b>IP</b>	-0.6964 (0.0173)	1		
<b>IA</b>	0.9645 (0.0000)	-0.7334 (0.0102)	1	
<b>HI</b>	-0.8069 (0.0027)	0.6065 (0.0479)	-0.8882 (0.0003)	1

Performing multiple regressions with  $\ln(a)$  as the response variable, and  $\ln(P)$ ,  $\ln(A)$  and  $\ln(H/L)$  as predictor variables, gives the following:  
 $\ln(a) = -9.4525 + 0.4484\ln(P) + 1.1642\ln(A) + 0.4681\ln(H/L)$ , with  $R^2 = 0.94$  and  $RMSE = 0.71$  It was found that only area  $\ln(A)$  is significant and an important predictor variable of  $a$ , ( $p=0.001$ ). The step-wise regression also confirmed that the results of the

regression analysis that only  $\ln(A)$  was the significant predictor of  $\ln(a)$ . The model in step-wise regression is:  $\ln(a) = -3.4262 + 0.9225\ln(A)$  or  $a = e^{-3.4262}A^{0.9225}$ ; with  $R^2 = 0.92$  and  $RMSE = 0.70$ .

A plot of the residuals versus fitted values in Figure 4.17 shows that there is a violation of random scattering and the constancy of variance of residuals.

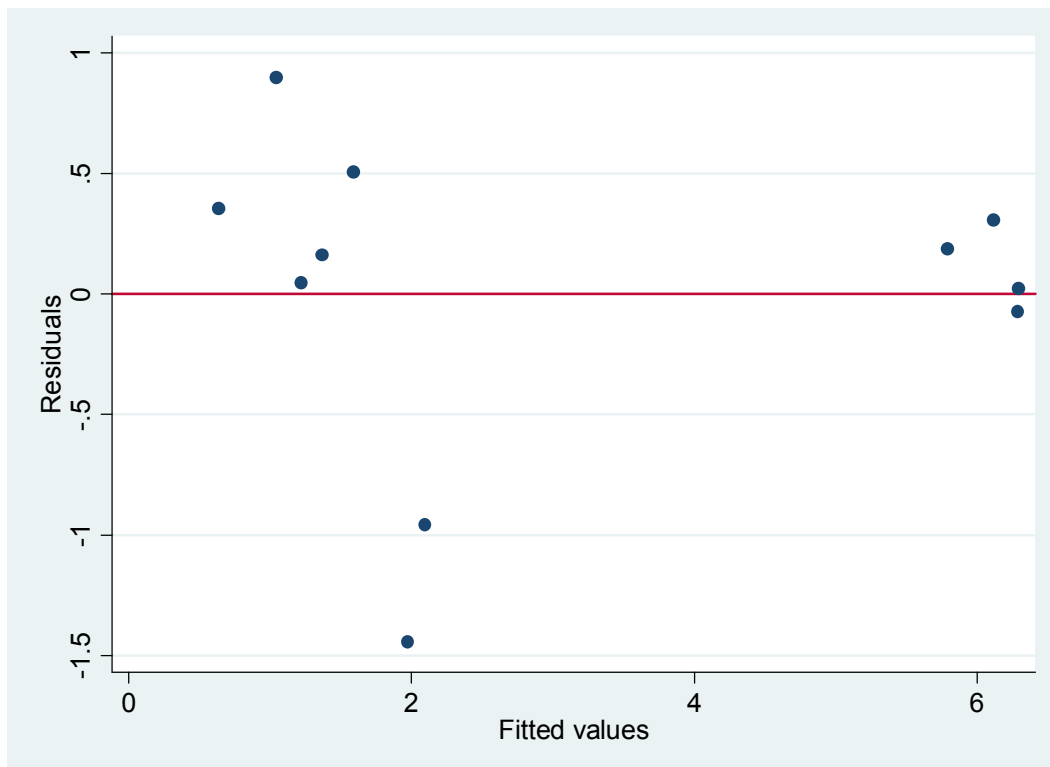


Figure 4. 17 Plotted graph of residual versus fitted values for Model 3.9

Model 3.10 with equation  $a = b_0P^{b_1}A^{b_2}H^{b_3}L^{b_4}$  can be written in the log scale as follows:

$$\ln(a) = \ln(b_0) + b_1 \ln(P) + b_2 \ln(A) + b_3 \ln(H) + b_4 \ln(L)$$

The scatter matrix of the variables  $\ln(a)$ ,  $\ln(P)$ ,  $\ln(A)$ ,  $\ln(H)$  and  $\ln(L)$  as shown in Figure 4.18 reveals that  $\ln(a)$  is positively related to area  $\ln(A)$  and  $\ln(L)$ , and negatively related to precipitation  $\ln(P)$  and hypsometric fall  $\ln(H)$ .

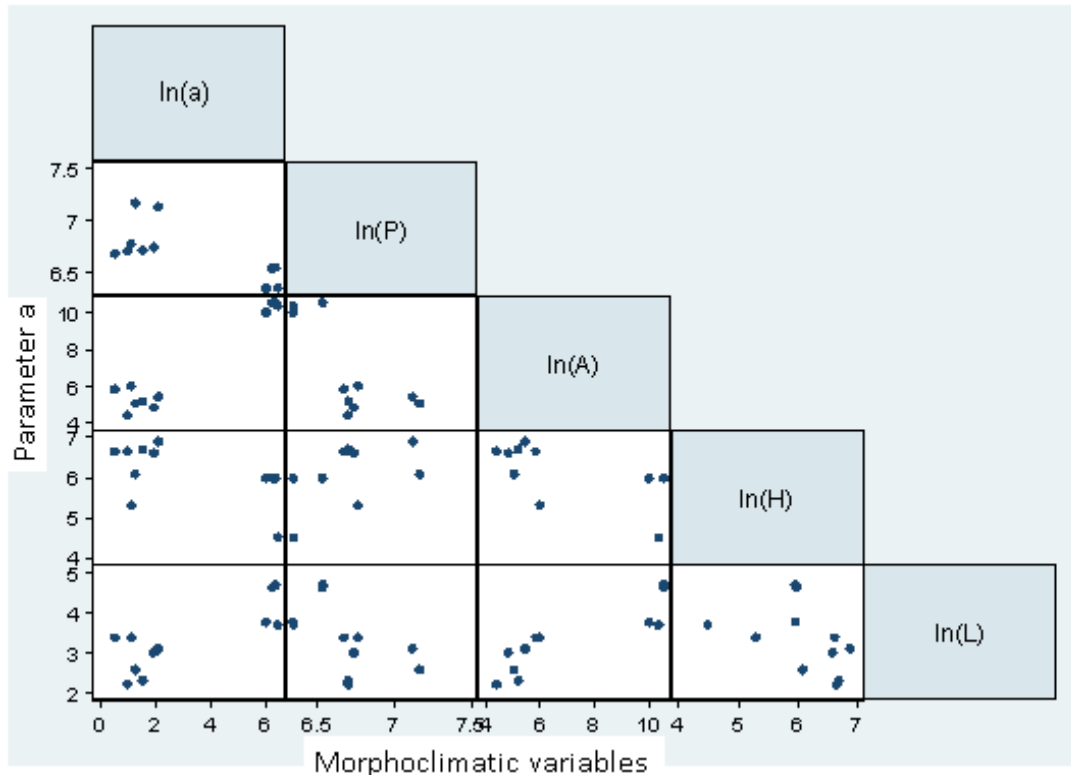


Figure 4. 18 Scatter matrix for the variables  $a$ ,  $P$ ,  $A$ ,  $H$  and  $L$  for Model 3.10

However, the correlation matrix in Table 4.8 indicates that  $\ln(a)$  is significantly correlated with three predictor variables;  $\ln(P)$ ,  $\ln(A)$ , and  $\ln(L)$  at the significance level of 5%. Note that the correlation matrix indicates that the predictor variables are highly correlated or there is some collinearity between  $\ln(A)$  and  $\ln(P)$  ( $p$ -value=0.0102), between  $\ln(H)$  and  $\ln(A)$  ( $p$ -value=0.0487), and between  $\ln(L)$  and  $\ln(A)$  ( $p$ -value=0.0004).

Table 4. 8 Correlation matrix for variables  $a$ ,  $P$ ,  $A$ ,  $H$  and  $L$  for Model 3.10

	<b>la</b>	<b>IP</b>	<b>IA</b>	<b>IH</b>	<b>IL</b>
<b>la</b>	1				
<b>IP</b>	-0.6964 (0.0173)	1			
<b>IA</b>	0.9645 (0.0000)	-0.7334 (0.0102)	1		
<b>IH</b>	-0.5476 (0.0812)	0.4929 (0.1234)	-0.6047 (0.0487)	1	1
<b>IL</b>	0.8005 (0.0031)	-0.5319 (0.0921)	0.8794 (0.0004)	-0.4327 (0.1838)	

Performing multiple regressions with  $\ln(a)$  as the response variable, and  $\ln(P)$ ,  $\ln(A)$ ,  $\ln(H)$  and  $\ln(L)$  as predictor variables, result in:

$$\ln(a) = -10.5170 + 0.8077\ln(P) + 1.2855\ln(A) + 0.3366\ln(H) - 0.8848\ln(L),$$

with  $R^2 = 0.95$  and  $RMSE = 0.73$ . However, note that only area  $\ln(A)$  is significant variable predictor of  $a$  ( $p$ -value=0.009). The model in step-wise regression or backward elimination confirms that only  $\ln(A)$  is significant predictor of  $\ln(A)$  and the resulting model is:  $\ln(a) = -3.4262 + 0.9225\ln(A)$  or  $a = e^{-3.4262} A^{0.9225}$ ; with  $R^2 = 0.93$  and  $RMSE = 0.70$ . This model is the same as the one found using of Model 3.9.

#### 4.3.4 Estimation of the parameter $b$

An inspection of the values of parameter  $b$  in Table 4.8 indicates that  $b$  is close to 0.5 for all stations. Hence  $b$  may be independent from the values of variables  $P$ ,  $A$ ,  $H$  and  $L$ . The scatter matrix of the variables  $b$ ,  $P$ ,  $A$ ,  $H$  and  $L$  displayed in Figure 4.20 confirms that there is no relationship between  $b$  and predictor variables  $P$ ,  $A$ ,  $H$  and  $L$ .

According to the results, using the fitting Models 3.7 to 3.10, the scatter matrix, correlation matrix, multiple linear regressions and stepwise regression showed that none of the prediction variables has an influence on the value of  $b$ . The parameter  $b$  should then be constant. Multiple linear regression and stepwise regression show that  $b$  was estimated by  $b = b_0 = 0.5067$  for Model 3.7. It was found that  $b = b_0$  satisfies all models from 3.7 to 3.10,  $b = b_0$  and  $b_1 = b_2 = b_3 = b_4 = 0$ .

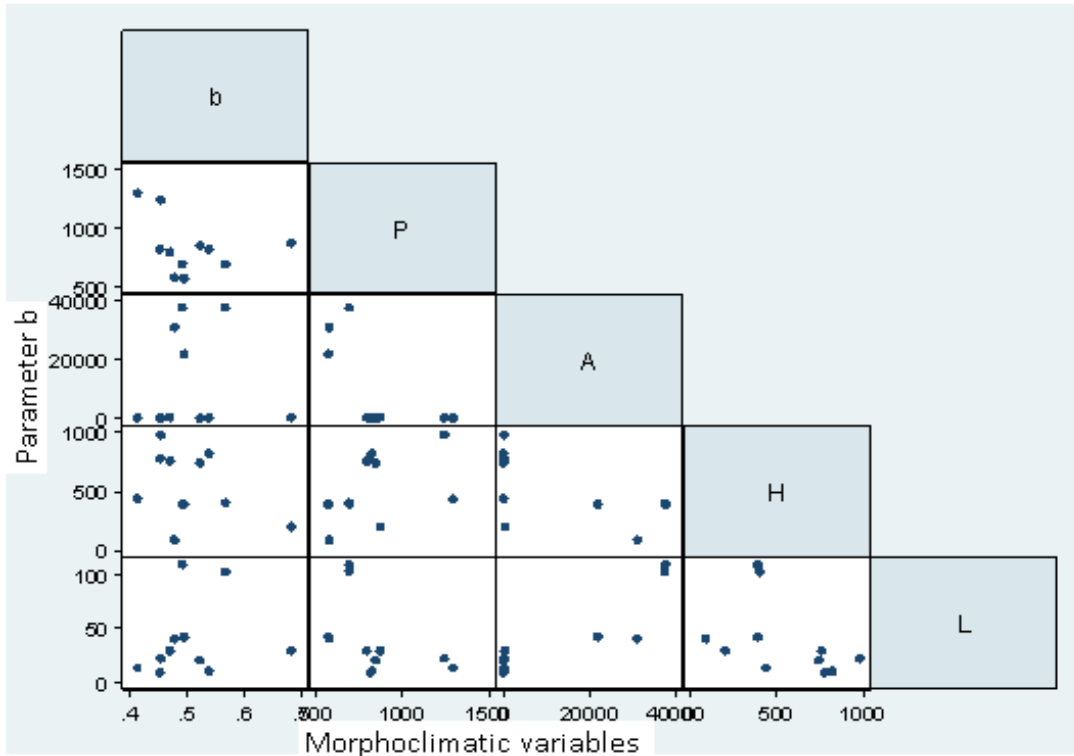


Figure 4. 19 Scatter matrix for the variables  $b$ ,  $P$ ,  $A$ ,  $H$  and  $L$  for Models 3.7 to 3.10

Table 4. 9 Correlation matrix for variables  $b$ ,  $P$ ,  $A$ ,  $H$  and  $L$  for Models 3.7 to 3.10

	<b>b</b>	<b>P</b>	<b>A</b>	<b>H</b>	<b>L</b>
<b>b</b>	1				
<b>P</b>	-0.2992 (0.3714)	1			
<b>A</b>	0.0556 (0.8711)	-0.6319 (0.0370)	1		
<b>H</b>	-0.3588 (0.2786)	0.4505 (0.1644)	-0.6075 (0.0474)	1	
<b>L</b>	0.1975 (0.5605)	-0.4595 (0.1551)	0.8867 (0.0003)	-0.4334 (0.1829)	1

For all Models 3.8 to 3.10,  $\ln b = -0.6882$ , hence  $b = 0.5067$ . It was concluded that with this value of the parameters, the calibration or power model can be written as:

$$a = e^{-1.6053} (A/L)^{1.2538} \text{ and } b = 0.5067; Q = e^{-1.6053} (A/L)^{1.2538} D^{-0.5067}.$$

### 4.3.5 Summary of regionalization

In summary, using Equation 3.3 the discharge ( $Q$ ) for a given probability of exceedance ( $D$ ) at ungauged sites can be estimated using the catchment specific drainage area ( $A$ ) divided by the length ( $L$ ). Then, the model in the power Equation 3.3 can be written as:

$$Q = e^{-1.6053} (A/L)^{1.2538} D^{-0.5067} \quad \text{Equation (4.1)}$$

The regional Equation 4.1 can be used at any ungauged sites within the catchment to be studied, mainly in the mountainous regions.

For Models 3.8 to 3.10, the same procedure of starting with a scatter matrix was used, followed by the correlation matrix, multiple regression analysis and step-wise regression. The result shows that  $b = 0.5067$  or  $\log b = -0.69$ . Hence, the parameter  $b$  is approximately 0.5. The results of the above discussion are summarised in Table 4.10.

Table 4. 10 Performance of Regional model

Models		$R^2$	RMSE ( $m^3 \cdot s^{-1}$ )	$P$ -value	Equations
3.7	MRA	0.99	30.24	$A = 0.000$ $L = 0.014$	
	STEPWISE	0.99	27.85		$a = 54.8895 + 0.0209A - 2.8805L$
3.8	MRA	0.94	0.72	0.000	
	STEPWISE	0.93	0.70		$a = e^{-1.6053} (A/L)^{1.2538}$
3.9	MRA	0.94	0.71	0.001	
	STEPWISE	0.92	0.70		$a = e^{-3.4262} A^{0.9225}$
3.10	MRA	0.95	0.73	0.009	
	STEPWISE	0.92	0.73		$a = e^{-3.4262} A^{0.9225}$

#### 4.4 Verification

In this section, the regional model developed was evaluated at two other locations, the Mac-Mac River gauging station (X3H003) on the South African side and the Ressano Garcia gauging station (E-23) on the Mozambican side along Inkomati River Catchment, which were not used in the calibration procedure. Tables 3.2 and 3.3 contain all the characteristics of the stations and the morphoclimatic characteristics of these drainage catchments.

Equation 4.1 was used to check if it fits the data of the two selected gauging stations. The Flow Duration Curves of observed and estimated discharges were plotted, using the model in Equation 4.1.

The result in Figure 4.21 shows that the estimated discharge was well-estimated in the high and low flows. The Mozambican gauging station (Ressano Garcia E-23) was also used for verification. Figure 4.22 shows that the estimated values are very high and located in the high flows range. The correlation between observed versus estimated values seems to be good, except in the interval from 0% to approximately 18% exceedance probability. As a consequence, the accuracy of the model will be affected.

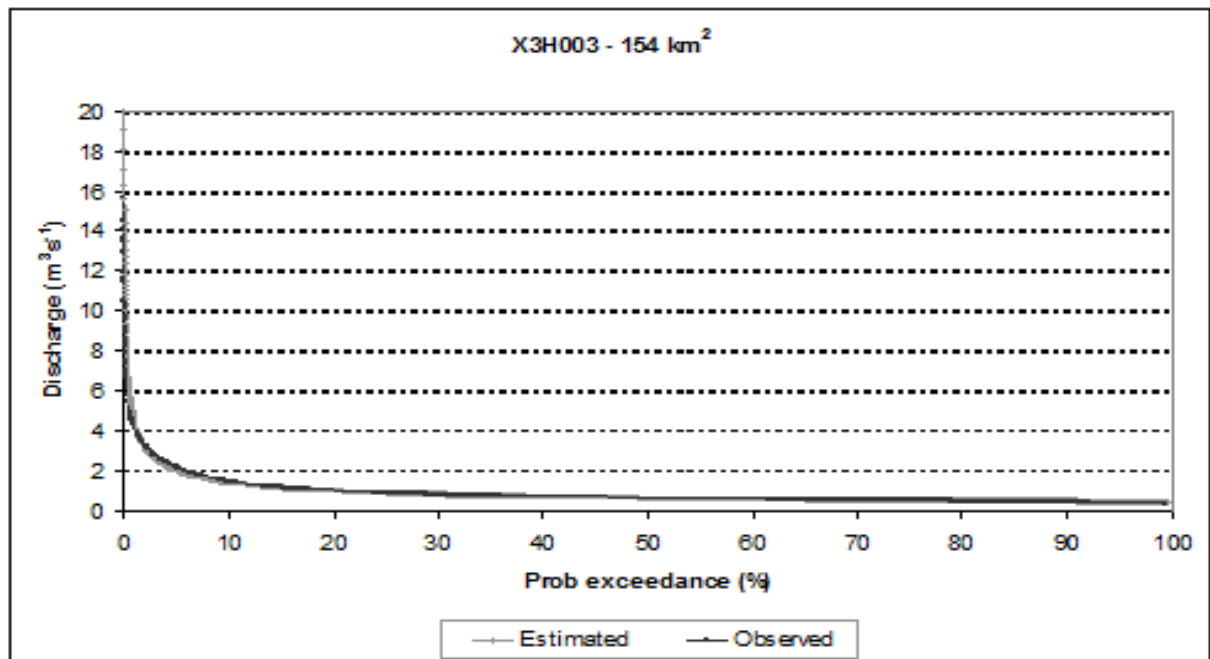


Figure 4. 20 Flow Duration Curves at the Geelhoutboom gauging station X3H003

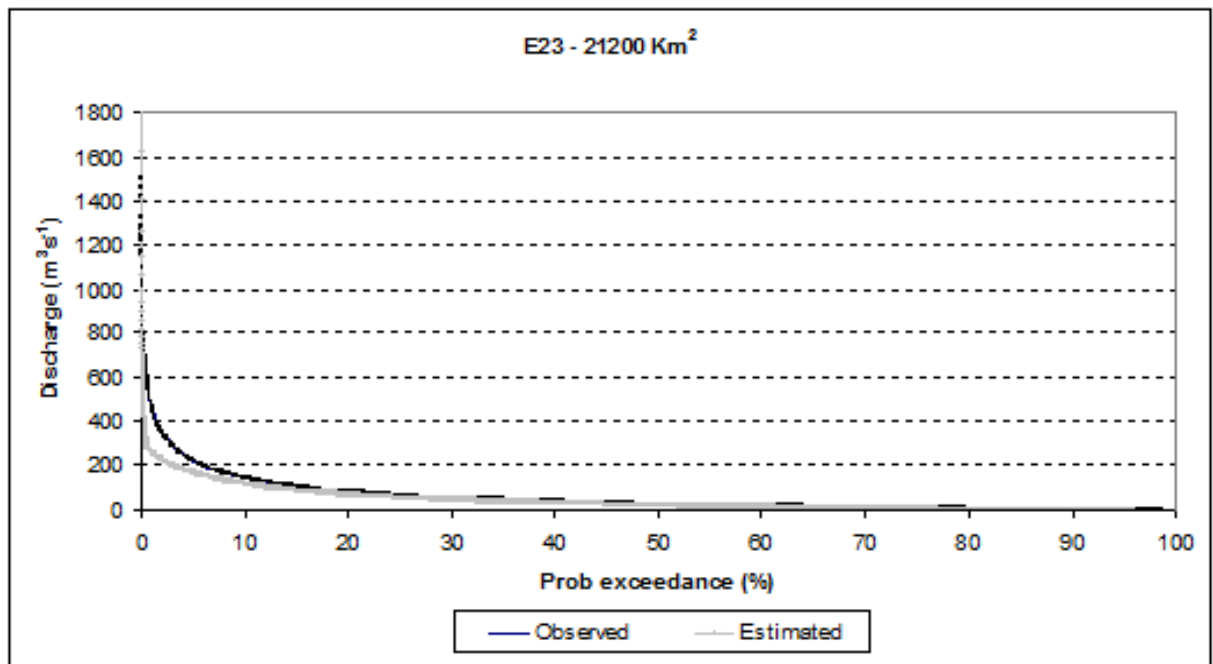


Figure 4. 21 Flow Duration Curves at the Ressano Garcia gauging station E-23

The accuracy of the regional models was examined from observed and estimated discharges by calculating the root mean square error, using Equation 3.11. The results of the analysis showed that the estimated accuracy was satisfactory and equal to  $RMSE=3\%$  for the Mac-Mac River gauging station X3H003 and presented good accuracy of prediction, taking into account the root mean square error ( $RMSE$ ). The result of the analysis for the Ressano Garcia gauging station E-23 showed that the estimated accuracy was not satisfactory because the root mean square error was equal to  $RMSE=22\%$ . The error in the regional prediction at this station was therefore high and was unacceptable.

#### 4.5 Calculation of the power at Mac-Mac River and Ressano Garcia gauging stations (X3H003 and E-23)

Power was estimated using Equation 2.3 for an assumed head of 25m based on topography and for assumed overall plant efficiencies of 50% and 70%. The 10%, 60% and 90% flow exceedance percentiles were used in the calculations, taking into consideration high, medium and low discharges.

The results are summarized in Table 4.11 and indicate that the Mac-Mac River gauging station X3H003 and Ressano Garcia gauging station E-23 can produce power, using the

potential power generated values of the same probabilities of exceedance. The amount of power that can be obtained from a stream depends on the quantity of water flow, the suitable height which the water falls (head) and the plant efficiency to convert mechanical energy to electrical energy (Ramachandra *et al.*, 2004; Hussein and Raman, 2010).

Table 4. 11 Results of power from observed discharge at two selected stations

Station	Discharge ( $\text{m}^3 \cdot \text{s}^{-1}$ )			Head (m)	Efficiency (%)	Specific . weight ( $\gamma$ ) ( $\text{N} \cdot \text{m}^{-3}$ )	Power ( $P_i$ ) (kw)		
	10%	60%	90%				10%	60%	90%
X3H003	1.444	0.555	0.394	25	50	9.8	17.7	6.7	4.8
X3H003	1.444	0.555	0.394	25	70	9.8	24.8	9.5	6.8
E-23	142.8	14.6	1.0	25	50	9.8	1,749.3	178.9	12.3
E-23	142.8	14.6	1.0	25	70	9.8	2,449.0	250.4	0.2

## 5. DISCUSSION, CONCLUSIONS AND RECOMMENDATIONS

In this study, the main objectives were to: (i) derive and verify a simple methodology to estimate daily streamflow quantiles at gauged sites, using flow duration curves (FDCs), (ii) to regionalise the FDCs in order to estimate daily streamflow quantiles at ungauged sites, and (iii) to demonstrate the use of the regionalised FDCs to estimate potential hydropower production at selected sites in the Inkomati River Catchment.

In this study, the results indicate that most of the South African gauging stations are located in higher-lying mountainous regions, where a high average rainfall occurs (Smakhtin and Toulouse, 1998). The results indicate that the Mozambican side has lower rainfall, declivity and less favourable conditions for hydropower generation than on the South African side. This is attributed to the large catchments and flood plain areas (Viola *et al.*, 2010; Nobert *et al.*, 2011).

FDCs can be divided into five flow duration intervals, namely, high flows (0-10% exceedance), moist or wet conditions (10-40% exceedance) and medium range flows (40-60% exceedance), dry or drought conditions (60-90% exceedance) and low flows (90-100% exceedance) (Viola *et al.*, 2010; Nobert *et al.*, 2011). The results for the gauges in South Africa indicate that the rivers are perennial, as also shown by (Smakhtin, 2001a).

The differences in the low flow regions of the superimposed curves (FDCs) may be partly attributed to the inaccuracies of low-flow measurements, but they are mostly due to the fact that some observed records (e.g. gauging stations X2H072, X3H007 and X3H011) include the period of the most severe drought on record, while the others do not. Some of the rivers in the region, which are normally perennial, ceased to flow for a short period and that has affected the shape of some flow duration curves in the area of extreme low flows (Smakhtin *et al.*, 1997; Smakhtin, 1997; Smakhtin and Toulouse, 1998; Smakhtin, 2001b). Most of the rivers in South Africa are perennial, with a clear wet season from December to March. This season is followed by a long recession period, with minimum flows from July to September.

Vogel and Fennessey (1994); Vogel and Fennessey (1995) state that the shape of the FDC can be determined by rainfall pattern, the size and the physiographic characteristics of the

catchment. The shape can also be influenced by water resources development (e.g. regulated flow, such as the Inkomati River Catchment) and type of land-use (Smakhtin, 2001b). Water resource management is one of the most important issues that can help to understand the impact of land-use changes on streamflow. Therefore, it can be useful in predicting the change of the Flow Duration Curve due to land-use changes (Shao *et al.*, 2009a), while steep curves indicate a small or variable baseflow contribution (Smakhtin and Toulouse, 1998; Smakhtin, 2001b; Patel, 2007).

The strength of using FDCs to estimate streamflow in gauged stations was corroborated by many authors in literature (Mimikou and Kaemaki, 1985a; Vogel and Fennessey, 1994; Vogel and Fennessey, 1995; Castellarin *et al.*, 2004; Rojanamon *et al.*, 2007; Younis and Hasan, 2014). The FDC method was successfully applied in this study, to estimate streamflow quantiles in the Inkomati River Catchment in South Africa. The results obtained in this study showed that the gauging stations had reliable streamflow data, namely Moamba, Chinhanganine, Magude, Chobela, Sassenheim, Bellevue, Glenthorpe, Kindergoed, Ethna and Geelhoutboom gauging stations, FDC was vigorous, reliable and successful. However, stations with unreliable streamflow data, including Ressano Garcia, Machatuine, Bobole, Incoluane, M. major, Sabie, Nsikazi River, White Water River and Marite River, were not used in the analysis.

The morphoclimatic parameters, such as catchment area, hypsometric fall, mean annual precipitation and river length were utilized in this study, to identify sites with potential catchments for hydropower production. Regionalisation was performed based on these site characteristics.

In this study, the FDCs of gauging stations previously selected in the Inkomati River were constructed and fitted by five distribution equations, namely, the exponential, power, logarithmic, quadratic and cubic equations. The calibration of FDCs at the selected stations demonstrated that the power model was the best fit for all the stations, with an average coefficient of determination  $R^2$  equal to 0.91. This finding was different from that of previous researches, such as (Mimikou and Kaemaki, 1985b), who proposed to use cubic equation in modelling the FDC. The power model was therefore selected for use in the regionalisation of the FDC models because it showed the highest average value of  $R^2$  and

seven times than other models. It can be concluded that the Flow Duration Curves of observed and estimated discharges were well-estimated, especially in the South African gauging stations. For all the sites, the power model was to be the best estimator of FDC at gauged sites.

The regionalisation approach was applied, in order to overcome limitations related to the scarcity of the gauged sites in the catchment, mainly in the remote and inaccessible areas. Multiple regression analysis allowed for the derivation of a regional equation, which was used to estimate streamflow at ungauged sites within the Inkomati River Catchment. For regionalisation, the drainage area and the length of the main river were the most significant factors for streamflow quantile estimation at ungauged sites. Scatter matrices, correlation matrices, multiple linear regressions, stepwise regression and the plotting of residual errors were used to obtain suitable regional equation.

Verification was performed to evaluate the accuracy of the regional model, using the root mean square error (*RMSE*), which is expressed in percentage. The root mean square error, which is an accuracy estimator, was used to determine how well estimated streamflow compared with observed streamflow. The streamflow in the regional model was well estimated in the Mac-Mac River gauging stations as indicated by the low root mean square error of 3%. However, for the Ressano Garcia, the model was not satisfactory, as depicted by the high root mean square error of 22%. Possible reasons for high root mean square error could be attributed to a reduction in streamflow due to water usage. It could also be caused by agriculture practices, including irrigation water abstraction, which are likely to reduce streamflows to downstream areas.

The power was calculated, based on flow, head height and plant efficiency, to convert mechanical energy to electrical energy, as given by Equation 2.3. The results of power obtained from observed discharge at two selected gauging stations (Mac-Mac River and Ressano Garcia), both are situated in the South African sides, respectively, were shown in Table 4.11. The power produced in these two gauging stations at 10% of probability exceedance, was higher than the power produced at 60% and 90% of probability exceedance. These results might probably be caused by the high, values of the discharge, especially in Ressano Garcia, where the catchment area is bigger than the Mac-Mac River.

The amount of power is given in kilowatts/day. The power produced in these gauging stations showed that micro-, mini- or small hydropower plants could be set up, according to the classification of hydropower plants (Balat, 2006). In this study, it was concluded that this kind of hydropower plant could provide an ideal way of producing electricity in rural and mountainous areas, where the demand is scattered and relatively low.

In this study, the development of a regional model was undertaken, where the model in Equation 3.8 was selected to be the best model to explain the spatial variation of the parameters of the flow duration curves. The drainage area ( $A$ ) and the length of the river ( $L$ ) are the most significant parameters.

The different results obtained in this study and in literature can be attributed to the different time scales of the analyses, different geographic regions and different climate characteristics. Through this study, the FDC approach showed its ability to represent and assess high flows and low flows, using observed and estimated discharges (Shao *et al.*, 2009b; Warburton, 2010). Applying the regionalisation of FDCs, it was possible to determine a regional equation (Equation 4.1 in Table 4.10) in the Results Chapter. This equation can be used at ungauged sites, such as the Inkomati River Catchment, mainly on the South African side (Mimikou and Kaemaki, 1985b).

The Mac-Mac River gauging station (X3H003) was not used in the development of the model and was selected from the Sabie sub-catchments on the South African side for independent evaluation of the method, because it is located upstream in the mountainous regions. The Ressano Garcia gauging station (E-23) is also located upstream of the Moamba gauging station (E-22) and it is also characterized by high topography, compared with other stations on the Mozambican side. The result supports the recommendations by (Franchini and Suppo, 1996; Rojanamon *et al.*, 2007), where the model that gives the smallest *RMSE* value can be used to predict flow at the ungauged sites, which are located within the catchment area. The results obtained from verification and accuracy of the regional models suggests that land use change is one of the factors that have influenced the flow pattern at the Ressano Garcia gauging station.

One of these two gauging stations used in the independent evaluation of the method is located on the South African side in the mountains and has a relatively small drainage area with higher MAP, compared with the MAP on the Mozambican side. This shows that the flows at higher altitudes exhibit larger variability, compared with flows at lower altitudes (Arora *et al.*, 2005). (Castellarin *et al.*, 2004; Rojanamon *et al.*, 2007) stated that the conditions mentioned are favourable for the development of small hydropower plants. The Ressano Garcia gauging station E-23 is located upstream on the Mozambican side. It has high values of flow at certain times, mainly during the rainy season. As a result, the values of potential power which could be produced are also very high. However, the region is located in a floodplain, where the conditions mentioned are not favourable for the installation of SHPs.

It was also concluded that most of the stations suitable for the installation of SHPs in the Inkomati River Catchment fall in the South African side. Possible reasons are (i) availability of perennial streams, and (ii) good terrain characteristics (e.g. suitable head and available streamflow rate). By contrast, most of the sites on the Mozambican side are characterized by regions with low topography (< 600m elevation), large catchment areas and high discharges. Hence, it is recommended that the Mozambican side might not potentially be suitable for SHPs, and further investigation is required.

This result suggests that the reduction in streamflow at the border station of Ressano Garcia can be attributed to other factors, such as the use of water upstream in Komatipoort side. Another direct effect of agriculture on streamflow takes place through irrigation water abstraction, as large volumes of water are diverted from the river system, consequently reducing the flows to downstream areas.

It is recommended, therefore, that the network of the meteorological and hydrological stations be improved to cover larger areas and more catchments, particularly in Mozambique. For further investigation, the procedures followed in this research should be carefully applied to other regions, taking into consideration the similar geomorphologic features, such as homogeneity in terms of climate, topography, hydrology and other relevant factors.

The accurate application of the FDC method and the monitoring of the rivers regimes should be done on a national level, to help the water resources managers and planners to develop and implement the best water management practices.

## 6. REFERENCES

- Al-Hallaq, A.H. and B.S.A. Elaish. 2008. Determination of Mean Areal Rainfall in the Gaza Strip Using Geographic Information System (GIS) Technique. *Journal of Pure & Applied Sciences* 5.
- Alejandrino, A.A. and T.A. McNally. 1983. Regionalized flow duration for Philippines. *Journal of Water Resources Planning and Management* 109: 320-330.
- Archfield, S.A., P.A. Steeves, J.D. Guthrie and K.G.R. III. 2013. Towards a publicly available, map-based regional software tool to estimate unregulated daily streamflow at ungauged rivers. *Geoscientific Model development* 6: 101-115.
- Arora, M., N. Goel, P. Singh and R. Singh. 2005. Regional flow duration curve for a Himalayan river Chenab. *Nordic hydrology* 36: 193-206.
- Aslan, Y., O. Arslan and C. Yasar. 2008. A sensitivity analysis for the design of small-scale hydropower plant: Kayabogazi case study. *Renewable Energy* 33: 791-801.
- Associates, S.A. 2003. Three Basins Study - National Water Resources Development Plans for Maputo, Umbeluzi and Inkomati River Basins and Joint Water Resources Development Study of Maputo, Umbeluzi and Inkomati National River Basins. Sweco in association with Consultec and Impacto, Maputo.
- Bakis, R. and A. Demirbas. 2004. Sustainable development of small hydropower plants (SHPs). *Energy sources* 26: 1105-1118.
- Balat, M. 2006. Hydropower systems and hydropower potential in the European Union countries. *Energy sources* 28: 965-978.
- Ballance, A., D. Stephenson, R. Chapman and J. Muller. 2000. A geographic information systems analysis of hydro power potential in South Africa. *Journal of Hydroinformatics* 2: 247-254.
- Bartle, A. 2002. Hydropower potential and development activities. *Energy Policy* 30: 1231-1239.
- Bayraktar, H., F.S. Turalioglu and Z. Sen. 2005. The estimation of average areal rainfall by percentage weighting polygon method in Southeastern Anatolia Region, Turkey. *Atmospheric research* 73: 149-160.
- Bekoe, E.O., F.Y. Logah, K. Kankam-Yeboah and B. Amisingo. 2012. Low flow characterization of a coastal river in Ghana. *International Journal of Modern Engineering Research* 2(5): 3210-3219.

- Berk, R.A. 1988. Casual inference for statistical data. In N. J. Smelser, ed Hand book of sociology. Beverly Hills: *Sage Publications*, pp 155-172.
- Blanco, C., Y. Secretan and A. Mesquita. 2008. Decision support system for micro-hydropower plants in the Amazon region under a sustainable development perspective. *Energy for Sustainable Development* 7: 25-33.
- Castellarin, A., G. Camorani and A. Brath. 2007. Predicting annual and long-term flow-duration curves in ungauged basins. *Advances in Water Resources* 30: 937-953.
- Castellarin, A., G. Galeati, L. Brandimarte, A. Montanari and A. Brath. 2004. Regional flow-duration curves: reliability for ungauged basins. *Advances in Water Resources* 27: 953-965.
- Cheng, L., M. Yaeger, A. Viglione, E. Coopersmith, S. Ye and M. Sivapalan. 2012. Exploring the physical controls of regional patterns of flow duration curves - Part 1: Insights from statistical analyses. *Hydrology Earth System Science Discussion* 9: 7001-7034.
- Consultec and BKS. 2001. Joint Inkomati Basin Study (JIBS). Consultec in association with BKS. Maputo.
- Copestake, P. and A.R. Young. 2008. How much water can a river give? Uncertainty and the flow duration curve. *BHS 10th National Hydrology Symposium. Exter*. p. 59-66.
- Corston, R. and A.M. Colman. 2003. A crash course in SPSS for Windows for version 10 and 11 2nd ed. Wiley, *Malden, MA*.
- Dudhani, S., A. Sinha and S. Inamdar. 2006. Assessment of small hydropower potential using remote sensing data for sustainable development in India. *Energy policy* 34: 3195-3205.
- Fennessey, N. and R.M. Vogel. 1990. Regional flow-duration curves for ungauged sites in Massachusetts. *Journal of Water Resources Planning and Management* 116: 530-549.
- Fiedler, F.R. 2003. Simple, Practical Method for Determining Station Weights Using Thiessen Polygons and Isohyetal Maps. *Journal of Hydrologic Engineering* 8(4): 219.
- Franchini, M. and M. Suppo. 1996. Regional analysis of flow duration curves for a limestone region. *Water resources management* 10: 199-218.
- Ganora, D., P. Claps, F. Laio and A. Viglione. 2009. An approach to estimate nonparametric flow duration curves in ungauged basins. *Water Resources management* 45: 1-34.

- Hussein, I. and N. Raman. 2010. Reconnaissance studies of micro-hydro potential in Malaysia. International conference on Energy and Sustainable Development: Issues and Strategies IEEE. Chiang Mai, Thailand. p. 1-10.
- JIBS. 2001. *Joint Incomati Basin Study Report Phase 2*. Maputo/Johannesburg.
- Kaldellis, J. 2007. The contribution of small hydro power stations to the electricity generation in Greece: Technical and economic considerations. *Energy Policy* 35: 2187-2196.
- Karamouz, M., F. Szidarovszky and B. Zahraie. 1991. *Water resources systems analysis*. Lewis Publishers.
- Kaygusuz, K. 2002. Sustainable development of hydroelectric power. *Energy sources* 24: 803-815.
- Kennedy, P. 2003. *A guide to Econometrics*. MIT Press, Cambridge, MA.
- Kim, J. 2004. Regionalization of daily flow characteristics using GIS and Spatial Interpolation Algorithm: The case of Brazos River Basin  
1-23.
- Kusre, B., D. Baruah, P. Bordoloi and S. Patra. 2010. Assessment of hydropower potential using GIS and hydrological modeling technique in Kopili River basin in Assam (India). *Applied Energy* 87: 298-309.
- Kutner, M.H., C.J. Nachtsheim and J. Neter. 2004. *Applied Linear Regression Models*. McGraw Hills, Irwin.
- McCuen, R.H. 1993. *Microcomputer applications in statistical hydrology*. 1st ed. Prentice Hall, Gale.
- Mimikou, M. and S. Kaemaki. 1985a. Regionalization of flow duration characteristics. *Journal of Hydrology* 82: 77-91.
- Mimikou, M. and S. Kaemaki. 1985b. Regionalization of flow duration characteristics. *Journal of Hydrology* 82: 77-91.
- Mohamoud, Y.M. 2008. Prediction of daily flow duration curves and streamflow for ungauged catchments using regional flow duration curves. *Hydrological sciences journal* 53: 706-724.
- NDW. 1991. *Monography of the Incomati River Basin*. Mozambique.
- Niadas, I.A. 2005. Regional flow duration curve estimation in small ungauged catchments using instantaneous flow measurements and a censored data approach. *Journal of hydrology* 314: 48-66.

- Nobert, J., J. Ndayizeye and S. Mkhandi. 2011. Regional flow duration curve estimation and its application in assessing low flow characteristics for ungauged Catchment. A case study of Rwegura Catchment-Burundi. *Nile Basin Water Science & Engineering Journal* 4(1): 14-23.
- Paish, O. 2002. Small hydro power: technology and current status. *Renewable and Sustainable Energy Reviews* 6: 537-556.
- Patel, J.A. 2007. Evaluation of low flow estimation techniques for ungauged catchments. *Water and Environment Journal* 21: 41-46.
1997. Integrating ArcView and Spatial Analyst Extension with the PRISM Climate Expert System. International Users Conference, *Environmental System Research Institute*, San Diego, CA.
- Ramachandra, T., R.K. Jha, S.V. Krishna and B. Shruthi. 2004. Spatial decision support system for assessing micro, mini and small hydel potential. *Journal of Applied Sciences* 4: 596-604.
- Ramachandra, T. and B. Shruthi. 2007. Spatial mapping of renewable energy potential. *Renewable and Sustainable Energy Reviews* 11: 1460-1480.
- Rojanamon, P., T. Chaisomphob and T. Bureekul. 2009. Application of geographical information system to site selection of small run-of-river hydropower project by considering engineering/economic/environmental criteria and social impact. *Renewable and Sustainable Energy Reviews* 13: 2336-2348.
- Rojanamon, P., T. Chaisomphob and W. Rattanapitikon. 2007. Regional flow duration model for the Salawin river basin of Thailand. *Science Asia: Journal of Science Society Thailand* 33: 411-419.
- Shao, Q., L. Zhang, D. Yongqin and P.S. Vijay. 2009a. A new method for modelling flow duration curves and predicting streamflow regimes under altered land-use conditions. *Hydrological sciences journal* 54: 606-622.
- Shao, Q., L. Zhang, D. YONGQIN and P.S. VIJAY. 2009b. A new method for modelling flow duration curves and predicting streamflow regimes under altered land-use conditions/Une nouvelle méthode de modélisation des courbes de débits classés et de prévision des régimes d'écoulement sous conditions modifiées d'occupation du sol. *Hydrological sciences journal* 54: 606-622.

- Shoaib, S.A., A. Bardossy, T. Wgener, Y. Huang and N. Sultana. 2013. A different light in predicting ungauged basins: Regionalization approach based on Eastern USA catchments. *Jordan Journal of Civil Engineering and Architecture* 7(3): 364-378.
- Smakhtin, V. 2001a. Low flow hydrology: a review. *Journal of Hydrology* 240: 147-186.
- Smakhtin, V. 2001b. Low flow hydrology: a review. *Journal of Hydrology* 240: 147-186.
- Smakhtin, V., D. Hughes and E. Creuse-Naudin. 1997. Regionalization of daily flow characteristics in part of the Eastern Cape, South Africa. *Hydrological sciences journal* 42: 919-936.
- Smakhtin, V. and M. Toulouse. 1998. Relationships between low-flow characteristics of South African streams. *Water SA-Pretoria* 24: 107-112.
- Smakhtin, V.Y. 1997. Regional low-flow studies in South Africa. *Iahs Publications*: 125-132.
- Taucale, F. 2007. *Environmental Profile of the Inkomati River Basin in Mozambique*. Eduardo Mondlane University, Department of Geography, Maputo.
- Tsoutsos, T., E. Maria and V. Mathioudakis. 2007. Sustainable siting procedure hydroelectric plants: The Greek experience. *Energy Policy* 35: 2946-2959.
- Vaz, A.C. and P. Van der Zaag. 2003. *Sharing the Incomati Waters: cooperation and competition in the balance, from potential conflict to cooperation potential*. Final text. Maputo - Mozambique, Harare - Zimbabwe UNESCO-IHE/IHP/WWAP., Paris. p. 102.
- Viola, F., L. Noto, M. Cannarozzo and G.L. Loggia. 2010. Regional flow duration curves for ungauged sites in Sicily. *Hydrology and Earth System Sciences Discussions* 7: 7059-7078.
- Vogel, R.M. and N. Fennessey. 1994. Flow-duration curves. I: New interpretation and confidence intervals. *Journal of Water Resources Planning and Management* 120: 485-504.
- Vogel, R.M. and N.M. Fennessey. 1995. Flow Duration Curves II: a Review of Applications in Water Resources Planing. *Journal of the American Water Resources Association* 31: 1029-1039.
- Warburton, M. 2010. Interactive comment on “Confirmation of ACRU model results for applications in land use and climate change studies” by ML Warburton et al. *Hydrology and Earth System Sciences* 14: 2399-2414.

- Younis, A.M. and I.F. Hasan. 2014. Prediction of flow duration curve for seasonal rivers in Iraq. *Jordan Journal of Civil Engineering* 8(1): 30-42.
- Yu, P.S., T.C. Yang and Y.C. Wang. 2002. Uncertainty analysis of regional flow duration curves. *Journal of Water Resources Planning and Management* 128: 424-430.
- Yüksek, Ö. and K. Kaygusuz. 2006. Small hydropower plants as a new and renewable energy source. *Energy Sources, Part B: Economics, Planning, and Policy* 1: 279-290.
- Yuksel, I. 2008. Hydropower in Turkey for a clean and sustainable energy future. *Renewable and Sustainable Energy Reviews* 12: 1622-1640.
- Yuksel, I. 2007. Development of hydropower: a case study in developing countries. *Energy Source, Part B. Economics, Planning and Policy* 2: 113-121.

## 7. APPENDICES

### 7.1 Appendix 1

Flow duration curves were plotted from all selected gauging stations on the Mozambican and South African sides. These Figures are results of the assessment and reliability of Mozambican and South African observed flow data. The plots of daily FDCs (logarithmic scale) are presented in Figures 7.1 to 7.12

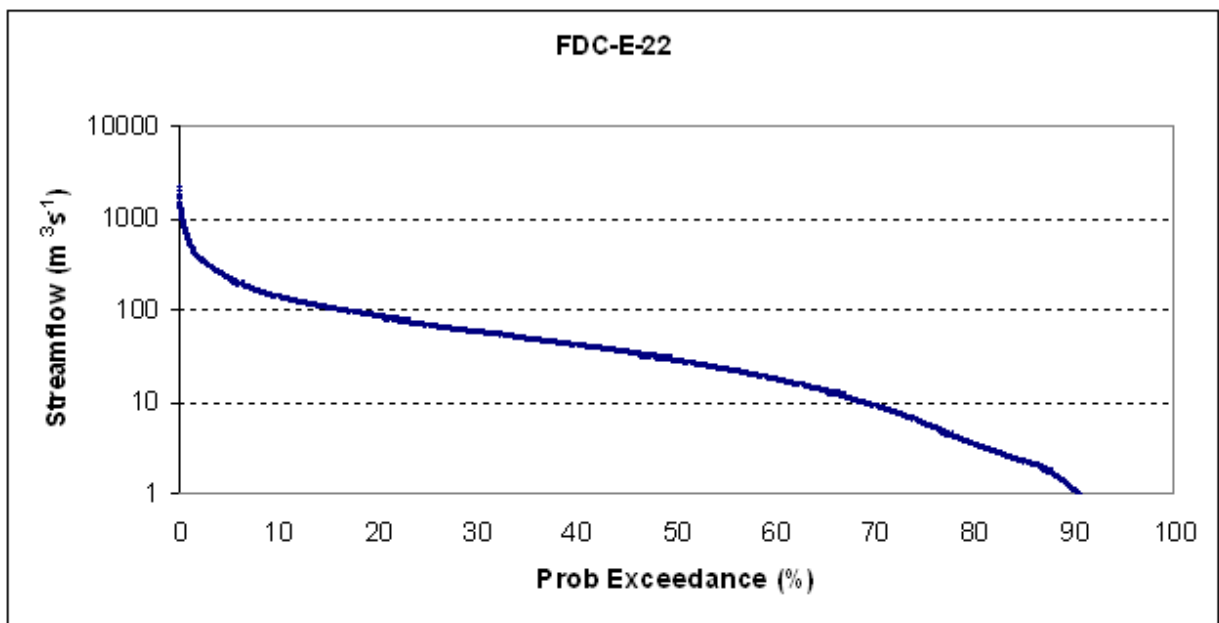


Figure 7.1 Flow Duration Curve on logarithmic scale at Moamba station

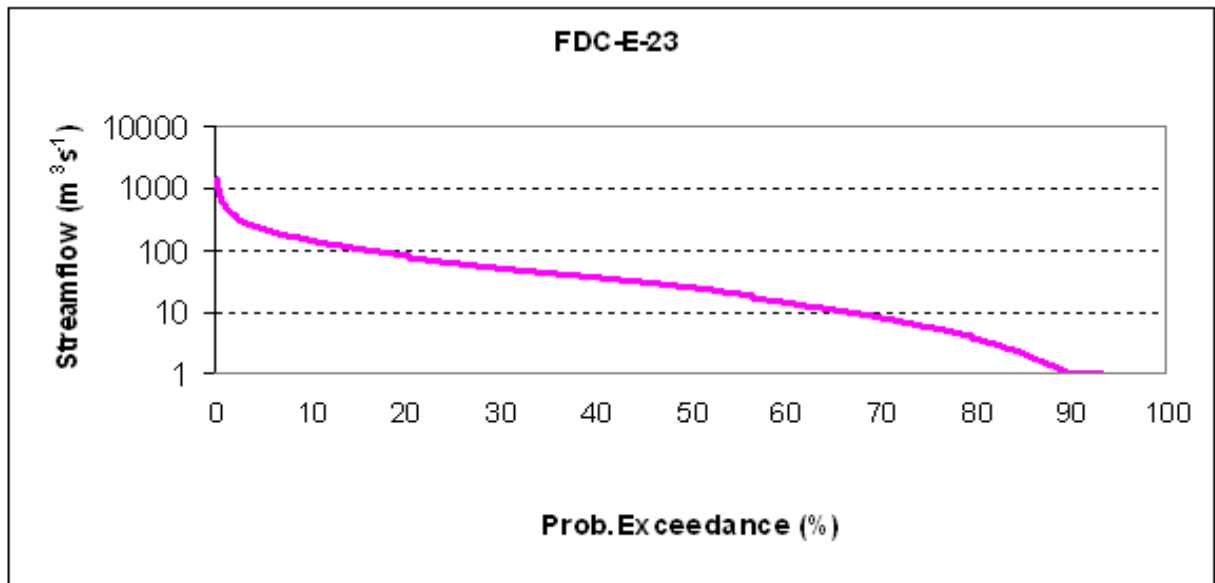


Figure 7.2 Flow Duration Curve on logarithmic scale at Ressano Garcia station

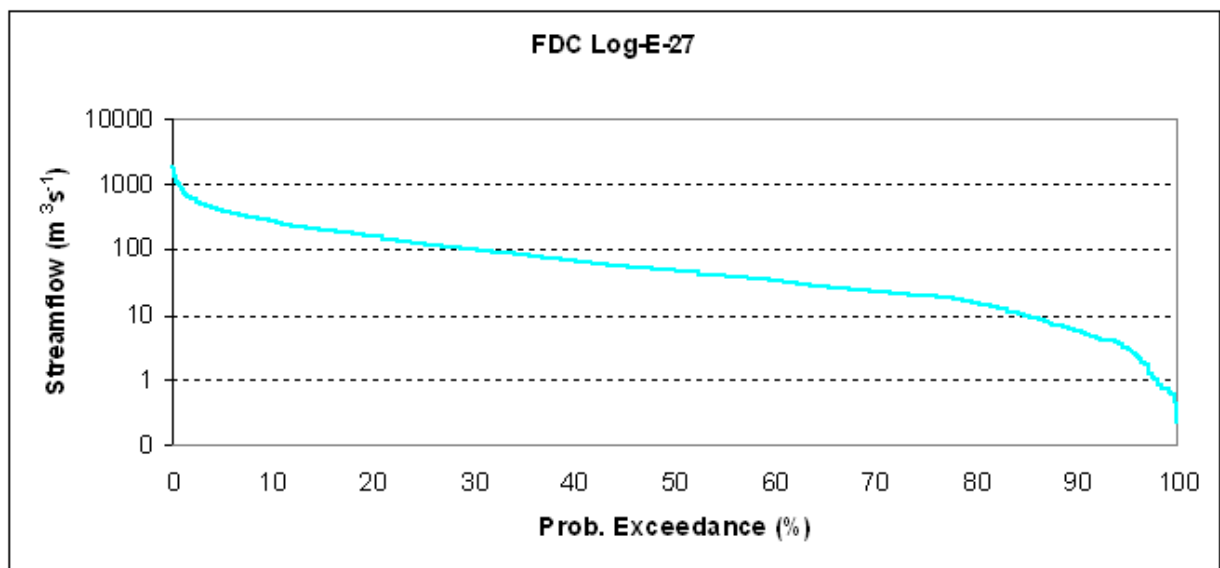


Figure 7.3 Flow Duration Curve on logarithmic scale at Chinhuanine station

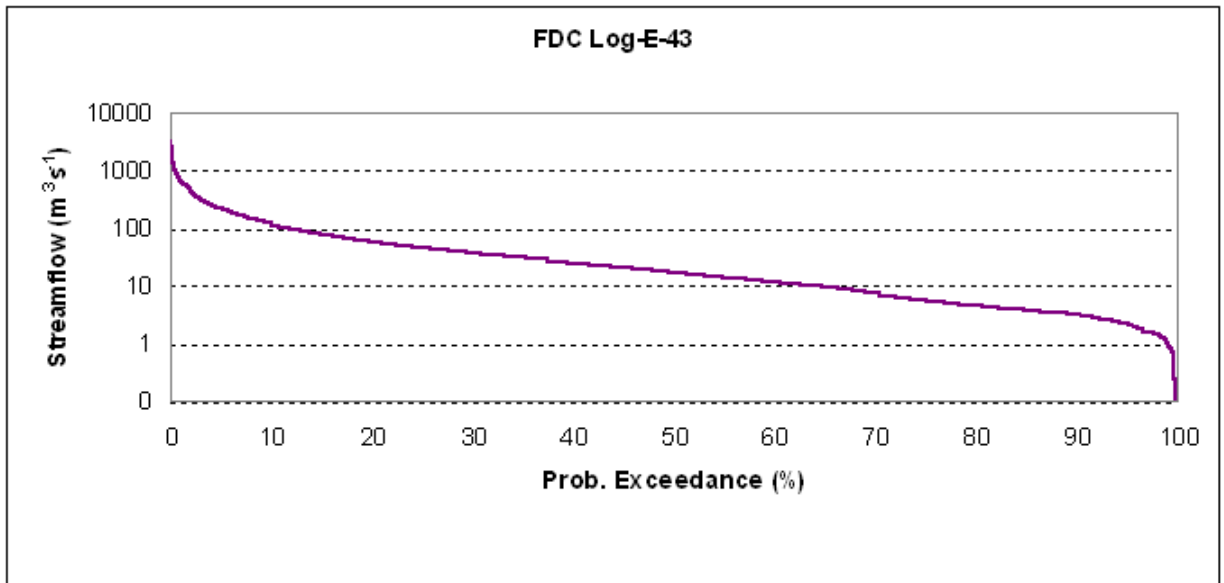


Figure 7. 4 Flow Duration Curve on logarithmic scale at Magude station

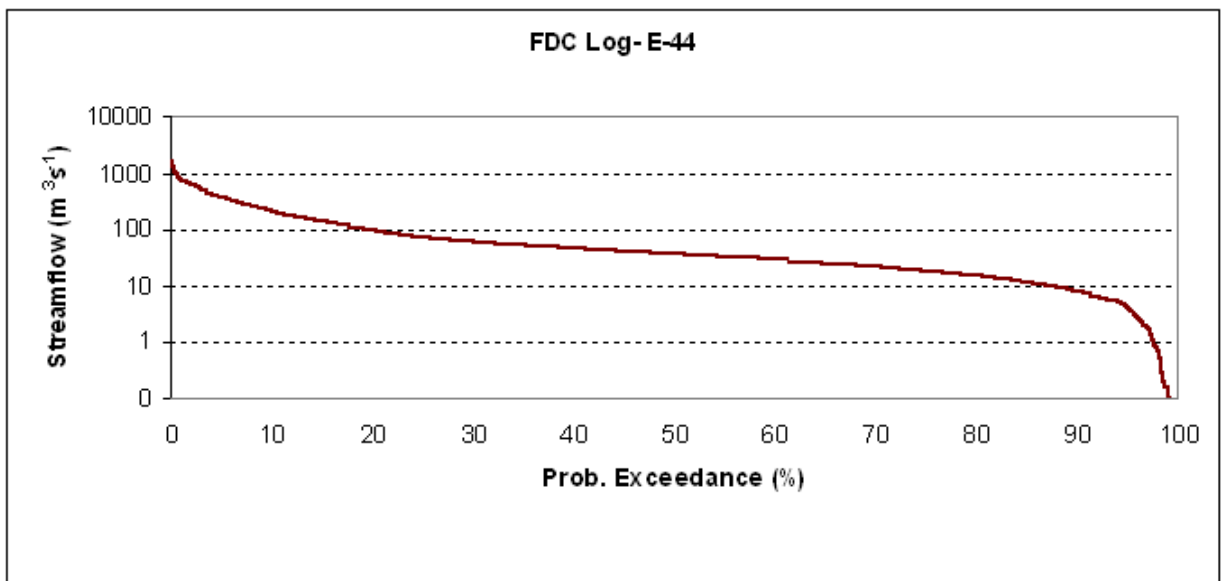


Figure 7. 5 Flow Duration Curve on logarithmic scale at Chobela station

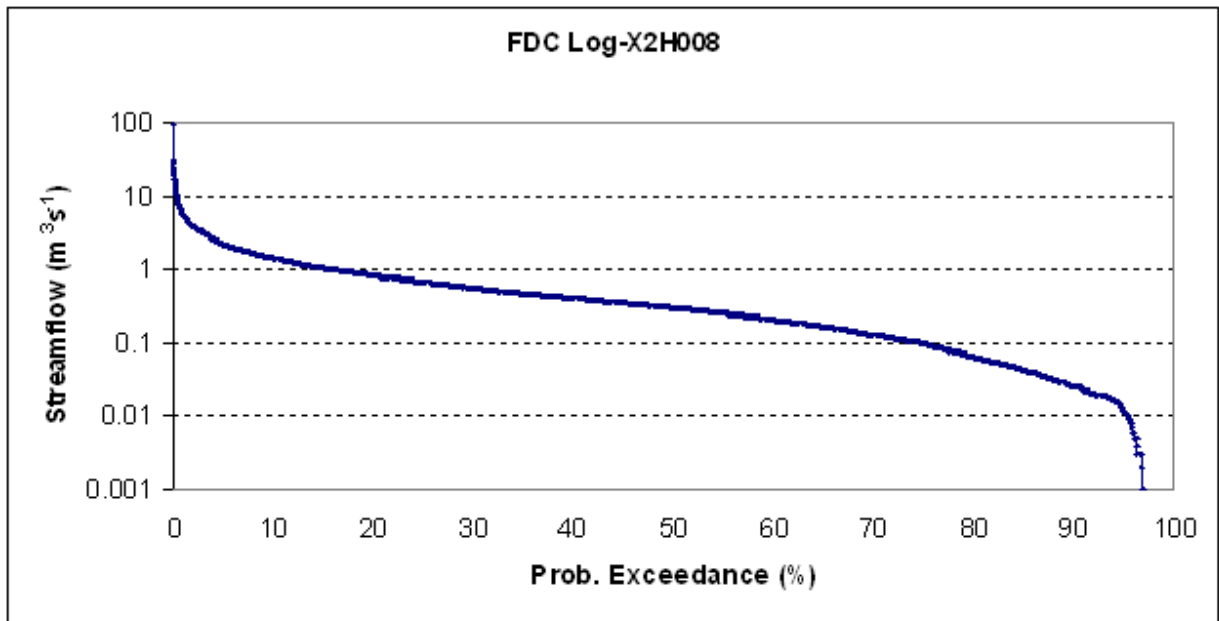


Figure 7.6 Flow Duration Curve on logarithmic scale at Sassenheim station

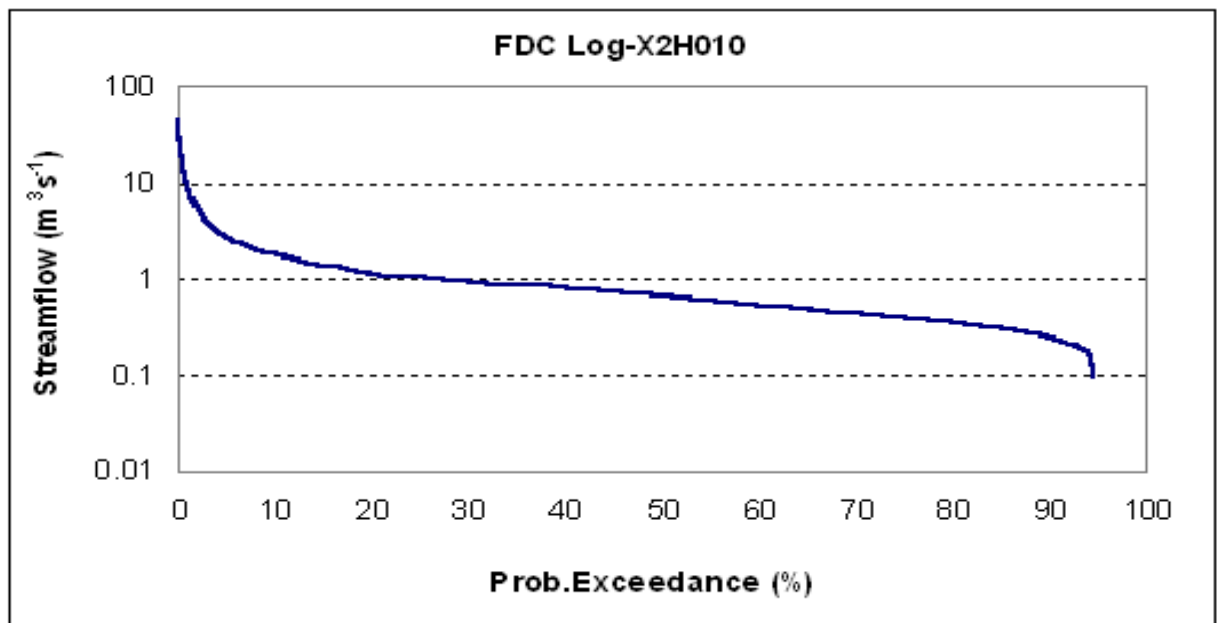


Figure 7.7 Flow Duration Curve on logarithmic scale at Bellevue station

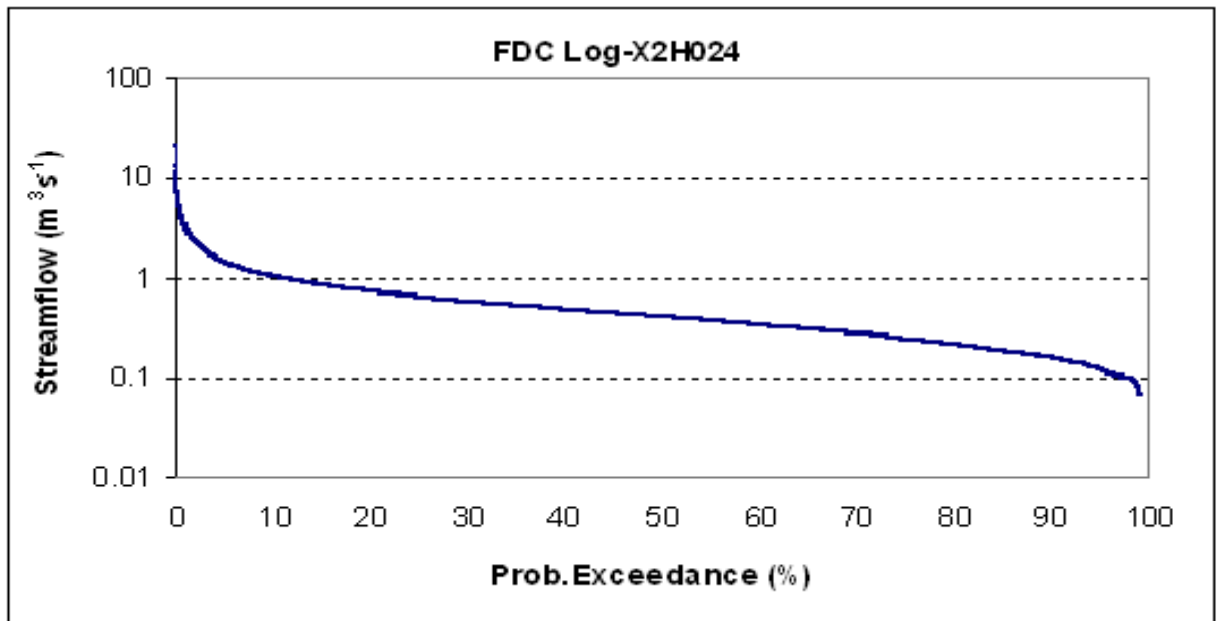


Figure 7.8 Flow Duration Curve on logarithmic scale at Glenthorpe station

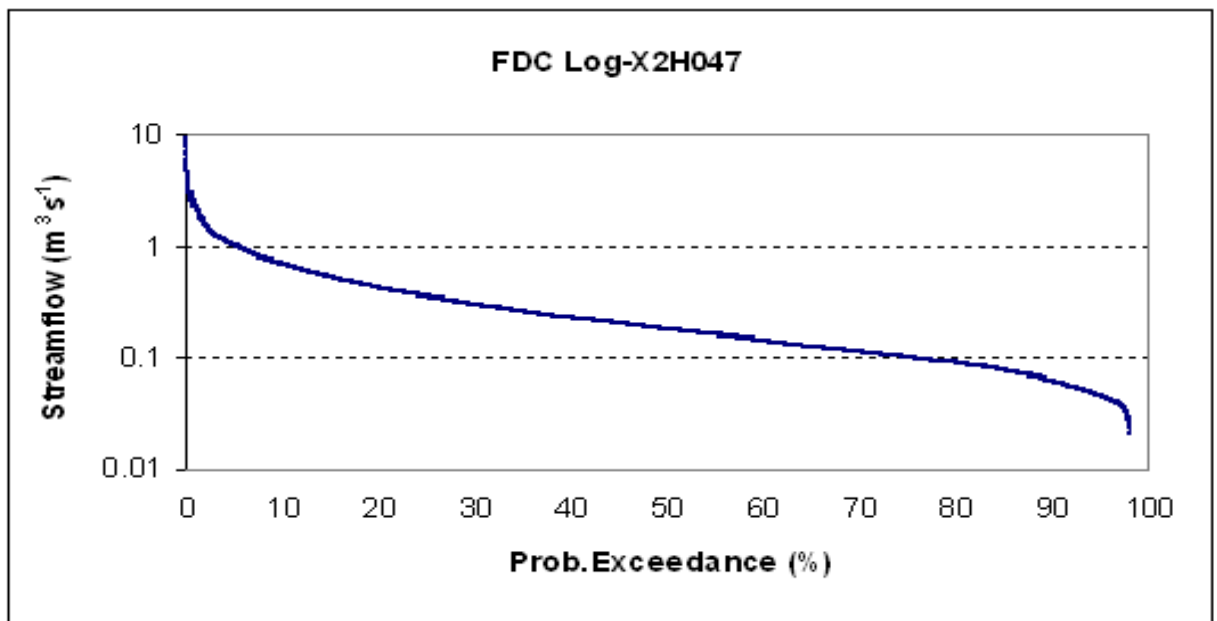


Figure 7.9 Flow Duration Curve on logarithmic scale at Kindergoed station

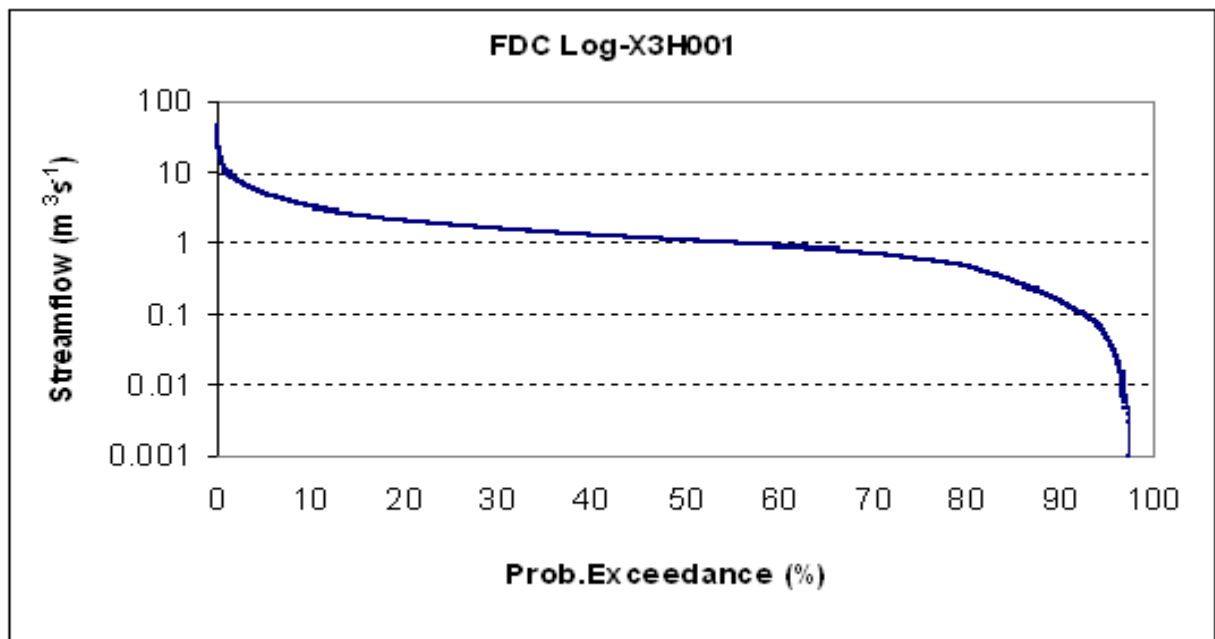


Figure 7. 10 Flow Duration Curve on logarithmic scale at Sabie station

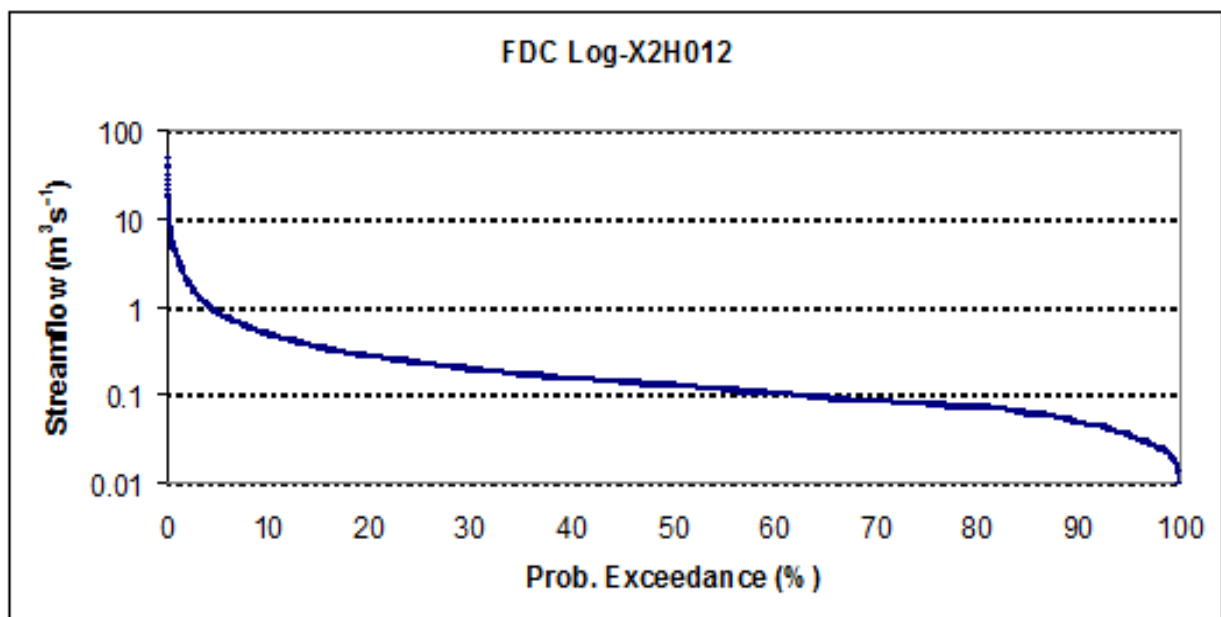


Figure 7. 11 Flow Duration Curve on logarithmic scale at Dawsonsspruit station

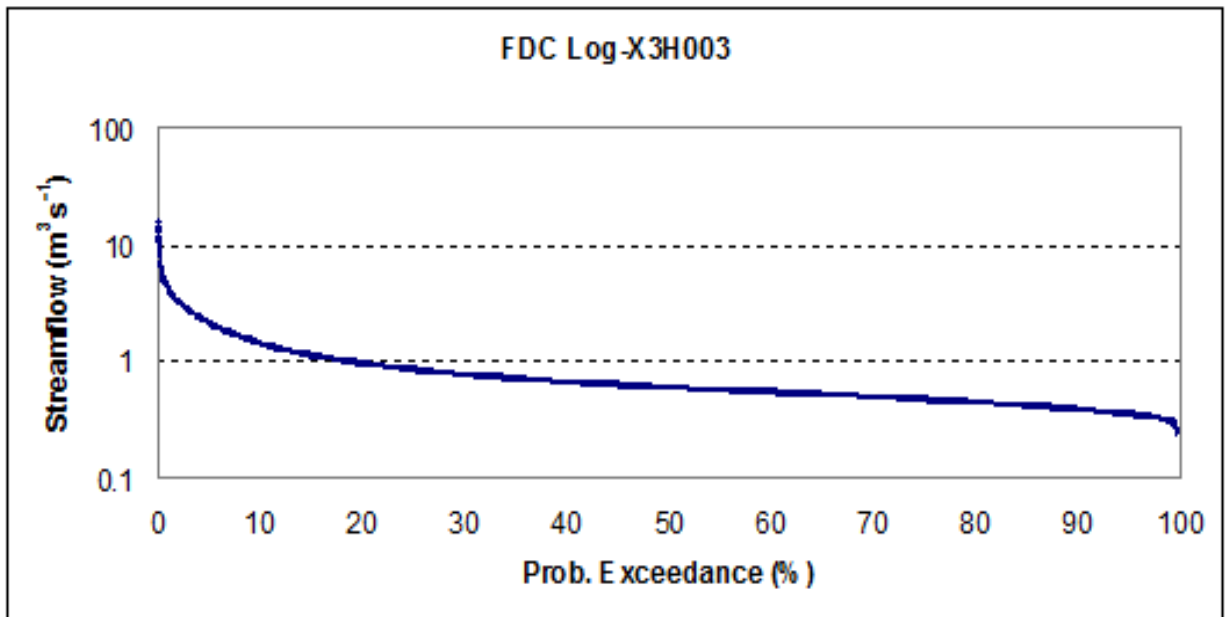


Figure 7. 12 Flow Duration Curve on logarithmic scale at Geelhoutboom station

## 7.2 Appendix 2

Various mathematical models were used for the calibration of the FDCs at gauging stations. The results of the regression analysis in the calibration of flow duration models for all gauging stations are summarized in Tables 7.1 and 7.10

Table 7. 1 Results of analysis of the mathematical models at Moamba station

<b>Equations</b>	<b>R<sup>2</sup></b>	<b>Coefficients</b>
$Q = 763.617 \exp(-0.199D)$	0.82	a=763.617 b=-0.199
$Q = 394.638D^{-0.496}$	0.88	a=394.638 b=-0.496
$Q = 442.304 - 105.504 \ln D$	0.80	a=442.304 b=-105.504
$Q = 295.466 - 9.087D + 0.66D^2$	0.54	a=295.466 b=-9.087 c=0.66
$Q = 395.254 - 21.059D + 0.366D^2 - 0.001D^3$	0.64	a=395.254 b=-21.059 c=0.366 d=-0.001

Table 7.2 Results of analysis of the mathematical models at Chinhanganine station

<b>Equations</b>	<b>R<sup>2</sup></b>	<b>Coefficients</b>
$Q = 835.568 \exp(-0.984D)$	0.89	a=835.568 b=-0.984
$Q = 615.186D^{-0.478}$	0.87	a=615.186 b=-0.478
$Q = 685.701 - 160.766 \ln D$	0.90	a=685.701 b=-160.766
$Q = 480.034 - 14.441D + 0.104D^2$	0.68	a=480.034 b=-14.441 c=0.104
$Q = 626.249 - 31.978D + 0.543D^2 - 0.003D^3$	0.98	a=626.249 b=-31.978 c=0.543 d=-0.003

Table 7.3 Results of analysis of the mathematical models at Magude station

Equations	R <sup>2</sup>	Coefficients
$Q = 2031.254 \exp(-0.791D)$	0.84	a=2031.254 b=-0.791
$Q = 501.126D^{-0.567}$	0.87	a=501.126 b=-0.567
$Q = 520.425 - 128.61 \ln D$	0.59	a=520.425 b=-128.61
$Q = 328.203 - 11.256D + 0.087D^2$	0.34	a=328.203 b=-11.256 c=0.087
$Q = 760.253 - 262.855D + 0.178D^2 - 0.001D^3$	0.81	a=760.253 b=-262.855 c=0.178 d=-0.001

Table 7.4 Results of analysis of the mathematical models at Chobela station

Equations	R <sup>2</sup>	Coefficients
$Q = 962.257 \exp(-0.152D)$	0.92	a=962.257 b=-0.152
$Q = 551.742D^{-0.492}$	0.84	a=551.742 b=-0.492
$Q = 616.412 - 146.649 \ln D$	0.84	a=616.412 b=-146.649
$Q = 429.257 - 13.704D + 0.103D^2$	0.61	a=429.257 b=-13.704 c=0.103
$Q = 800.840 - 247.431D + 0.122D^2 - 0.001D^3$	0.99	a=800.840 b=-247.431 c=0.122 d=-0.001

Table 7.5 Results of analysis of the mathematical models at Sassenheim station

Equations	R <sup>2</sup>	Coefficients
$Q = 10.405 \exp(-0.312D)$	0.78	a=10.405 b=-0.312
$Q = 4.618D^{-0.538}$	0.92	a=4.618 b=-0.538
$Q = 4.786 - 1.152 \ln D$	0.71	a=4.786 b=-1.152
$Q = 5.759 - 1.619D + 0.000D^2$	0.80	a=5.759 b=-1.619 c=0.000
$Q = 6.381 - 2.055D + 0.001D^2 - 0.000D^3$	0.86	a=6.381 b=-2.055 c=0.001 d=-0.000

Table 7. 6 Results of analysis of the mathematical models at Bellevue station

Equations	R <sup>2</sup>	Coefficients
$Q = 28.618 \exp(-0.901D)$	0.81	a=28.618 b=-0.901
$Q = 6.966D^{-0.523}$	0.90	a=6.966 b=-0.523
$Q = 6.946 - 1.644 \ln D$	0.58	a=6.946 b=-1.644
$Q = 8.620 - 2.459D + 0.000D^2$	0.69	a=8.620 b=-2.459 c=0.000
$Q = 9.853 - 3.346D + 0.003D^2 - 0.000D^3$	0.79	a=9.853 b=-3.346 c=0.003 d=-0.000

Table 7.7 Results of analysis of the mathematical models at Glenthorpe station

Equations	R <sup>2</sup>	Coefficients
$Q = 2.471 \exp(-0.531D)$	0.76	a=2.471 b=-0.531
$Q = 2.696D^{-0.454}$	0.97	a=2.696 b=-0.454
$Q = 2.702 - 0.596 \ln D$	0.80	a=2.702 b=-0.595
$Q = 3.049 - 0.759D + 0.000D^2$	0.84	a=3.049 b=-0.759 c=0.000
$Q = 3.327 - 0.953D + 0.001D^2 - 0.000D^3$	0.89	a=3.327 b=-0.953 c=0.001 d=-0.000

Table 7. 8 Results of analysis of the mathematical models at Kindergoed station

Equations	R <sup>2</sup>	Coefficients
$Q = 2.101 \exp(-0.089D)$	0.81	a=2.101 b=-0.089
$Q = 1.701D^{-0.471}$	0.93	a=1.701 b=-0.471
$Q = 1.807 - 0.413 \ln D$	0.83	a=1.807 b=-0.413
$Q = 2.076 - 0.540D + 0.000D^2$	0.90	a=2.076 b=-0.540 c=0.000
$Q = 2.238 - 0.652D + 0.000D^2 - 0.000D^3$	0.93	a=2.238 b=-0.652 c=0.000 d=-0.000

Table 7.9 Results of analysis of the mathematical models at Sabie station

Equations	R <sup>2</sup>	Coefficients
$Q = 9.843 \exp(-0.083D)$	0.82	a=9.843 b=-0.083
$Q = 8.129D^{-0.455}$	0.93	a=8.129 b=-0.455
$Q = 8.750 - 1.984 \ln D$	0.85	a=8.750 b=-1.984
$Q = 9.829 - 2.495D + 0.000D^2$	0.82	a=9.829 b=-2.495 c=0.000
$Q = 10.740 - 3.124D + 0.002D^2 - 0.000D^3$	0.68	a=10.740 b=-3.124 c=0.002 d=-0.000

Table 7. 10 Results of analysis of the mathematical models at Dawsonsspruit station

Equations	R <sup>2</sup>	Coefficients
$Q = 29.262 \exp(-3.459D)$	0.82	a=29.262 b=-3.459
$Q = 3.124D^{-0.682}$	0.97	a=3.124 b=-0.682
$Q = 2.834 - 0.699 \ln D$	0.37	a=2.834 b=-0699
$Q = 3.778 - 1.145D + 0.000D^2$	0.49	a=3.778 b=-1.145 c=0.000
$Q = 4.475 - 1.623D + 0.001D^2 - 0.000D^3$	0.59	a=4.475 b=-1.623 c=0.001 d=-0.000